Characterization of novel Modified Vaccinia virus Ankara (MVA)-based vaccines targeting hemagglutinin proteins from influenza A virus subtypes H2N2, H2N9 and H5N8

von Gabriel Maiwald

Inaugural-Dissertation zur Erlangung der Doktorwürde

(Dr. rer. biol. vet.)

der Tierärztlichen Fakultät der Ludwig-Maximilians-Universität München

Characterization of novel Modified Vaccinia virus Ankara (MVA)-based vaccines targeting hemagglutinin proteins from influenza A virus subtypes H2N2, H2N9 and H5N8

von Gabriel Maiwald, MSc ETH

aus Wien (Österreich)

München 2025

Aus dem Veterinärwissenschaftlichen Department der Tierärztlichen Fakultät

der Ludwig-Maximilians-Universität München

Lehrstuhl für Virologie

Arbeit angefertigt unter der Leitung von:

Univ.-Prof. Dr. Markus Meißner

Mitbetreuung durch:

Dr. Alina Tscherne, MSc

Gedruckt mit Genehmigung der Tierärztlichen Fakultät

der Ludwig-Maximilians-Universität München

Dekan: Univ.-Prof. Dr. Reinhard K. Straubinger, Ph.D.

Berichterstatter: Univ.-Prof. Dr. Markus Meißner

Korreferent: Priv.-Doz. Dr. Matthias Eddicks

Tag der Promotion: 26. Juli 2025

Diese Arbeit widme ich meinen Eltern.

Euch verdanke ich eure großzügige Förderung mit Leidenschaft, Hingabe und Liebe seit ich ein Kind war. Ihr habt immer an mich geglaubt. Danke ***Mama****, für alles, was du für mich gemacht hast, was du für meine Entwicklung beigetragen hast, schaust, dass es mir gut geht und dass du immer für mich da bist. Danke* ***Papa****, dafür, dass du meine Talente wahrgenommen hast und schon immer mein Mentor gewesen bist. Ich hab euch lieb!*

TABLE OF CONTENTS

I. ABBREVIATIONS

AmpR	ampicillin resistance gene
BCG	Bacillus Calmette-Guérin (vaccine)
BSA	bovine serum albumin
BSL	biosafety level
CDC	U.S. Centers for Disease Control and Prevention
CEV	cell-associated enveloped virus
COVID-19	coronavirus disease 2019
CPE	cytopathic effect
CVA	Chorioallantois Vaccinia virus
Da	Dalton
DAPI	4′,6-Diamidin-2-phenylindol
DdRp	DNA-dependent RNA polymerase
Del-III	deletion site III
dsRNA	double-stranded RNA
E	envelope protein
ECDC	European Centre for Disease Prevention and Control
EEV	extracellular enveloped virus
EFSA	European Food Safety Authority
ELISA	Enzyme-linked immunosorbent assay
ELISpot	Enzyme-linked immunosorbent spot
EMA	European Medicines Agency
EV	extracellular virus
FBS	fetal bovine serum
HA	hemagglutinin
HPAIV	highly pathogenic avian influenza virus
hpi	hours post infection
HRP	horseradish peroxidase
IAV	influenza A virus
IBV	influenza B virus
IC_{50}	half maximal inhibitory concentration
ICS	intracellular cytokine staining
ICTV	international committee on taxonomy of viruses
IEV	intracellular enveloped virus
IF	immunofluorescence
IFN-γ	interferon gamma
IL	interleukin
IM	intramuscular
IMV	intracellular mature virus
IS	immunostaining
IVCs	individually ventilated cages
kb	kilo - base pairs

LB	lysogeny broth
LoD	limit of detection
LPAIV	low pathogenic avian influenza virus
M1 protein	matrix protein
M2 protein	ion channel
MDCK	Madin-Darby Canine Kidney
MERS	middle east respiratory syndrome
MOI	multiplicity of infection
MV	mature virus
MVA	Modified Vaccinia virus Ankara
NA	neuraminidase
NEP	nuclear export protein
NLRP3	nucleotide-binding oligomerization domain-like receptor protein 3
nM	nanomolar (nmol/l)
NSAID	non-steroidal anti-inflammatory drugs
OD	optical density
PAMP	pathogen associated molecular pattern
PBS	phosphate-buffered saline
PEI	Paul Ehrlich Institute
PFU	plaque-forming units
PIV	parainfluenza virus
PMA	phorbol myristate acetate
PNGase F	Peptide -*N*-Glycosidase F
prM	pre-membrane protein
RdRp	RNA-dependent RNA polymerase
RKI	Robert Koch Institute
RNP	ribonuclear protein
RSV	respiratory syncytial virus
RT-PCR	reverse transcription polymerase chain reaction
SARS-CoV-2	severe acute respiratory syndrome coronavirus type 2
SFC	spot-forming cells
SPF	specific pathogen free
TBEV	tick-borne encephalitis virus
Th	T-helper (cell)
TLR	Toll-like receptor
TMB	3′3′,5′5′-Tetramethylbenzidine
TNF-α	Tumor necrosis factor alpha
VACV	vaccinia virus
WB	Western blot
WHO	World Health Organization

II. INTRODUCTION

Influenza A Virus (IAV) is listed as a high-risk pathogen for a possible next pandemic by the World Health organization (WHO) (WHO, July 2024). Similar to what has been observed during the latest coronavirus disease 2019 (COVID-19) outbreak, an IAV outbreak would lead to many preventable deaths, restrictions of personal liberty and vast economic damage. Especially children, elderly and immunosuppressed individuals are at high risk to become infected with influenza A viruses and develop severe symptoms, including high fever, coughing, body ache and multi organ failure (Moghadami, 2017). Although there are effective and approved vaccines against influenza available, the fast mutation rate and regular occurring reassortment events of genetic information between distinct IAV subtypes dramatically hamper the effectiveness of these vaccines. Thus, adaptions of seasonal vaccine formulations must be done annually, and the regular booster immunizations dramatically decreases the willingness of the population to receive the vaccinations. Therefore, the development of effective and broadly reactive vaccines must be promoted as recognized by the WHO (WHO, November 2024).

The aim of this thesis was to generate and characterize candidate vaccines targeting the hemagglutinin (HA) of IAV subtypes with pandemic potential. Modified Vaccinia virus Ankara (MVA) served as a backbone for antigen delivery, which is a well-researched pox virus strain unable to replicate in cells of mammalian origin due to its strict attenuation. HA gene sequences of IAV subtypes H2N9, H2N2 and H5N8 were stably incorporated into the backbone virus. In *in vitro* cell culture infections, the recombinant MVA candidate vaccines demonstrated genetic stability, unimpaired protein expression and replicative capacity in the producer DF-1 (chicken embryo fibroblast) cell line, thus, confirming their suitability for vaccine production at industrial scale. In humanized *HLA-A2.1-/HLA-DR1-transgenic H-2 class I-/class II-knockout* mice, two immunizations with the recombinant MVA vaccines elicited both a strong T-cell- and antibody-mediated immune response. These first promising results support the further development of the generated MVA-based vaccines for pandemic preparedness against

influenza A viruses.

III. LITERATURE REVIEW

1. Influenza A virus

Influenza, mainly caused by Alphainfluenzavirus influenzae (= influenza A virus, IAV) and Betainfluenzavirus influenzae (= influenza B virus, IBV), is a leading cause of morbidity and mortality globally. In fact, IAV and IBV cause 3 to 5 million severe cases and 290,000 to 650,000 deaths annually (WHO, March 2024). While IBV contributes to seasonal flu and could potentially become a pandemic concern, IAV is evidently the major threat due to antigenic drift and animal reservoirs (Sharma et al., 2019). Transmission of both IAV and IBV occurs via coughing, sneezing, indirect transmission via contact with contaminated objects or inhalation of aerosols (Javanian et al., 2021).

IAV is a respiratory virus and causes symptoms such as fever, dry cough, body aches and rhinitis in humans with a symptom onset around 1-4 days after infection (Javanian et al., 2021; WHO, February 2025). Typically, infected individuals recover after 7 days, however, especially elderly individuals, children and immunocompromised have a high risk to develop severe symptoms and complications, which is a socioeconomic burden for society causing hospitalizations every year (Moghadami, 2017). Hence, seasonal vaccination of those individuals is a high priority, however, the coverage of a broad spectrum of influenza strains is a challenging endeavor (Javanian et al., 2021).

1.1. Nomenclature of influenza A viruses

Subtypes of IAV are distinguished via their HA and neuraminidase (NA) variants. There are 18 HA and 11 NA proteins, most of which circulate in aquatic birds. The most relevant subtypes to cause infections in humans are H1N1, H1N2, H3N2, H5N1, H5N6, H7N2, H7N4 and H7N9 (Goneau et al., 2018; Wu et al., 2014). The nomenclature of a specific strain follows the scheme: IAV / origin / location / (lab number) / isolation year / subtype. An example is the IAV strain of the subtype H2N9 that was isolated in 2019 from a ruddy turnstone with the lab number 374 in Delaware (A/Ruddy/Turnstone/-Delaware/374/2019(H2N9)) (Bull World Health

Organ, 1980).

1.2. Influenza A viruses throughout the 20th and 21st century

IAV has caused four pandemics over the last 100 years. In the 20th century, pandemic outbreaks occurred in 1918, 1957 and 1968. The Spanish flu pandemic of 1918, which was caused by IAV subtype H1N1, is estimated to have caused 50 million deaths worldwide. High mortality was observed among younger adults and in individuals living in low-income countries. The Asian flu pandemic occurred in 1957, which was caused by the IAV H2N2 subtype, where the reassorted hemagglutinin was from avian origin. The Hong Kong flu pandemic was caused by IAV H3N2 subtype and spread in 1968. Interestingly, the neuraminidase of both the Asian flu and Hong Kong flu were shared between H3N2 and H2N2. IAV H1N1 subtype, which caused the Spanish flu, made again its way into headlines in 2009. The swine flu pandemic entailed reassorted segments of strains which had already circulated in swine for a decade. However, segments were determined to be of avian origin. Although it is difficult to predict which subtype will cause the next epidemic, it is worth mentioning that the subtypes H5Nx, H7Nx and H9N2 caused various outbreaks and endemic events in birds so far (Kuiken et al., 2023; Globig et al., 2018; Laurie & Rockman, 2021; Li et al., 2019; Lycett et al., 2019; McArthur, 2019; Editorial Lancet, 2018; Ungchusak et al., 2005). Furthermore, numbers of wild birds infected with the highly pathogenic H5N1 subtype, with the HA which was originally detected in 1996 in goose in China, are rising (Brüssow, 2024).

1.3. Current circulating influenza A virus subtypes with pandemic potential

Until now, IAV remains a global health concern. Latest reports from the WHO and Centers for Disease Control and Prevention (CDC) confirmed infection of dairy cows with the IAV subtype H5N1 in several states of the US followed by detection in humans (WHO, August 2024; CDC, February 2025). Furthermore, the virus was also found in wild birds and cats (Burrough et al., 2024). Over the last few years, it has been estimated that about 300 million wild birds died due to IAV (United Nations, December 2024).

The most recent human cases were reported in February 2025 (CDC, February 2025). A 2-years-old child got infected, most likely due to contact with an infected chicken, and died from a severe influenza virus A infection. (Khmer Times, February 2025). Previously further human cases were reported. For instance, the IAV subtype H5N2 was involved in the death of a man in Mexico, where the virus was circulating in poultry farms (RKI, November 2024). These reports highlight the relevance of IAV in terms of public health and the necessity to implement effective countermeasures, research and vigilance. Risk assessment should involve increased research on viral properties (susceptibility to antivirals, genomic characteristics, receptor binding, transmission in animal models), human population attributes (disease severity, antigenic relatedness, population immunity) and viral ecology and epidemiology (geographic distribution, infection in animals, human infection) (Harrington et al., 2021).

1.4. Pandemic prevention strategies

Future zoonosis should be prevented by innovative approaches of therapeutics and vaccines. Vaccines are the most effective countermeasures against newly emerging infectious diseases (Pollard & Bijker, 2021). For decades, a tremendous effort is being made by researchers all over the world to develop a universal flu vaccine. Besides, it is important to monitor the virus in both farm animals and wildlife, especially pigs and birds. Testing of poultry is routinely performed, and wild birds are surveilled based on risk for highly pathogenic avian influenza viruses (HPAIV) or tested once sick animals are identified. Additional pandemic prevention countermeasures include the surveillance of individuals in close contact with these animals, such as pig farmers, hunters and attendants of agricultural fairs. Moreover, environmental monitoring of wild water habitats, water supplies and wastewater could act as an early warning system and would help in predicting the evolutionary development of future strains (ECDC, October 2022; He et al., 2020). Furthermore, live-animal markets should be restricted to minimize the risk of interspecies transmission of novel and pathogenic influenza subtypes (ECDC, October 2022). Additionally, there are several countermeasures which could be implemented to mitigate the risk of pandemic and seasonal influenza. As

experienced during the COVID-19 pandemic, precautionary measures, including hand hygiene, respiratory etiquette, face masks, surface and object cleaning, increasing ventilation, isolation of sick individuals, school or workplace measures and closures, avoidance of crowding and reduced travelling dramatically decreased the cases of severe acute respiratory syndrome coronavirus type 2 (SARS-CoV-2) infections (WHO, September 2019; Talic et al., 2021), but also decreased the cases of IAV and IBV infections in humans (Soo et al., 2020).

1.5. Clinical presentation and treatment

IAV infections cause fever, dry cough, body aches and nausea in infected humans. Severity of the disease and elevated risk for complications is seen in elderly, immunocompromised patients and children. Transmission of the virus occurs mainly via sneezing and coughing and symptoms onset occur typically 1-4 days after infection. In severe cases, antiviral treatment should be initiated within 48 hours after initial symptoms. Complications include primary viral pneumonia, secondary bacterial pneumonia, and non-pulmonary related complications. A clinical presentation facilitates an accurate diagnosis of influenza. Over the last years, several tests to detect IAV were developed, including rapid tests, nucleic acid amplification via reverse transcription polymerase chain reaction (RT-PCR), hemagglutination assay and culturing (Eisfeld et al., 2014; Javanian et al., 2021; K. Mehta et al., 2018; Moghadami, 2017).

There are two major classes of therapeutics, namely NA inhibitors (e.g., Oseltamivir), which block viral cleavage activity of NA, and Adamantanes, which act on the ion channel M2. NA inhibitors are the preferred treatment of choice as influenza viruses became resistant to Adamantanes due to their rapid mutation rates (Javanian et al., 2021; K. Mehta et al., 2018; Moghadami, 2017; Raza & Ashraf, 2024). However, also resistance to NA inhibitors has been reported recently due to mutations in the enzyme’s active site. Interestingly, higher resistance rates against IAV treatment were observed in younger patients. Strikingly high resistance rates were observed in the 2008 and 2009 influenza seasons depending on geographical location, which emphasizes the potential selection of resistant strains and global spread (K. Mehta et al., 2018; Raza & Ashraf, 2024). NA

inhibitors are usually given to people with severe clinical manifestations or to high-risk individuals such as people over the age of 65, children, pregnant women, people with chronic diseases, immunocompromised or severely obese individuals. Notably, NA inhibitors can be taken as preventive measure after exposure (Javanian et al., 2021; K. Mehta et al., 2018). A therapeutic approach should follow as soon as possible after initial symptoms. Symptomatic treatment of severe cases takes place with non-steroidal anti-inflammatory drugs (NSAID) and hydration (Javanian et al., 2021; K. Mehta et al., 2018; Moghadami, 2017; Raza & Ashraf, 2024). The limited therapeutic approaches highlight the importance of developing effective vaccines against the virus.

1.6. Structure of influenza A virus

IAV belongs to the *Orthomyxoviridae* family and is a single-stranded (ss) RNA virus with a segmented RNA genome of negative polarity. It has an envelope with glycosylated surface proteins which are vital for its life cycle (see **Figure 1**). HA is required for binding to host cell receptors via sialic acid residues and endosomal fusion. Steric orientation of those residues determines host susceptibility. Notably, HA is cleaved by proteases into two subunits, HA1 and HA2, for activation. Besides, HA is the major target of neutralizing antibodies, which is acquired after both infection and vaccination (Bouvier & Palese, 2008; Cheung & Poon, 2007). Contrary, NA is responsible for cleavage of sialic acid residues, releasing newly formed viral particles. It also plays a role in virus internalization creating a rolling movement of viral particles on the cell surface increasing viral uptake. For optimal replication efficiency, NA and HA must be present in balanced numbers to each other (McAuley et al., 2019). The ion channel M2 establishes ion flux for the pH dependent viral-host membrane fusion of HA (Cheung & Poon, 2007).

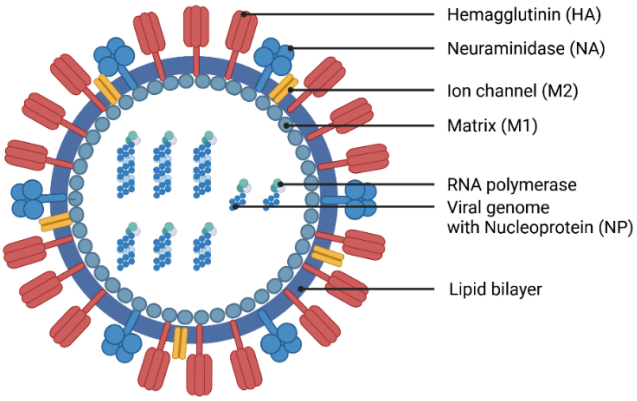

Figure 1: Structure of influenza A virus. IAV consists of a segmented genome, which is found within an enveloped virus, having two major proteins, HA and NA, on the surface. HA (red) is required for viral binding and fusion to the host cell, while NA (blue) is vital for cleavage of sialic acids to release newly formed viral particles. Ion channel M2 (yellow) is needed for generation of acidic pH within the virion required for conformational change of the matrix protein M1. M1 coats the viral genome, which is surrounded by the nucleoprotein (NP). Both proteins are necessary for viral uncoating. Created with BioRender.com

1.7. Underlying mechanisms for rapid adaption of the virus

In terms of IAV evolution, pig farms, where humans are in contact with increasingly large reservoirs, and globalization are factors, which contribute to the adaption of the virus on the human interface (Kessler et al., 2021; McArthur, 2019). The segmented genome of IAV is the underlying key concept for the pandemic potential of the virus. On the one hand, recombination of genomic segments between an avian and seasonal human strain creates a new subtype allowing spillover from bird and pig reservoirs to humans. This occurs when those two viruses infect the same host cell (antigenic shift). On the other hand, the high mutation rate of IAV enables antigenic drift of certain subtypes (see **Figure 2**) (Chan et al., 2021; Goneau et al., 2018). In addition, transmission of human strains to animals can lead again to the generation of novel strains and subsequent infection of humans (Nelson & Vincent, 2015). Adaption to the new host via point mutations could lead to greater concern following previous underestimation (He et al., 2020).

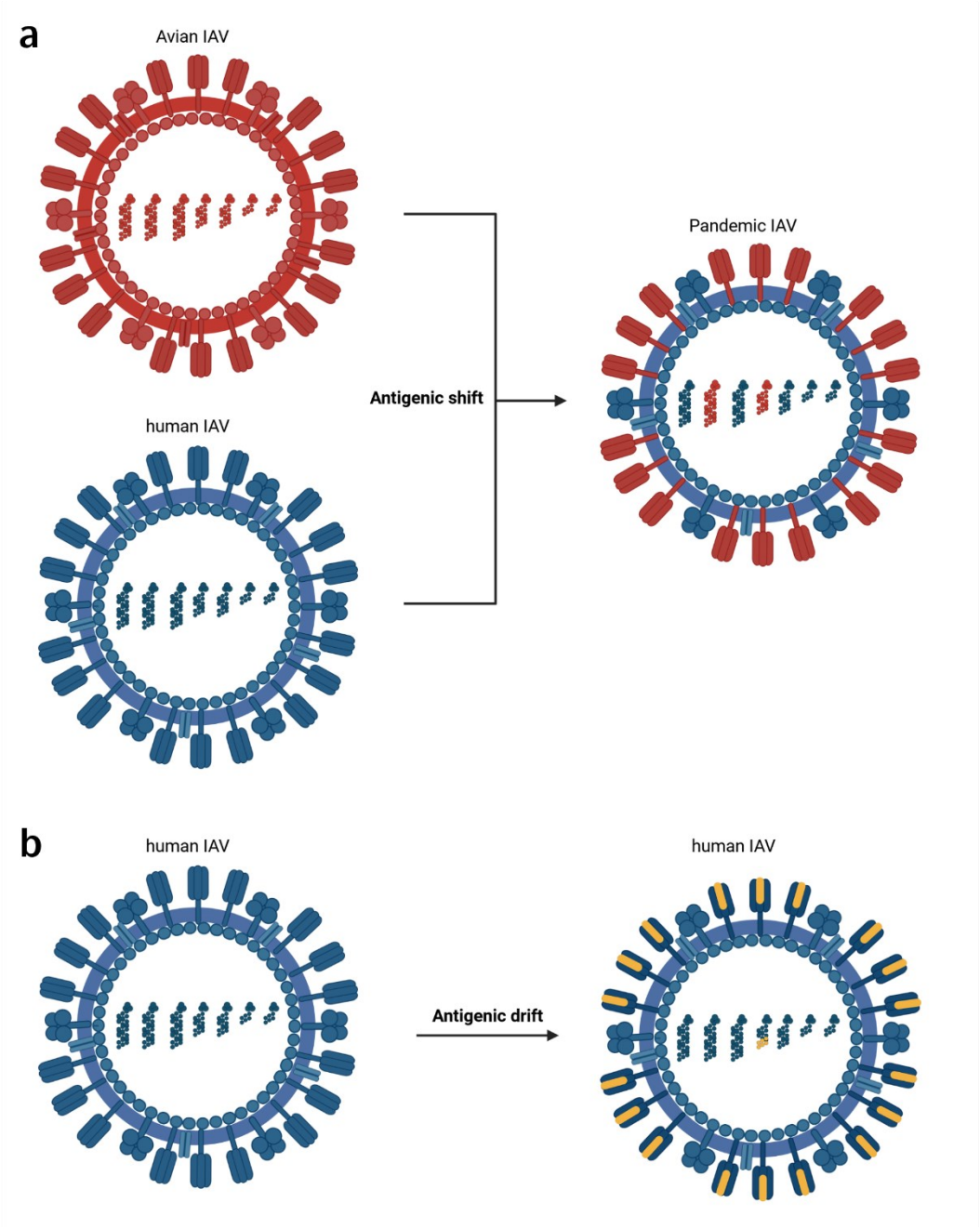

Figure 2: Evolution of IAV occurs via two main mechanisms: **(a)** Antigenic shift and antigenic drift **(b)**. While antigenic drift represents the slow adaption of the virus, antigenic shift alters the virus rapidly and hence lays the foundation for zoonotic transmission. Adapted from (Krammer, 2018). Created with BioRender.com

1.8. Hemagglutinin

The surface protein, HA, is a trimer consisting of two subunits, which are both N-glycosylated (see **Figure 3**). HA1 is shaped like a head, while HA2 is referred to as the stem domain. The receptor binding site of HA consists of three loops and one helix and is located on the HA1 subunit. As previously mentioned, HA binds via sialic acid residues to host cells, and the steric

configuration of those residues determines host susceptibility. While human IAV bind via α2,6-linked glycosidic bond, avian IAV bind via α2,3-linked sialic acids (Skehel & Wiley, 2000; Wilks et al., 2012; Wilson et al., 1981; Wu & Wilson, 2020). During viral entry, the polypeptide HA0 (75 kDa) is cleaved into the subunits HA1 (55 kDa) and HA2 (25 kDa) (Zhirnov et al., 2002). HA1 binds to sialic acid residues and HA2 mediates endosomal fusion after conformational change triggered by the endosome's acidic pH (Wang et al., 2015). HA of HPAIV are cleaved by furin in the Golgi apparatus of infected cells. HA of low pathogenic avian influenza viruses (LPAIV) can be cleaved via four different modes of action: I) extracellularly by soluble trypsin-like proteases such as plasmin, II) by serine proteases in the endosome of target cells, III) by transmembrane serin proteases on the way to the cell membrane of infected cells or IV) by transmembrane serin proteases on the surface of infected cells (Bertram et al., 2010). Since furin proteases are ubiquitous and the HA of HPAIV has a polybasic cleavage site, the virus can replicate readily in every tissue explaining its pathogenicity in birds. HA of LPAIV has only a monobasic cleavage site which is accessible to a limited number of proteases, residing in the respiratory and gastrointestinal tract, which limits infection (Bertram et al., 2010).

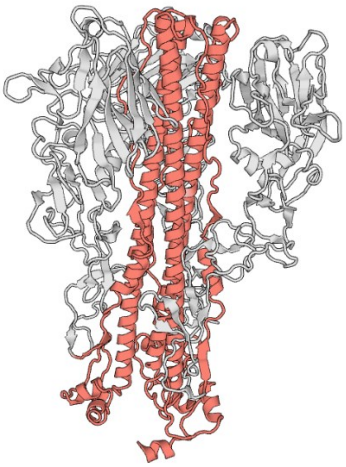

Figure 3: HA trimeric structure. Each monomer comprises of two subunits, namely HA1 (gray) and HA2 (red). The polypeptide HA0 is cleaved into HA1 and HA2 for activation during the viral life cycle. The receptor binding site is located on the HA1 subunit. HA1 resembles a globular head, while HA2 is considered as stem region (Source: SWISS-MODEL, https://swissmodel.expasy.org/repository/uni-prot/P03436?template=7zj7.1.A&-range=30-515, Biozentrum of the University of Basel and Swiss Institute of Bioinformatics).

1.9. Life cycle of IAV

During the life cycle, IAV attaches to sialic acid residues of the host cell with its HA protein and enters via endocytosis (see **Figure 4**). Low pH of the endosome triggers the conformational change of HA, allowing fusion with the endosomal membrane and the activation of the ion channel activity of the M2 protein (Bouvier & Palese, 2008). A conserved region at the N-terminus of the HA2 subunit, named fusion peptide, plays a key role for the fusion process, which ultimately interacts with the endosomal membrane by anchoring into the membrane after structural rearrangement (Cross et al., 2009). After endosomal fusion, ribonuclear proteins (RNPs) are released into the cytoplasm and cellular proteins, guided by nuclear localization signals, transport RNPs into the nucleus. Viral RNA-dependent RNA polymerase (RdRp) synthesizes two positive-sense RNA strands - mRNA for protein synthesis and a complementary strand which is transcribed to negative-sense genomic RNA. Viral mRNA is then polyadenylated and the 5’ cap snatched from the host cell before being exported to the cytoplasm and translated to proteins. The export is guided by viral proteins M1 and nuclear export protein (NEP). Proteins are synthesized on membrane-bound ribosomes at the endoplasmic reticulum, folded and post-translational modified in the Golgi apparatus. In the assembly phase, eight RNA segments are selectively packaged into each virion and newly formed viral particles are released at the cell membrane via budding. In this process, HA requires cleavage from sialic acid residues by NA activity (Bouvier & Palese, 2008).

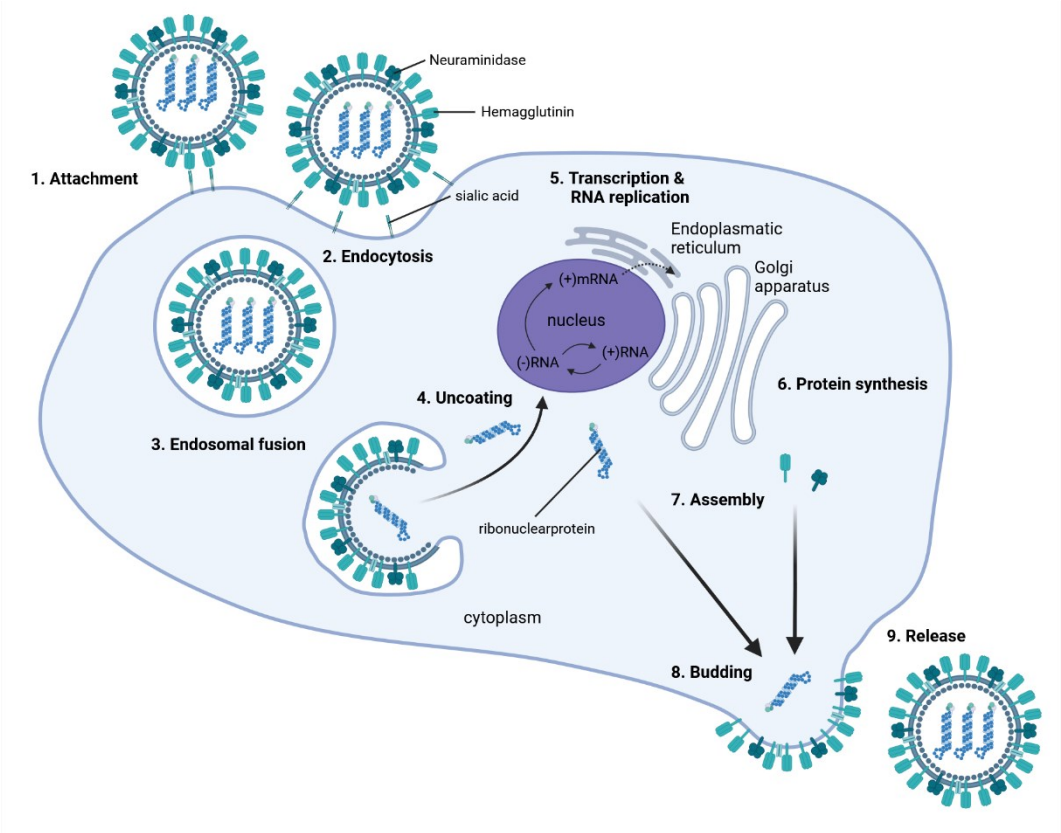

Figure 4: The life cycle of IAV. IAV enters the host cell via attachment of HA to sialic acid residues and endocytosis. Fusion with the endosome mediates uncoating of viral genome which is transcribed and translated into new viral genome and proteins. Progeny virus is assembled and released via budding. Adapted from (Nuwarda et al., 2021). Created with BioRender.com

2. Modified Vaccinia virus Ankara

The here presented recombinant vaccines targeting IAV are based on the Modified Vaccinia virus Ankara. MVA is a well characterized vaccine strain, used as viral vector in vaccine development against emerging infections and offers established clinical safety. It is a non-replicating attenuated virus (in mammalian cells) possessing strong immunogenicity. A block in the morphogenesis allows for the expression of viral and foreign proteins, while being unable to replicate in mammalian cells (Gilbert, 2013; Kreijtz et al., 2014; Volz & Sutter, 2017).

2.1. History of MVA

MVA is derived from the Vaccinia virus (VACV) strain Ankara, which was used as a smallpox vaccine in Turkey. This virus was cultivated on chorioallantois membranes of chicken eggs and was subsequently named

Chorioallantois Vaccinia Virus (CVA) (Herrlich & Mayr, 1954). CVA was then serially passaged on chicken embryo fibroblasts (CEF) and renamed to MVA after the 516th passage. Early testing demonstrated that MVA had lost the ability to induce strong cytopathic effects compared to its ancestor strain VACV which made it suitable for vaccine production (Herrlich & Mayr, 1954; Stickl & Hochstein-Mintzel, 1971). In fact, smaller lesions were observed compared to CVA after inoculation of chorioallantois membranes, but were similar to a variola or fowlpox inoculation, indicating a maintained immunogenicity. In one study, rabbits were inoculated with MVA which did not develop typical skin lesions (Mayr et al., 1975; Stickl & Hochstein-Mintzel, 1971). In another study, mice received intracerebral injections with both MVA or CVA, however, only the MVA injected mice survived, whereas the CVA group died (Mayr et al., 1975; Stickl & Hochstein-Mintzel, 1971). Studies in macaques also revealed loss of virulence as intracranial injection of MVA did not cause a systemic disease in contrast to CVA (Stickl & Hochstein-Mintzel, 1971). MVA was further developed as safer smallpox vaccine and subsequently received market authorization in 1977 after successful clinical trials (Stickl et al., 1974). Between 1977 and 1980, the vaccine was administered to approximately 120,000 people before the smallpox vaccination program was stopped in Germany. No cases of the severe adverse events associated with conventional VACV vaccination were documented in the recipients of the MVA vaccine (Mahnel & Mayr, 1994).

2.2. Structure and characteristics of MVA

MVA belongs to the family *Poxviridae*. The virus has a brick shaped envelope, which is about 240 – 300 nm in size and its DNA genome is about 130 – 375 kb long (see **Figure 5**) (Damon, 2011; Moussatche & Condit, 2015). MVA is a subspecies of Vaccinia virus and is a member of the genus *Orthopoxviruses* (ICTV, 2024). The capsid protects the genome from the external environment and the core wall is made of viral proteins, including A3, A4, A10, L4 and F17. Interestingly, lateral bodies, which are located between the core and first membrane are believed to take part in antiviral mechanisms. The virus is enveloped by up to two membranes (Damon, 2011; Moussatche & Condit, 2015). Glycosylated proteins are embedded in

the outer membrane, while proteins of the inner membrane are not glycosylated (Modrow S. et al., 2021).

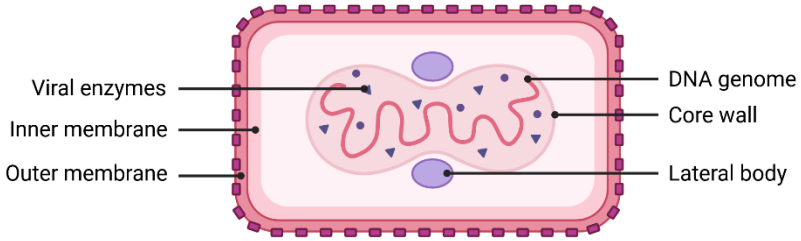

Figure 5: Structure of Poxviruses. The genomic DNA is enclosed by viral enzymes and the core membrane, followed by two outer membranes. Lateral bodies are denoted in purple. Created with BioRender.com

The documented genome of MVA, which was characterized from isolate MVA-F6 after the 572nd passage, is shown in **Figure 6**. As described above, the serial passaging of MVA on avian cells caused a strict attenuation. This resulted in large deleted regions (in total 30,000 bp), referred to as six major deletion sites (deletion site I to VI), and mutations in virus-host interaction genes. Host range genes define the tropism of viruses. Interestingly, the host range gene C7L is conserved, whereas K1L was lost during the serial passages. Both genes are vital for late gene expression. Due to the strict attenuation, MVA fails to replicate in cells of mammalian origin (Volz & Sutter, 2017; Antoine et al., 1998; Backes et al., 2010; Meyer et al., 1991; Werden et al., 2008). Hence, MVA is considered a non-replicating attenuated DNA virus suitable for human application. It was discovered that protein and DNA synthesis remained unimpaired, as the life cycle is blocked at the step of virion assembly. MVA also lacks many immune evasion factors and interference with host defense mechanisms is hampered (Volz & Sutter, 2017). Studies of immunoregulatory pathways showed that MVA induced chemotaxis, migration of leukocytes to site of infection and NF-κβ activation (Lehmann et al., 2009). Overall, MVA regulatory proteins activate induction of apoptosis, interferons, and inflammatory cytokines at an early stage (Volz & Sutter, 2017). Notably, MVA elicits a T-helper (Th) 1 skewed immune response, with interleukin (IL)-6 and tumor necrosis factor alpha (TNF-α) being the major cytokines involved (Ramírez et al., 2000). Upon intramuscular (IM) immunization, MVA infects not only myocytes but also

antigen-presenting cells, possibly contributing to its excellent immunogenicity (Altenburg et al., 2017). Infection of dendritic cells prompts cytokine production, activation of costimulatory molecules for T cell stimulation and cell death (Döring et al., 2021).

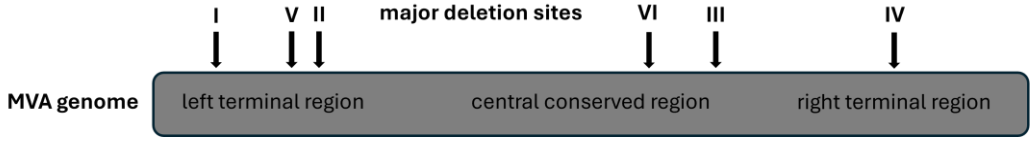

Figure 6: Schematic representation of the MVA genome. MVA, after 572nd passages of CVA on CEF, harbors six major deletion sites as denoted in the picture. Key characteristic of its attenuation is its replication deficiency on mammalian cells. Adapted from (Volz & Sutter, 2017).

2.3. Life cycle of MVA

The various stages of MVA's life cycle are illustrated in **Figure 7**. MVA's entry into host cells depends in which form the virus is present. The first mechanism of action refers to the intracellular mature virus (IMV), also named mature virus (MV), which is enveloped by one membrane. IMV enters via fusion or endocytosis followed by endosome fusion. The second mechanism of actions refers to the extracellular enveloped virus (EEV), also named extracellular virus (EV), which possesses two membranes. EEV enters via membrane shedding and direct fusion. In the next step, the core is transported via microtubules into the cytoplasm for uncoating. DNA is then transcribed into mRNA by a viral DNA-dependent RNA poly-merase (DdRp). Early transcribed genes are essential for DNA replication and virus-host interaction factors, while intermediate genes are required for transcription factors of late genes, which are translated into viral proteins and enzymes. Subsequently, progeny virions are formed in virus factories within the cytoplasm (Greseth & Traktman, 2022; Moss, 2006; Roberts & Smith, 2008).

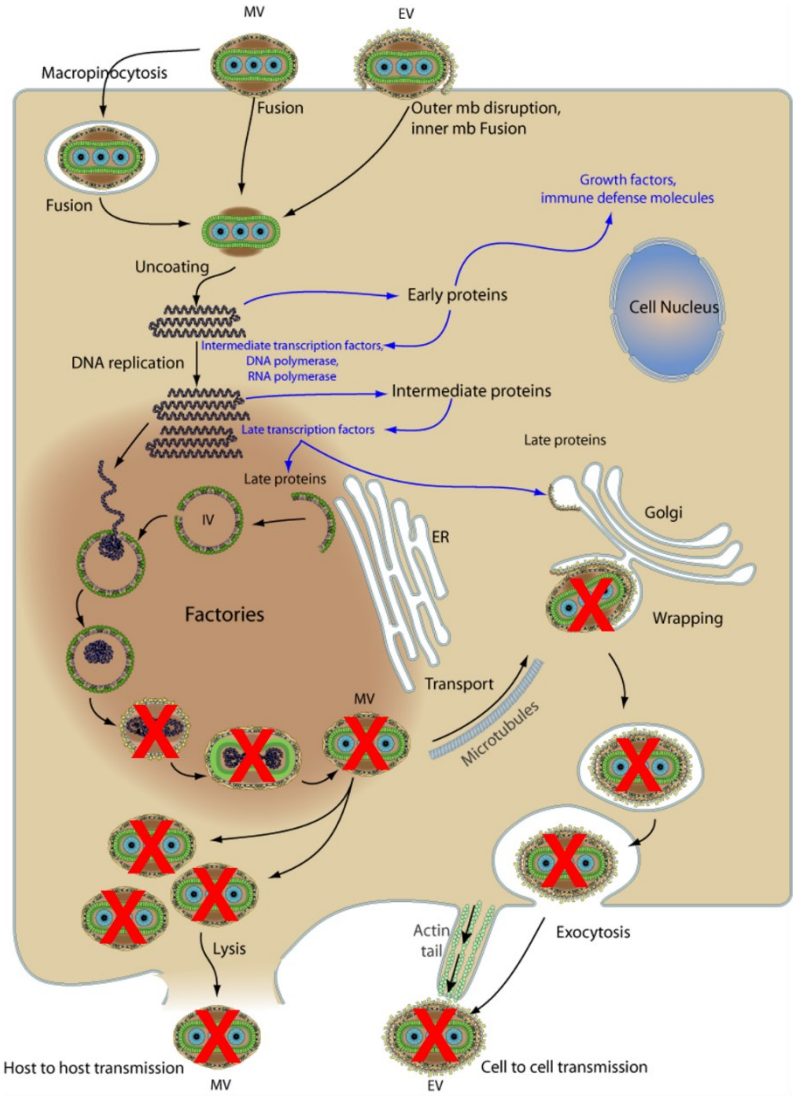

Figure 7: Life cycle of MVA in mammalian cells. Expression and translation of early, intermediate and late proteins is unimpaired. Replication is blocked at the step of virion assembly. Adapted from ViralZone, https://viralzone.expasy.org/4399, Swiss Institute of Bioinformatics.

Next steps in the viral life cycle do not occur in cells of mammalian origin but in chicken cells (see **Figure 8**). Proteins are cleaved and packed together with DNA to form infectious IMVs. IMVs can be released via cell lysis. If not released, virions are transported for wrapping in two membranes, which originate from endosomal or trans-Golgi cisterna. Viral proteins play a crucial role in the wrapping process. Although their exact role is not yet fully understood, all of them are either incorporated into the membrane or associated with membrane wrapping (Greseth & Traktman, 2022; Roberts & Smith, 2008). For instance, F13 is associated with phospholipase activity (Husain & Moss, 2002). The intracellular enveloped

virus (IEV) is then transported to the cell periphery and crosses the actin cortex before the outer IEV membrane can fuse with the plasma membrane. Actin polymerization leads the now called cell-associated enveloped virus (CEV), which is the cell-retained version of EEVs, to infect neighboring cells, and are formed by the exocytosis of IEVs. EEVs are capable of infecting distant cells, resulting in comet-shaped plaque formation on a cell monolayer. Primary plaques are accompanied by a comet tail formed by secondary plaques. EEVs are the main route of virus spread and relatively resistant to neutralizing antibodies and the complement system (Greseth & Traktman, 2022; Roberts & Smith, 2008).

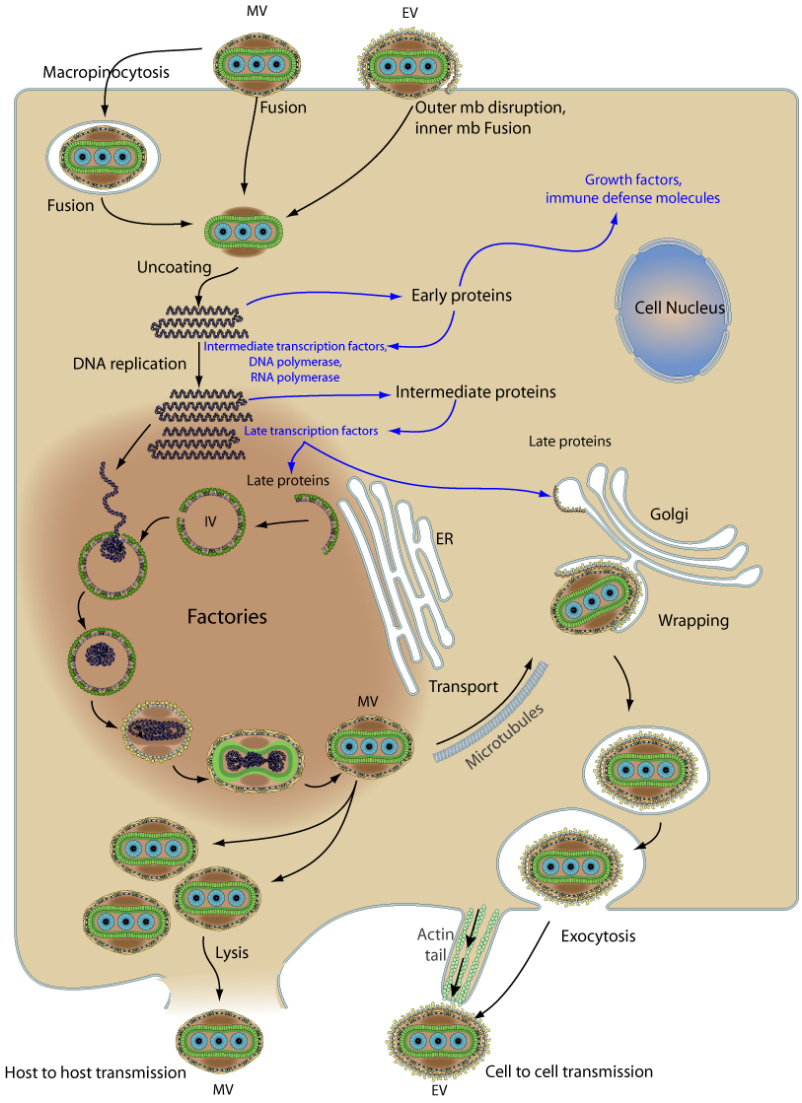

Figure 8: Life cycle of MVA on chicken cells. Expression and translation of early, intermediate and late proteins is followed by virion assembly. (Source: ViralZone, https://viralzone.expasy.org/4399, Swiss Institute of Bioinformatics)

2.4. MVA as a versatile vaccine platform

After MVA's use as a smallpox vaccine in Germany, MVA was tested as a eukaryotic cloning vector that could be used to express heterologous genes (Volz & Sutter, 2017). For example, Sutter and Moss exploited MVA's non-replicating characteristic to deliver foreign sequences that were introduced into deletion site III, leading to the induction of antibody and cytotoxic T-cell responses in mice (Sutter & Moss, 1992; Sutter et al., 1994). MVA's loss of virus-host interaction factors makes it an interesting platform to study Vaccinia virus regulators involved in host cell tropism, inflammatory response and immunogenicity (Volz & Sutter, 2017). MVA has also been used for research and vaccine development against malaria (Schneider et al., 1998), AIDS (Abaitua et al., 2006), tuberculosis (Goonetilleke et al., 2003), West Nile fever (Volz et al., 2016), Middle East Respiratory Syndrome (MERS) (Song et al., 2013), COVID-19 (Tscherne et al., 2021) and Ebola (Tapia et al., 2016). For example, studies in mice, immunized with MVA delivering SARS-CoV- spike (S) protein, protected mice against SARS-CoV-2 infection, accompanied by the induction of a strong cellular and humoral immune response (Bisht et al., 2004; Chen et al., 2005; Tscherne et al., 2021). Similarly, MERS-CoV-S was delivered by MVA in mice and camels, inducing secretion of neutralizing antibody (Alharbi et al., 2022; Song et al., 2013). Noteworthy, concerns about using smallpox as biological weapon have been raised. Fortunately, MVA entails superior characteristics as preventive vaccine and post exposure immunization in case of re-emergence of smallpox, as it is well-tolerated in individuals with immunodeficiencies or skin diseases (Henderson et al., 1999; Rotz et al., 2002; Volz & Sutter, 2017).

MVA is also being used as vaccine platform against poorly addressed respiratory viruses such as parainfluenza virus (PIV) 3 and human respiratory syncytial virus (RSV). For both viruses, experimental vaccines were developed, which yielded in protection in animal models (Durbin et al., 1999; Durbin et al., 1998; Wyatt et al., 1996). Particularly, recombinant MVA delivering fusion or hemagglutinin-neuraminidase proteins of parainfluenza virus 3, elicited high levels of virus-specific antibodies, while the candidate vaccine against hemagglutinin-neuraminidase reduced viral loads more

efficiently upon challenge. Both vaccines protected from disease in a macaque model (Durbin et al., 1999; Durbin et al., 1998). MVA was also utilized to address Nipah disease. In one study, MVA was used to deliver the Nipah glycoprotein G, and a strong cellular immune response was established after immunization of type I interferon receptor-deficient (IFNAR−/−) mice (Kalodimou et al., 2019). In addition, MVA-based vaccines against Tick-borne encephalitis virus (TBEV) were used in a heterologous approach. Pre-membrane (prM) and envelope (E) proteins of TBEV were delivered by MVA and induced full protection of mice. The titer of induced virus-neutralizing antibodies was similar compared to the inactivated virus vaccine FSME-IMMUN® (Kubinski et al., 2023).

A more recent example of MVA as a successful vaccine is its use against Mpox, formerly known as monkeypox, which was addressed with Imvanex (also known as Imvamune or Jynneos) (EMA, 2013). A systematic review assessed vaccine effectiveness with real-world data (Mason et al., 2024). Pre-exposure prophylaxis achieved a vaccine effectiveness ranging from 35% to 86% after prime-boost immunization. Post-exposure prophylaxis of two studies amounted to 78% and 89% vaccine effectiveness with a prime only immunization. The vaccine was reported to also reduce Mpox related hospitalization and severity of clinical presentation.

MVA is not only used for vaccine development against infectious diseases, but also as a cancer therapeutic. For instance, one study by Drexler and colleagues elicited a cytotoxic T-cell response directed against melanoma (Drexler et al., 1999). Another study revealed the use of MVA to deliver the suicide gene FCU1 to cancer cells, which lead to the production of an enzyme capable of converting the prodrug 5-fluorocytosine. 5-fluorocytosine suppressed the tumor growth more potent than an adenovirus-based equivalent (Erbs et al., 2008). Recombinant MVAs can also be used to target nasopharyngeal carcinoma by delivering the Epstein-Barr virus latent membrane protein 2A. In a preclinical study, a strong cellular and humoral immune response against the Epstein-Barr virus latent membrane protein 2A was elicited, resulting in the killing of tumor cells (Sun et al., 2025). Another oncolytic study showed that MVA replicates in tumor cells with lower expression of the zinc finger antiviral protein and reduced

tumors (Li et al., 2025).

2.5. Advantages over alternative vaccine technologies

Two MVA-based vaccines received marketing authorization namely the pox vaccine Imvanex (EMA, 2013) and the Ebola vaccine Mvabea (EMA, 2020). Another four candidates (MVA/HIV62B, MVA-NSmut, TherVacB, CMV-MVA Triplex) are being tested in clinical studies (NCT02852005; NCT01701336; NCT06513286; NCT06075745), which highlights that MVA is appropriate for use as vaccine platform.

MVA-based vaccines are genetically stable, highly immunogenic and therefore do not require adjuvants (Volz & Sutter, 2017). In addition, MVA offers a high safety profile. In one clinical study, participants were monitored up to 180 days and no severe or serious adverse events were reported (Koch et al., 2020). Pain, swelling, induration, headaches, fatigue and malaise were the most common side effects and disappeared quickly without complications or long-term sequelae. Compatibility with comorbidities is another clinical advantage of the platform. MVA was administered to high-risk groups including immunocompromised individuals, in which no severe adverse events were reported (Kennedy & Greenberg, 2009). In other clinical studies, local reactions were the most frequently reported conditions (Vollmar et al., 2006; von Krempelhuber et al., 2010).

Another advantage is that MVA represents a non-replicating viral vector, eliminating the risk of vaccination illness (Robert-Guroff, 2007). Furthermore, the nature of MVA allows a multivalent approach by delivering different viral proteins at the same time. Delivery of homologous antigens was already demonstrated with an MVA-based vaccine against Epstein-Barr virus with five entry glycoproteins, which had superior neutralizing antibody activity to a monovalent approach (Escalante et al., 2024).

In another study, a heterologous MVA-based vaccine against TBEV with the prM and E performed as good as an inactivated virus vaccine in terms of antibody-mediated protection (Kubinski et al., 2023). Compared to adenoviral vectors, for which vector immunity is reported, hindering antigen delivery (Sakurai et al., 2022), vector immunity to MVA does not diminish

vaccine efficacy of subsequent MVA-based vaccination under optimal conditions (Altenburg et al., 2018). However, cellular immunity can be dampened. This should be taken into consideration together with the knowledge of the correlate of protection for the corresponding pathogen when designing MVA-based vaccines.

Unlike conventional live-attenuated or inactivated influenza vaccines, MVA can be handled at biosafety level (BSL) 1 conditions (Altenburg et al., 2014), which facilitates vaccine development and production. In contrast to mRNA-based vaccines, MVA is superior in handling of vaccine stocks due to its stability (Rheinbaben et al., 2007; Crommelin et al., 2021; Uddin & Roni, 2021). As a study exemplifies, it can be stored for 12 months at temperatures above the freezing point, for 6 h up to 40°C and potency upon freeze-thawing cycles, agitation or temperature variations is maintained (Capelle et al., 2018). Unsophisticated delivery of MVA is another advantage over other technologies involving mRNA. Formulation of mRNA vaccines must address various properties of mRNA. mRNA is relatively unstable, readily degraded and quite large, hindering the passage of the plasma membrane (Wadhwa et al., 2020). In contrast, MVA-based vaccines allow to deliver the antigen by simply infecting host cells.

Here, we aimed to establish a repertoire of IAV-HA vaccines against the potential pandemic IAV subtypes H2N2, H2N9 and H5N8. We first aimed to generate a series of candidate vaccines and to characterize them *in vitro* using standardized quality control procedures. Furthermore, we aimed to test the candidate vaccines *in vivo*, to explore the humoral immune responses and to identify potential human H2 and H5-specific T cell epitopes using humanized *HLA-A2.1-/HLA-DR1-transgenic H-2 class I-/class II-knockout* mice.

IV. OBJECTIVES

Although there are effective vaccines available against IAV, the emergence of new reassorted subtypes with the ability to cause severe diseases in human and birds, makes it necessary to adapt the vaccines on a regular basis. The aim of this thesis was to develop novel MVA-based candidate vaccines against IAV targeting HA proteins of the subtypes H2N2, H2N9 and H5N8. This study describes the following milestones on the way to develop the new candidate vaccines MVA-IAV-H2R, expressing HA from subtype A/Ruddy/Turnstone/Delaware/-374/2019(H2N9), MVA-IAV-H2S, expressing HA from subtype A/Singapore/1/1957(H2N2) and MVA-IAV-H5G, expressing HA from subtype A/seal/Germany-SH/AI05379/2021-(H5N8):

(i) Design and generation of recombinant MVA delivering full-length IAV-HA antigens (MVA-IAV-H2R, MVA-IAV-H2S and MVA-IAV-H5G)

(ii) *In vitro* characterization of recombinant MVA-IAV vaccines following standardized quality control procedures:

   a. Genetic stability and integrity

   b. Unimpaired protein expression

   c. Replicative capacity

(iii) *In vivo* characterization of recombinant MVA-IAV candidate vaccines in regard to the induction of adaptive immune responses in humanized *HLA-A2.1-/HLA-DR1-transgenic H-2 class I-/class II-knockout* mice:

   a. Immunization experiments

   b. Determination of IAV-specific $CD8^+$ and $CD4^+$ T cell responses

   c. Humoral immune responses against IAV by determining binding antibody responses

V. MATERIALS

1. Plasmids

Table 1: Expression and Shuttle plasmids

Plasmid	Company
pEX-K248-H2Ruddy	Eurofins Genomics GmbH (Ebersberg, Germany)
pEX-K248-H2Singapore	Eurofins Genomics GmbH (Ebersberg, Germany)
pEX-K248-H5Germany	Eurofins Genomics GmbH (Ebersberg, Germany)
pIIIsynIIred	LMU
pIIIsynIIred-IAV- A/Ruddy/Turnstone/-Delaware/374/2019(H2N9) (pSynII-red-H2R)	LMU
pIIIsynIIred-IAV- A/Singapore/f1/1957(H2N2) (pSynII-red-H2S)	LMU
pIIIsynIIred-IAV- A/seal/Germany-SH/AI05379/-2021(H5N8) (pSynII-red-H5G)	LMU

2. Oligonucleotides

Table 2: Oligonucleotides used for PCR analysis.

Name	Sequence (5'→3')	PCR
III-3´ (forward)	GTACCGGCATCTCTAGCAGT	Del-III
III-5´ (reverse)	TGACGAGCTTCCGAGTTCC	Del-III
MVA-Del I for	CTTTCGCAGCATAAGTAGTATGTC	Six major deletion
MVA-Del I rev	CATTACCGCTTCATTCTTATATTC	Six major deletion
MVA-Del II for	GGGTAAAATTGTAGCATCATATACC	Six major deletion
MVA-Del II rev	AAAGCTTTCTCTCTAGCAAAGATG	Six major deletion
MVA-Del III for	GATGAGTGTAGATGCTGTTATTTTG	Six major deletion
MVA-Del III rev	GCAGCTAAAAGAATAATGGAATTG	Six major deletion
MVA-Del IV for	AGATAGTGGAAGATACAACTGTTACG	Six major deletion
MVA-Del IV rev	TCTCTATCGGTGAGATACAAATACC	Six major deletion
MVA-Del V for	CGTGTATAACATCTTTGATAGAATCAG	Six major deletion
MVA-Del V rev	AACATAGCGGTCTACTAATTGATTT	Six major deletion
MVA-Del VI for	CTACAGGTTCTGGTTCTTTATCCT	Six major deletion
MVA-Del VI rev	CACGGTCAATTAACTATAGCTCTG	Six major deletion

C7L for	ATGGGTATACAGCACGAA	C7L
C7L rev	CATGGACTCATAATCTCT	C7L
H5-Germany for 1	GAAAAAACACACAACGGGAAG	insert
H5-Germany rev 1	TGCCCCACAGTATCAAGAG	insert
H5-Germany for 2	AAACCCAACCACCTACATTTC	insert
H5-Germany rev 2	TTCACTCCGCTTATTTCTTCTC	insert
H2-Ruddy for 1	TCAATCCCTGAGATAGCGAC	insert
H2-Ruddy rev 1	AACACATCCAGAAAGAAATCCC	insert
H2-Ruddy for 2	GCCAACAATTCCACAGAAAAAG	insert
H2-Ruddy rev 2	TGATGATACCCATACCAGCC	insert
H2-Singapore for	CTCATTCTCCTGTTCACAGC	insert
H2-Singapore rev	CCATACCAACCATCAACCATTC	insert

3. Antibodies

3.1. Primary antibodies

Table 3: Primary antibodies used for Western blot (WB), immunofluorescence staining (IF) and intracellular cytokine staining (ICS) listed with catalogue numbers (Cat. No.).

Name	Cat. No.	Company	Method
Polyclonal Rabbit anti-Influenza A Virus H2	LS-C486849	LifeSpan BioSciences (Seattle, Washington)	IF (1:2000), WB (1:2000)
Influenza A H5N8 HA Polyclonal	PA5-81709	Thermo Fisher Scientific (Waltham, Massachusetts)	IF (1 µg/ml)
Vaccinia Virus (Lister Strain) rabbit polyclonal antibody	BP1076	OriGene Technologies (Rockville, Maryland)	PFU titration (2 – 2.5 µg/ml)
Anti-hemagglutinin antibody, Influenza A virus H5N8 antibody, clone 7H6C	MABF2811	Merck Millipore (Burlington, Massachusetts)	WB (1:2000)
PE/Cyanine 7 anti-mouse CD3 antibody	100220	Biolegend (San Diego, California)	ICS (2 µg/ml)
Brilliant Violet 421™ anti-mouse CD4 antibody	100443	Biolegend (San Diego, California)	ICS (1:600)
Alexa Fluor® 488 anti-mouse CD8a	100723	Biolegend (San Diego, California)	ICS (1.25 µg/ml)

antibody			
TruStain FcX™ (anti-mouse CD16/32) antibody	101320	Biolegend (San Diego, California)	ICS (1 µg/ml)
APC anti-mouse IFN-ɣ antibody	505810	Biolegend (San Diego, California)	ICS (0.67 µg/ml)
PE anti-mouse TNF-α antibody	506306	Biolegend (San Diego, California)	ICS (0.67 µg/ml)

3.2. Secondary antibodies

Table 4: Secondary antibodies used for Western blot (WB), immunofluorescence staining (IF) and intracellular cytokine staining (ICS) listed with catalogue numbers (Cat. No.).

Name	Cat. No.	Company	Method
Goat anti-rabbit IgG (H+L) highly cross-adsorbed secondary antibody, Alexa Fluor™ 488	A11034	Thermo Fisher Scientific (Waltham, Massachusetts)	IF (2 µg/ml)
Peroxidase AffiniPure™ goat anti-rabbit IgG (H+L)	111-035-144	Jackson ImmunoResearch (West Grove, Pennsylvania)	PFU titration (0.16 µg/ml)
Anti-rabbit IgG, HRP-linked antibody	7074	Cell Signaling Technology (Danvers, Massachusetts)	WB (1:5000), ELISA (1:5000)
Polyclonal goat anti-mouse, conjugated with HRP	P0447	Agilent (Santa Clara, California)	WB (1:2000)
Goat anti-mouse IgG (H+L) Secondary antibody, HRP	62-6520	Thermo Fisher Scientific (Waltham, Massachusetts)	ELISA (0.5 µg/ml)

4. Peptides

Table 5: Selected HA A/Singapore/1/1957(H2N2) specific overlapping peptides.

Peptide ID	Amino acid sequence	Pools
HA H2-S p1	MAIIYLILLFTAVRG	H2S-P1
HA H2-S p2	YLILLFTAVRGDQIC	H2S-P1
HA H2-S p3	LFTAVRGDQICIGYH	H2S-P1
HA H2-S p4	GTYVSVGTSTLNKRS	H2S-P7
HA H2-S p5	TRPKVNGLGSRMEFS	H2S-P1
HA H2-S p6	VNGLGSRMEFSWTLL	H2S-P1
HA H2-S p7	GSRMEFSWTLLDMWD	H2S-P1
HA H2-S p8	EFSWTLLDMWDTINF	H2S-P1
HA H2-S p9	TLLDMWDTINFESTG	H2S-P1
HA H2-S p10	MWDTINFESTGNLIA	H2S-P1
HA H2-S p11	INFESTGNLIAPEYG	H2S-P1
HA H2-S p12	HPLTIGECPKYVKSE	H2S-P1
HA H2-S p13	IGECPKYVKSEKLVL	H2S-P1
HA H2-S p14	PKYVKSEKLVLATGL	H2S-P1
HA H2-S p15	KSEKLVLATGLRNVP	H2S-P2, H2S-P8
HA H2-S p16	EKMNTQFEAVGKEFS	H2S-P2
HA H2-S p17	TQFEAVGKEFSNLER	H2S-P2
HA H2-S p18	AVGKEFSNLERRLEN	H2S-P2
HA H2-S p19	EFSNLERRLENLNKK	H2S-P2
HA H2-S p20	LDVWTYNAELLVLME	H2S-P2
HA H2-S p21	TYNAELLVLMENERT	H2S-P2
HA H2-S p22	ELLVLMENERTLDFH	H2S-P3
HA H2-S p23	LMENERTLDFHDSNV	H2S-P3
HA H2-S p24	ERTLDFHDSNVKNLY	H2S-P3
HA H2-S p25	DFHDSNVKNLYDKVR	H2S-P3
HA H2-S p26	IKGVKLSSMGVYQIL	H2S-P3
HA H2-S p27	KLSSMGVYQILAIYA	H2S-P3
HA H2-S p28	VAGSLSLAIMMAGIS	H2S-P3
HA H2-S p29	LSLAIMMAGISFWMC	H2S-P3
HA H2-S p30	IMMAGISFWMCSNGS	H2S-P3

Table 6: Selected HA A/Ruddy/Turnstone/Delaware/-374/2019(H2N9), specific overlapping peptides.

Peptide ID	Amino acid sequence	Pools
HA H2-R p1	MTITFLILLFTVVKG	H2R-P1
HA H2-R p2	FLILLFTVVKGDQIC	H2R-P1
HA H2-R p3	LFTVVKGDQICIGYH	H2R-P1
HA H2-R p4	ECDRLLSVPEWSYIV	H2R-P1
HA H2-R p5	LLSVPEWSYIVEKEN	H2R-P1
HA H2-R p6	PEWSYIVEKENPVNG	H2R-P1
HA H2-R p7	YIVEKENPVNGLCYP	H2R-P1
HA H2-R p8	KENPVNGLCYPGSFN	H2R-P1
HA H2-R p9	QRTLYQNVGAYVSVG	H2R-P8
HA H2-R p10	GAYVSVGTSTLNKRS	H2R-P8
HA H2-R p11	TRPKVNGQGGRMEFS	H2R-P1
HA H2-R p12	VNGQGGRMEFSWTLL	H2R-P1
HA H2-R p13	GGRMEFSWTLLETWD	H2R-P1
HA H2-R p14	EFSWTLLETWDVINF	H2R-P1
HA H2-R p15	TLLETWDVINFESTG	H2R-P1
HA H2-R p16	TWDVINFESTGNLIV	H2R-P1
HA H2-R p17	INFESTGNLIVPEYG	H2R-P2
HA H2-R p18	STGNLIVPEYGFKIS	H2R-P2, H2R-P8
HA H2-R p19	LIVPEYGFKISKRGS	H2R-P2
HA H2-R p20	FHNIHPLTIGECPKY	H2R-P2
HA H2-R p21	HPLTIGECPKYVKSD	H2R-P2
HA H2-R p22	IGECPKYVKSDRLVL	H2R-P2
HA H2-R p23	PKYVKSDRLVLATGL	H2R-P2
HA H2-R p24	KSDRLVLATGLRNVP	H2R-P2
HA H2-R p25	TQKAVDGITNKVNSV	H2R-P2
HA H2-R p26	VDGITNKVNSVIEKM	H2R-P2
HA H2-R p27	EKMNTQFEAVGKEFN	H2R-P2
HA H2-R p28	TQFEAVGKEFNNLER	H2R-P2
HA H2-R p29	AVGKEFNNLERRLEN	H2R-P2
HA H2-R p30	EFNNLERRLENLNKK	H2R-P3
HA H2-R p31	LDVWTYNAELLILME	H2R-P3
HA H2-R p32	TYNAELLILMENERT	H2R-P3
HA H2-R p33	ELLILMENERTLDYH	H2R-P3
HA H2-R p34	LMENERTLDYHDSNV	H2R-P3
HA H2-R p35	ERTLDYHDSNVRNLY	H2R-P3
HA H2-R p36	DYHDSNVRNLYDKVR	H2R-P3
HA H2-R p37	IKGVKLSNMGVYQIL	H2R-P3

HA H2-R p38	KLSNMGVYQILAIYA	H2R-P3
HA H2-R p39	IYATVAGSLSLAIMI	H2R-P3
HA H2-R p40	VAGSLSLAIMIAGIS	H2R-P3
HA H2-R p41	LSLAIMIAGISFWMC	H2R-P3
HA H2-R p42	IMIAGISFWMCSNGS	H2R-P3

Table 7: Selected HA A/Ruddy/Turnstone/Delaware/-374/2019(H2N9), and A/Singapore/1/1957(H2N2) specific overlapping peptides, which are shared between the two subtypes.

Peptide ID	Amino acid sequence	Pools
HA H2-S+R p1	NNSTEKVDTILERNV	H2S-P4, H2R-P4
HA H2-S+R p2	EKVDTILERNVTVTH	H2S-P4, H2R-P4
HA H2-S+R p3	TILERNVTVTHAKDI	H2S-P4, H2R-P4
HA H2-S+R p4	RNVTVTHAKDILEKT	H2S-P4, H2R-P4
HA H2-S+R p5	LGNPECDRLLSVPEW	H2S-P4, H2R-P4
HA H2-S+R p6	TSGEQMLIIWGVHHP	H2S-P4, H2R-P4
HA H2-S+R p7	EYGFKISKRGSSGIM	H2S-P4, H2R-P4
HA H2-S+R p8	LVLATGLRNVPQIES	H2S-P4, H2R-P4
HA H2-S+R p9	TGLRNVPQIESRGLF	H2S-P4, H2R-P4
HA H2-S+R p10	NVPQIESRGLFGAIA	H2S-P4, H2R-P4
HA H2-S+R p11	IESRGLFGAIAGFIE	H2S-P4, H2R-P4
HA H2-S+R p12	GLFGAIAGFIEGGWQ	H2S-P5, H2R-P5
HA H2-S+R p13	AIAGFIEGGWQGMVD	H2S-P5, H2R-P5
HA H2-S+R p14	NSVIEKMNTQFEAVG	H2S-P5, H2R-P5
HA H2-S+R p15	LERRLENLNKKMEDG	H2S-P5, H2R-P5
HA H2-S+R p16	LENLNKKMEDGFLDV	H2S-P5, H2R-P5
HA H2-S+R p17	NKKMEDGFLDVWTYN	H2S-P5, H2R-P5
HA H2-S+R p18	EDGFLDVWTYNAELL	H2S-P5, H2R-P5
HA H2-S+R p19	QILAIYATVAGSLSL	H2S-P5, H2S-P9, H2R-P5, H2R-P9
HA H2-S+R p20	GISFWMCSNGSLQCR	H2S-P5, H2R-P5

Table 8: Selected HA A/seal/Germany-SH/AI05379/2021-(H5N8): specific overlapping peptides.

Peptide ID	Amino acid sequence	Pools
HA H5-G p1	MKNIVLLLAIVSLVK	H5G-P1
HA H5-G p2	VLLLAIVSLVKSDQI	H5G-P1
HA H5-G p3	AIVSLVKSDQICIGY	H5G-P1
HA H5-G p5	TEQVDTIMEKNVTVT	H5G-P1
HA H5-G p6	DTIMEKNVTVTHAQD	H5G-P1
HA H5-G p7	EKNVTVTHAQDILEK	H5G-P1
HA H5-G p8	PMCDEFIRVPEWSYI	H5G-P1
HA H5-G p9	EFIRVPEWSYIVERA	H5G-P1
HA H5-G p10	VPEWSYIVERANPAN	H5G-P1
HA H5-G p11	SYIVERANPANDLCY	H5G-P1
HA H5-G p12	ERANPANDLCYPGSL	H5G-P1
HA H5-G p13	NPTTYISVGTSTLNQ	H5G-P2
HA H5-G p14	YISVGTSTLNQRLVP	H5G-P2
HA H5-G p15	GTSTLNQRLVPKIAT	H5G-P2
HA H5-G p16	LNQRLVPKIATRSQV	H5G-P2
HA H5-G p17	SQVNGQRGRMDFFWT	H5G-P2
HA H5-G p18	GQRGRMDFFWTILKP	H5G-P2
HA H5-G p19	RMDFFWTILKPDDAI	H5G-P2
HA H5-G p20	FWTILKPDDAIHFES	H5G-P2
HA H5-G p21	MPFHNIHPLTIGECP	H5G-P2
HA H5-G p22	NIHPLTIGECPKYVK	H5G-P2
HA H5-G p23	LTIGECPKYVKSNKL	H5G-P3
HA H5-G p24	ECPKYVKSNKLVLAT	H5G-P3
HA H5-G p25	PLRERRRKRGLFGAI	H5G-P3
HA H5-G p26	RRRKRGLFGAIAGFI	H5G-P3
HA H5-G p27	RGLFGAIAGFIEGGW	H5G-P3
HA H5-G p28	GFIEGGWQGMVDGWY	H5G-P3
HA H5-G p29	ADKESTQKAIDGVTN	H5G-P3
HA H5-G p30	STQKAIDGVTNKVNS	H5G-P3
HA H5-G p31	AIDGVTNKVNSIIDK	H5G-P3
HA H5-G p32	VTNKVNSIIDKMNTQ	H5G-P3
HA H5-G p33	VNSIIDKMNTQFEAV	H5G-P4
HA H5-G p34	IDKMNTQFEAVGREF	H5G-P4
HA H5-G p35	NTQFEAVGREFNNLE	H5G-P4
HA H5-G p36	RIENLNKKMEDGFLD	H5G-P4
HA H5-G p37	LNKKMEDGFLDVWTY	H5G-P4
HA H5-G p38	MEDGFLDVWTYNAEL	H5G-P4

HA H5-G p39	FLDVWTYNAELLVLM	H5G-P4
HA H5-G p40	WTYNAELLVLMENER	H5G-P4
HA H5-G p41	AELLVLMENERTLDF	H5G-P4
HA H5-G p42	VLMENERTLDFHDSN	H5G-P4
HA H5-G p43	NERTLDFHDSNVKNL	H5G-P5
HA H5-G p44	LDFHDSNVKNLYDKV	H5G-P5
HA H5-G p45	VKLESIGTYQILSIY	H5G-P5
HA H5-G p46	SIGTYQILSIYSTAA	H5G-P5
HA H5-G p47	YQILSIYSTAASSLA	H5G-P5
HA H5-G p48	SIYSTAASSLALAIM	H5G-P5
HA H5-G p49	TAASSLALAIMMAGL	H5G-P5
HA H5-G p50	SLALAIMMAGLSLWM	H5G-P5
HA H5-G p51	AIMMAGLSLWMCSNG	H5G-P5
HA H5-G p52	AGLSLWMCSNGSLQC	H5G-P5

Table 9: HA A/Ruddy/Turnstone/Delaware/-374/2019(H2N9), and A/Singapore/1/1957(H2N2) specific peptides, which were predicted for MHC binding using the Immune Epitope Database.

Name	Subtype	MHC Allele	Position	Amino acid sequence	Pool
HA H2-S p43	H2N2	HLA-A*02:01	HA_{5-13}	YLILLFTAV	H2S-P6
HA H2-S p44	H2N2	HLA-A*02:01	$HA_{245-253}$	TLLDMWDTI	H2S-P6
HA H2-S p45	H2N2	HLA-A*02:01	$HA_{440-448}$	VLMENERTL	H2S-P6
HA H2-S p46	H2N2	HLA-A*02:01	$HA_{542-550}$	MMAGISFWM	H2S-P6
HA H2-R p47	H2N9	HLA-A*02:01	HA_{5-13}	FLILLFTVV	H2R-P6
HA H2-R p48	H2N9	HLA-A*02:01	$HA_{440-448}$	ILMENERTL	H2R-P6
HA H2-R p49	H2N9	HLA-A*02:01	$HA_{525-533}$	QILAIYATV	H2R-P6
HA H2-S+R p50	H2N2+ H2N9	HLA-A*02:01	HA_{33-41}	TILERNVTV	H2S-P7, H2R-P7
HA H2-S+R p51	H2N2 + N2N9	HLA-A*02:01	$HA_{326-334}$	VLATGLRNV	H2S-P7, H2R-P7
HA H2-S+R p52	H2N2+ H2N9	HLA-A*02:01	$HA_{398-406}$	KMNTQFEAV	H2S-P7, H2R-P7

HA H2-S+R p53	H2N2+ H2N9	HLA-A*02:01	$HA_{423-431}$	KMEDGFLDV	H2S-P7, H2R-P7
HA H2-S+R p54	H2N2+ H2N9	HLA-A*02:01	$HA_{428-436}$	FLDVWTYNA	H2S-P7, H2R-P7
HA H2-S+R p55	H2N2+ H2N9	HLA-A*02:01	$HA_{457-466}$	NLYDKVRMQL	H2S-P7, H2R-P7
HA H2-S+R p56	H2N2+ H2N9	HLA-A*02:01	$HA_{525-533}$	QILAIYATV	H2S-P7, H2R-P7
HA H2-S p57	H2N2	HLA-DRB1*01:01	HA_{7-21}	ILLFTAVRGDQICIG	H2S-P8, H2R-P8
HA H2-S p58	H2N2	HLA-DRB1*01:01	$HA_{208-222}$	VGTYVSVGTSTLNKR	H2S-P8, H2R-P8
HA H2-S p59	H2N2	HLA-DRB1*01:01	$HA_{259-273}$	GNLIAPEYGFKISKR	H2S-P8, H2R-P8
HA H2-S p60	H2N2	HLA-DRB1*01:01	$HA_{301-315}$	TTLPFHNVHPLTIGE	H2S-P8, H2R-P8
HA H2-S p61	H2N2	HLA-DRB1*01:01	$HA_{322-336}$	SEKLVLATGLRNVPQ	H2S-P8, H2R-P8
HA H2-S p62	H2N2	HLA-DRB1*01:01	$HA_{436-450}$	AELLVLMENERTLDF	H2S-P8, H2R-P8
HA H2-S-R p63	H2N2	HLA-DRB1*01:01	$HA_{522-536}$	GVYQILAIYATVAGS	H2S-P9, H2R-P9

Table 10: HA A/seal/Germany-SH/AI05379/2021-(H5N8) specific peptides, which were predicted for MHC binding using the Immune Epitope Database.

Peptide ID	MHC Allele	Position	Amino acid sequence	Pool
HA H5-G p54	HLA-A*02:01	HA_{6-14}	LLLAIVSLV	H5G-P6
HA H5-G p55	HLA-A*02:01	HA_{34-42}	TIMEKNVTV	H5G-P6
HA H5-G p56	HLA-A*02:01	$HA_{403-411}$	KMNTQFEAV	H5G-P6
HA H5-G p57	HLA-A*02:01	$HA_{433-441}$	FLDVWTYNA	H5G-P6
HA H5-G p58	HLA-A*02:01	$HA_{304-313}$	SMPFHNIHPL	H5G-P7
HA H5-G p59	HLA-A*02:01	$HA_{428-436}$	KMEDGFLDV	H5G-P7
HA H5-G p60	HLA-A*02:01	$HA_{445-453}$	VLMENERTL	H5G-P7
HA H5-G p61	HLA-A*02:01	$HA_{541-549}$	SLALAIMMA	H5G-P7
HA H5-G p62	HLA-A*02:01	$HA_{543-551}$	ALAIMMAGL	H5G-P7
HA H5-G p63	HLA-DRB1*01:01	HA_{92-106}	WSYIVERANPANDLC	H5G-P8
HA H5-G p64	HLA-DRB1*01:01	$HA_{211-225}$	TTYISVGTSTLNQRL	H5G-P8
HA H5-G p65	HLA-DRB1*01:01	$HA_{261-275}$	GNFIAPEYAYKIVKK	H5G-P8
HA H5-G p66	HLA-DRB1*01:01	$HA_{303-317}$	SSMPFHNIHPLTIGE	H5G-P8
HA H5-G p67	HLA-DRB1*01:01	$HA_{324-338}$	SNKLVLATGLRNSPL	H5G-P8
HA H5-G p68	HLA-DRB1*01:01	$HA_{185-199}$	REDLLILWGIHHSNN	H5G-P9
HA H5-G p69	HLA-DRB1*01:01	$HA_{526-540}$	IGTYQILSIYSTAAS	H5G-P9

The VACV-specific peptide $A6(L)_{(6-14)}$ VLYDEFVTI by Thermo Fisher Scientific (Waltham, Massachusetts) served as control.

5. Proteins

Table 11: Recombinant HA proteins of the subtypes H1N1, H2N2 and H5N8 were used for cross-reactivity assays and are listed with catalogue numbers (Cat. No.).

Protein	Cat. No.	Company
recombinant IAV-H1	11684-V08H	Sino Biological (Beijing, China)
recombinant IAV-H2	40119-V08B	Sino Biological (Beijing, China)
recombinant IAV-H5	40932-V08B1	Sino Biological (Beijing, China)

VI. METHODS

1. Cell culture

1.1. Cultivation and passaging of cells

Primary chicken embryonic fibroblast (CEF) cells were prepared from 11-days old chicken embryos (SPF eggs, VALO, Cuxhaven, Germany) following established protocols (Kremer et al., 2012; Tscherne et al., 2025). In brief, SPF eggs were opened with scissors without damaging the embryo. Head, legs and organs were removed from the embryo and the torso was washed with DPBS. Homogenization was conducted by pressing the torso through a 24 ml syringe. The tissue was then trypsinized with 100 ml 0.25% Trypsin-EDTA under constant stirring at 37°C for 10 min. The cell suspension was filtered through gauze and centrifuged in 50 ml falcon tubes at 1,800 g and 4°C for 10 min. Subsequently, the supernatant was discarded and the pellet was resuspended in 10 ml cell culture medium, which was Minimum Essential Medium Eagle (MEM) containing 10% heat-inactivated FBS and 1% MEM non-essential amino acid solution. 80 ml of the mixture was filtered again and 1 ml of the mixture and 29 ml of cell culture medium were added to a T175 cell culture flask. After incubation for 24 h at 37°C and 5% CO_2, cell monolayers were confluent. For subculturing, cells were washed with in-house produced PBS and incubated with 0.25% Trypsin-EDTA solution for detachment. Cell suspension was subsequently added to fresh cell culture medium (1:1) to inactivate enzymatic activity of Trypsin. Finally, cell suspension was added in required volumes to cell culture medium and transferred to a cell culture flask or cell culture plates. For infection experiments, cell culture medium was supplemented with 2% heat-inactivated fetal bovine serum (FBS) and 1% MEM non-essential amino acid solution.

DF-1 cells (ATCC® CRL-12203™) were cultured in VP-SFM medium containing 2% heat-inactivated FBS and 2% L-glutamine. For subculturing, cells were washed with Dulbecco's Phosphate Buffered Saline (DPBS) and incubated with TrypLE™ Select for detachment. Cell suspension was subsequently added to fresh cell culture medium (1:1) to inactivate

enzymatic activity of Trypsin. Finally, cell suspension was added in required volumes to cell culture medium and transferred to a cell culture flask or cell culture plates. For infection experiments, cell culture medium was supplemented with 2% glutamine only.

Vero cells (ATCC CCL-81) and human HaCaT cells (CLS Cell Lines Service GmbH, Eppelheim, Germany) were cultured in Dulbecco's Modified Eagle's Medium (DMEM) with high glucose containing 10% heat-inactivated FBS and 1% MEM non-essential amino acid solution and 1% HEPES solution. Cells were cultured at 37°C and 5% CO_2. For subculturing, cells were washed with in-house produced PBS and incubated with 0.25% Trypsin-EDTA solution for detachment. Cell suspension was subsequently added to fresh cell culture medium (1:1) to inactivate enzymatic activity of Trypsin. Finally, cell suspension was added in required volumes to cell culture medium and transferred to a cell culture flask or cell culture plates. For infection experiments, cell culture medium was supplemented with 2% heat-inactivated FBS, 1% MEM non-essential amino acid solution and 1% HEPES solution.

1.2. Freezing and thawing of cells

Cells were subcultured in T175 cell culture flasks before freezing. One flask of confluent cells was sufficient for 2 cryovials. Cells were trypsinized and centrifuged at 1,500 rpm for 5 min. Afterwards, the cell pellet was resuspended in freezing medium. Cell suspensions were distributed to pre-chilled cryovials at a volume of 1 ml each. The vials were then immediately frozen at -80°C in a freezing container before they were transferred to the liquid nitrogen tank the next day. A single vial was thawed to check for viability.

For thawing, cells were taken from the liquid nitrogen tank and thawed by putting the vial in a warm water bath immediately. Cells were slowly added to a 50 ml falcon tube pre-filled with 10 ml medium. Centrifugation followed at 1,000 rpm for 5 min. In the next step, the supernatant was discarded, and the cell pellet was resuspended in 20 ml cell culture medium. Finally, cell suspension was transferred to a T75 cell culture flask for culturing at 37°C and 5% CO_2.

2. Generation of recombinant MVA-IAV-HA vaccines

2.1. Construction of plasmids

Encoding sequences of full-length hemagglutinin (HA) proteins from IAV subtypes H2N2 (A/Singapore/1/1957; Genbank accession No.: ACF54477.1), H2N9 (A/Ruddy/Turnstone/Dela-ware/374/2019; Genbank accession No.: QHC83179.1) and H5N8 (A/seal/Germany-SH/-AI05379/2021; Isolate-ID: EPI_ISL_4805936) were modified *in-silico* by removing runs of cytosine or guanine and signals for Vaccinia virus (VACV)-specific early transcription termination. Expression of recombinant IAV-HA proteins was placed under transcriptional control of the VACV-specific late promoter PsynII (Kubinski et al., 2023; Tscherne et al., 2025). cDNA was synthesized by gene synthesis and subsequently cloned into the MVA transfer plasmid pIIIsynIIred. Therefore, plasmids containing the synthesized HA sequences (pEX-K248-H2Ruddy, pEX-K248-H2Singapore and pEX-K248-H5Germany) and the above-described shuttle plasmids were digested with restriction enzymes BamHI, NotI and XhoI, HindIII (H2N9) SalI, HindIII (H2N2) or BamHI, NotI (H5N8) at 37°C. Fragments were separated by electrophoresis on an agarose gel. The required sequences were cut under UV-light and subsequently extracted using the NucleoSpin Gel and PCR-Clean-up kit. Thereafter, ligation of the fragment with the vector followed in a ratio 3:1, while a vector alone, the fragment alone and water were used as controls. Ligase was added before incubation at 16°C overnight followed. MVA transfer plasmids pIIIsynIIred-IAV-A/Ruddy/Turnstone/Delaware/374/2019(H2N9) (pSynII-red-H2R), pIIIsynIIred-IAV-A/Singapore/1/1957(H2N2) (pSynIIred-H2S) and pIIIsynIIred-IAV-A/seal/Germany-SH/AI05379/2021(H5N8 (pSynIIred-H5G) were obtained.

For transformation, 10-beta competent *E. coli* (high efficiency) were thawed on ice before 1 µl of ligation reaction were added. After 30 min incubation on ice, heat shock transformation was carried out at 42°C for 50 sec. The mixture was shortly cooled on ice and subsequently, LB-medium was added. Incubation for 1 h at 37°C on a shaker followed. Subsequently, bacteria were centrifuged at 2,500 rpm for 5 min, the supernatant was discarded and the pellet was resuspended in 100 µl LB medium. Bacteria

were streaked on agar plates containing Ampicillin or Kanamycin and incubated overnight at 37°C.

LB-medium with Ampicillin or Kanamycin was added to tubes and bacterial colonies were picked with a pipet tip. The tip was then transferred to a tube with LB-medium plus Ampicillin or Kanamycin and tubes were put on a shaker at 37°C overnight. On the next day, resuspended bacteria were transferred to centrifuge tubes and plasmid DNA was extracted with the NucleoSpin® Plasmid Mini kit according to the manufacturer's manual. Restriction digestion followed to control expected plasmid sizes. Two positive picked colonies were chosen and amplified in Erlenmeyer flasks containing 120 ml LB-medium with Ampicillin or Kanamycin shaking overnight at 37°C. In the end, plasmid DNA was again extracted with the NucleoBond® Xtra Midi kit and underwent control digestion.

2.2. Generation of recombinant MVA-IAV-HA vaccines

Recombinant MVA vector viruses were generated following established protocols as published recently (Kremer et al., 2012; Tscherne et al., 2025). In brief, monolayers of 90% confluent CEF or DF-1 cells were grown in six-well tissue culture plates and infected with parental MVAp11GFP (Tscherne et al., 2024) and transfected with MVA transfer plasmids pSynIIred-H2R, pSynIIred-H2S or pSynIIred-H5G using X-tremeGENE HP DNA Transfection Reagent according to the manufacturer's manual. 48 hours post infection (hpi), cell cultures were collected and used to re-infect CEF or DF-1 cells to obtain recombinant MVA-IAV viruses. Viral suspensions were sonicated 3-times at 100% before further use.

Recombinant MVA-IAV-H2R (MVA-H2R), MVA-IAV-H2S (MVA-H2S) and MVA-IAV-H5G (MVA-H5G) were isolated via plaque isolation by screening for transient co-expression of the red fluorescent marker gene mCherry using 24-well cell culture plates. Upon loss of mCherry by intragenomic recombination, colorless plaques were incubated for 96 h until a cytopathic effect (CPE) was observed in cell culture. Subsequently, inoculum was used to infect monolayers of DF-1 cells grown in 6-well cell culture plates. Inoculum was collected 48 hpi to re-infect monolayers of DF-1 cells grown in a cell culture flask T25 with 48 h of incubation. Analogue procedure was

subsequently applied for formats of T75 and T175. Monolayers of DF-1 cells, grown in 20 T175 cell culture flasks, were inoculated with recombinant viruses and used to generate virus crude stock material by pooling the collected cell cultures and conducting ultracentrifugation for 3 h at 15,000 rpm and 4°C. The supernatant was discarded and pellets were resuspended in 10 mmol TRIS-buffered saline (pH 7.4). Viral titers were obtained by titration on CEF cells, followed by counting of plaque-forming units (PFU) (Tscherne et al., 2025).

To generate high titer vaccine preparations for *in vitro* characterization studies and *in vivo* immunizations studies in mice, recombinant MVA-IAV-HA vector viruses were amplified on monolayers of CEF or DF-1 cells grown in 40-50 T175 cell culture flasks. Pooled virus-cell suspensions were then sonicated 3-times (15 s at 25%) with centrifugation steps (2,000 rpm, 4 min, 4°C) in between. After each centrifugation step, the supernatant was collected and the sonication procedure was repeated after addition of TRIS-buffered saline (pH 7.4) to the pellet. After the last centrifugation, the supernatant was collected, and the pellet was discarded. The pooled viral suspensions were slowly added to centrifugation beakers pre-filled with 36% sucrose. Ultracentrifugation at 15,000 rpm and 4°C for 2 h followed. Afterwards, the supernatant was discarded, and pellet was resuspended in TRIS-buffered saline. Viral titers were obtained by titration on CEF, followed by counting plaque-forming units (PFU) (Tscherne et al., 2025).

2.3. Determination of plaque-forming units

For determination of plaque-forming units, CEF cells were grown in 6-well tissue culture plates. Virus stock was serially diluted in 10-fold dilution steps. Dilutions were then added to the wells in three biological replicates with each two technical replicates. After 2 h incubation at 37°C, inoculum was replaced with fresh medium. Incubation followed at 37°C for 48 h. Next, medium was discarded and cells were fixed with ice-cold Acetone/Methanol (1:1) for 5 min at room temperature. After removal of the fixative, plates were let dried. Subsequently, cells were blocked with PBS/3% FBS for 1 h at room temperature or at 4°C overnight. Anti-Vaccinia antibody (1:2000) diluted in PBS/3% FBS was used as primary antibody. Plates were incubated for 1 h, gently rocking. Cells were then washed three times with

PBS, before peroxidase-conjugated goat anti-rabbit IgG (0.16 µg/ml) was added as secondary antibody. After 1 h incubation, cells were washed twice with PBS. At last, KPL TrueBlue™ Peroxidase Substrate was added to stain for plaque-forming units. Plaque-forming units were counted for each serial dilution and the mean of the replicates was determined. Each dilution step corresponds to a decimal power of the virus titer.

3. *In vitro* characterization of recombinant MVA-IAV-HA vaccines

3.1. Polymerase chain reaction (PCR)

For DNA extraction, a commercially available NucleoSpin® Blood QuickPure kit was used following the manuals instructions. Genetic identity and stability of the MVA-IAV-HA candidate vaccines were examined by polymerase chain reaction (PCR) of extracted viral DNA using Taq DNA Polymerase following the manufacturer's instructions. The used oligonucleotide sequences for PCR are listed in **Table 2**. A 1% agarose gel was prepared by dissolving agarose in 1x TAE electrophoresis buffer. One kb DNA ladder served as reference and samples were supplemented with purple loading dye prior to loading 3 µl on the gel. Electrophoresis was performed at 50 V for ~ 1 h and gels were subsequently analyzed with the ChemiDoc™ MP Imaging System.

3.2. Low multiplicity of infection (MOI) passage

Genetic stability of recombinant MVA-IAV-HA vaccines was examined by passaging the viruses on DF-1 cells at low MOI (multiplicity of infection). Therefore, monolayers of cells grown in 6-well cell culture plates were inoculated with the recombinant MVA candidate vaccines at MOI of 0.05 in triplicates. Incubation for 48 h at 37°C followed. All replicates were collected and serial diluted in 10-fold dilution steps to a final dilution of 1:1000 for reinoculation of fresh seeded DF-1 cells. Analogue procedure followed to a total of five passages. Finally, triplicates from passage 1 and 5 were analyzed by PCR targeting all six major deletion sites to confirm genetic stability.

3.3. Immunofluorescence staining of recombinant proteins

Vero cells grown in 6-well tissue culture plates on cover slips were infected at MOI of 0.5 with recombinant MVA-H2R, MVA-H2S and MVA-H5G. Incubation at 37°C for 16-24 h followed. Then, cells were fixed for 10 min with 4% paraformaldehyde on ice and permeabilization was conducted with 0.5% Triton X-100 dissolved in PBS. After an additional washing step with PBS, cells were blocked 30 min with 0.5% bovine serum albumin (BSA) dissolved in PBS. Subsequently, cells were incubated with primary antibodies directed against IAV-H2 (1:2000) or IAV-H5 (1 µg/ml) for 1 h at room temperature. After three washing steps with PBS, cells were incubated with a polyclonal goat anti-rabbit antibody conjugated with Alexa 488 (2 µg/ml). Cells were washed twice with PBS. 4′,6-Diamidin-2-phenylindol (DAPI) solution was used to stain cell nuclei. Cover slips were transferred to an object slide and mounted with fluorescence mounting medium. Imaging was performed with the fluorescence microscope BZ-X700 in 100x magnification.

3.4. Western blot (WB) analysis

Unimpaired IAV-HA expression was tested by infecting Vero cells, grown in 6-well tissue culture plates, at MOI of 5 with recombinant MVA-H2S, MVA-H2R and MVA-H5G. At 0, 4, 8, 24 and 48 hpi, cell cultures were harvested and centrifuged for 1 min at 13,000 rpm and 4°C. The supernatants were discarded and cell pellets were washed with ice-cold PBS. Lysates were prepared by resuspending the pellets in 80 µl lysis buffer. After 30 min incubation on ice, centrifugation for 10 min at 13,000 rpm and 4°C followed. The supernatants, containing the extracted proteins, were stored at -80°C until further use.

Furthermore, Peptide-*N*-Glycosidase F (PNGase F) was used for deglycosylation of expressed IAV-HA proteins. Deglycosylation was performed according to the manufacturer´s manual. To confirm unimpaired protein expression over time, protein concentration was determined with the Pierce™ Coomassie (Bradford) Protein-Assay-Kit following the manufacturer's instructions. Protein separation was conducted by sodium dodecyl sulfate polyacrylamide gel electrophoresis (SDS-PAGE) with a 4-20% gel. Transfer to a nitrocellulose membrane followed by electroblotting

using an in-house transfer buffer. Electroblotting was performed at 100 V for 1 h. Subsequently, membranes were blocked in blocking buffer for 1 h at room temperature. Membranes were incubated over night at 4°C with primary antibodies (diluted in blocking buffer), targeting recombinant IAV-H2 or IAV-H5 diluted 1:2000 in 5% milk/PBS. Subsequently, blots were washed three times with PBS/0.05% Tween-20 before incubation with a secondary goat anti-rabbit horse radish peroxidase (HRP)-conjugated IgG antibody, or goat anti-mouse HRP-conjugated IgG antibody diluted 1:5000 or 1:2000, respectively, in 5% milk/PBS followed for 1 h at room temperature. Afterwards, membranes were washed three times with PBS/0.05% Tween-20 and developed with SuperSignal® West Dura Extended Duration substrate. Finally, chemiluminescence was captured with the ChemiDoc™ MP Imaging System.

3.5. Multiple step growth curve

Replicative capacity of recombinant MVA-IAV-HA viruses was analyzed in multiple-step-growth experiments by inoculation of DF-1 or HaCaT cells grown in 6-well tissue culture plates. Therefore, cell lines were infected at MOI of 0.05 and cell suspensions were collected 0, 4, 8, 24, 48, and 72 hpi. Infectivity in the collected cell cultures was determined by counting plaque-forming units (Tscherne et al., 2025). Anti-Vaccinia specific antibody (1:2000) was used as a primary antibody, while peroxidase-conjugated goat anti-rabbit IgG (0.16 µg/ml) was used as a secondary antibody. Subsequently, cells were washed three times with PBS and stained for plaques with KPL TrueBlue™ Peroxidase Substrate. Plaque-forming units were counted analogue to section 2.3. (Determination of plaque-forming units).

4. *In vivo* characterization of recombinant MVA-IAV-HA vaccines

4.1. Vaccination experiments in mice

Specific pathogen free 6 to 10- week-old *HLA-A2.1-/HLA-DR1-transgenic H-2 class I-/class II-knockout* mice (in-house bred) (Pajot et al., 2004) were kept in isolated cage units (IVCs) with free access to water and food. All

animal experiments were conducted in alignment with the European and national regulations for animal experimentation and Animal Welfare Act (European Directive 2010/63/EU; Animal Welfare Acts in Germany), approved by the government of Upper Bavaria (Munich, Germany; ROB-55.2-2532.Vet.02-22-80). Mice were immunized twice over a 21-day interval with 10^7 PFU of recombinant MVA-H2S, MVA-H2R, MVA-H5G or non-recombinant MVA (MVA), respectively, using the IM route. Blood samples were collected on days 18 and 35 post prime immunization and coagulated blood was centrifuged at 2,000 rpm for 20 min to separate the serum. Serum samples were stored at -80°C for further use.

4.2. Peptide design, prediction and generation

HA protein sequences of A/Singapore/1/1957 (H2N2) (GenBank ID: ACF54477.1), A/Ruddy/Turnstone/Delaware/374/2019 (H2N9) (GenBank ID: QHC83179.1) and A/seal/Germany-SH/AI05379/2021(H5N8) (GISAID ID: EPI_ISL_4805936) were obtained and potential immunogenic peptides were predicted using two strategies. For the first strategy, sets of 15mer peptides with 11mer overlap were designed from each of the above-mentioned sequences. They were then analyzed *in silico* to determine if they contained T cell epitopes specific to the MHC class I allele HLA-A*02:01 and the MHC class II allele HLA-DRB1*01:01. For the MHC class I prediction, the Immune Epitope Database (IEDB) tool “T Cell Prediction – Class I” was used, using the MHC-I binding and MHC-I processing methods (Dhanda et al., 2019; Reynisson et al., 2020; Yan et al., 2024) and a peptide length of 9-mer. Next, the results were screened for peptides with a maximum percentile rank of 5 and a maximum IC_{50} of 1000 nM. The 15-mer peptides that contained the top 9-mer peptides were then identified (see **Table 5, 6** and **8**). For the MHC class II prediction, the IEDB prediction tool “MHC-II Binding” was used, using the methods NetMHCIIpan 4.1 EL and NetMHCIIpan 4.1 BA (Nilsson et al., 2023; Reynisson et al., 2020; Dönnes & Kohlbacher, 2005) and a peptide length of 15-mer. The results were then screened for peptides with a maximum percentile rank of 15 and a maximum IC_{50} of 1000 nM. The most immunogenic 15-mer peptides were selected. Finally, the top overlapping peptides of the HA proteins of A/Singapore/1/1957 (H2N2) and A/Ruddy/Turnstone/Dela-ware/374/2019

(H2N9) were compared to identify those that were shared between the sequences (see **Table 7**).

For the second strategy, the entire sequence of the above-mentioned HA proteins was analyzed *in silico* for HLA-A*02:01- and HLA-DRB1*01:01-specific peptides. For the MHC class I prediction, the IEDB tool “T Cell Prediction – Class I” was used, using the same methods described above and peptide lengths of 8 to 11-mer (see **Table 9-10**). Next, results were screened for peptides with a maximum percentile rank of 5 and a maximum IC_{50} of 1000 nM. From this list, the top 10 peptides were selected. For the MHC class II prediction, IEBD prediction tool “MHC-II Binding” was used as described above. The results were then screened for peptides with a maximum percentile rank of 15 and a maximum IC_{50} of 1000 nM. The top 4-7 peptides were selected. All peptides were synthesized by Thermo Fisher Scientific on a 1 mg scale with more than 50% purity. Subsequently, peptides were dissolved in either PBS or DMSO to a concentration of 2 mg/ml and stored in aliquots at -20 °C.

4.3. Preparation of splenocytes

Whole spleens were isolated from euthanized mice and pressed through a 70 µm strainer with the plunger of a syringe and cells were collected in 5 ml RPMI medium. Then, the strainer was rinsed with 5 ml RPMI-10. After centrifugation at 2,000 rpm for 5 min, supernatant was discarded and 5 ml Red Blood Cell Lysis Buffer was added to lyse red blood cells. After 5 min, the reaction was stopped with 5 ml RPMI. Centrifugation at 2,000 rpm for 5 min followed. The supernatants were discarded and the white-brownish cell pellet was resuspended in 10 ml RPMI. Centrifugation at 2,000 rpm for 5 min was conducted. The supernatants were discarded and the pellets were resuspended in 5 ml RPMI. Cells were counted for further use.

4.4. T cell analysis by enzyme linked immuno spot assay (ELISpot)

ELISpot assay was performed to measure IFN-γ-producing T cells in spleens of vaccinated mice. At day 35 post prime vaccination, mice were euthanized and splenocytes were isolated as described above. Subsequently, ELISPOT assay was conducted using the ELISpot Plus Mouse IFN-γ (ALP) kit following the manufacturer´s instructions. $2x10^5$

splenocytes in 100 µl RPMI-10 were transferred into 96-well plates for stimulation with either individual peptides (2 µg/ml in RPMI-10) or pools of predicted (2 µg/ml per peptide in RPMI-10) or overlapping peptides (2 µg/ml per peptide in RPMI-10) (see **Table 5-10**). Non-stimulated cells, cells stimulated with phorbol myristate acetate (PMA) / ionomycin or with VACV-specific peptide VLYDEFVTI A6(L)$_{(6-14)}$ served as controls. Cells were incubated for 48 h at 37°C and plates were stained according to the manufacturer´s manual. Subsequently, single spots were counted using the automated ELISpot plate reader Bioreader® 7000 V.

4.5. T cell analysis by intracellular cytokine staining (ICS)

Intracellular cytokine staining was performed with isolated splenocytes from immunized mice as described in previous studies (Kalodimou et al., 2019; Tscherne et al., 2021). In brief, 1x10^6 cells were plated into 96-well round bottom plates and restimulated with either individual peptides (8 µg/ml) or peptide pools (8 µg/ml per peptide) (see **Table 9-10**) diluted in RPMI-10. Cells stimulated with the VACV-specific peptide VLYDEFVTI A6(L)$_{(6-14)}$ or PMA/Ionomycin, and non-stimulated cells served as controls. Cells were stimulated for 2 h at 37°C, before the Golgi blocking agent Brefeldin A was added. Then, cells were stimulated for another 4 h at 37°C and subsequently stained extracellularly with anti-mouse CD3 phycoerythrin (PE)/Cy7 (2 µg/ml), anti-mouse CD4 Brillant Violet 421 (1:600), anti-mouse CD8α Alexa Fluor 488 (1.25 µg/ml), purified anti-mouse CD16/CD32 (1 µg/ml) and Zombie aqua (1:1000). Afterwards, cells were fixed, permeabilized and stained intracellularly with anti-mouse IFN-γ allophycocyanin (APC) (0.67 µg/ml) and anti-mouse TNF-α PE (0.67 µg/ml). Data was acquired by using a flow cytometer and analyzed with the FlowJo software (version 10.10.0) by FlowJo LLC (Ashland, Oregon).

4.6. Antigen-specific enzyme-linked immunosorbent assay (ELISA)

IAV-HA specific IgG binding antibodies in the serum of prime-boost immunized mice were determined by ELISA. 96-well flat bottom ELISA plates were coated with 50 ng/well of recombinant IAV-H2 or IAV-H5 and incubated at 4°C overnight. On the next day, plates were blocked with

blocking buffer for 1 h at 37°C. In the next step, mouse sera were threefold serial diluted in dilution buffer, starting at a 1:100 dilution, and subsequently transferred to ELISA plates. After incubation for 1 h at 37°C, plates were washed three times with PBS supplemented with 0.05% Tween-20 and subsequently incubated with a HRP conjugated goat anti-mouse IgG (H+L) secondary antibody (0.5 µg/ml) diluted in dilution buffer for 1 h at 37°C. 3′3′,5′5′-Tetramethylbenzidine (TMB) Liquid Substrate System for ELISA was added and the reaction was stopped after 5 min by adding Stop Reagent for TMB Substrate. Finally, the absorbance was measured at 450 nm with a 620 nm reference wavelength using the Spark® plate reader. The cut off value was calculated by the mean 450 nm value of the MVA control group at a dilution of 1:100 plus 6 standard deviations (mean + 6 SD).

4.7. Statistical analysis

Statistical analysis was performed using Prism 5 (version 5.04) by GraphPad Software Inc. (La Jolla, California). Unpaired two-tailed t-test was used for the ELISpot and ICS data. Optical density (OD) values of ELISA data were calculated as geometric means and Log_2 transformed before one-way ANOVA Tukey test was pursued.

.

VII. RESULTS

1. Generation of recombinant MVA-IAV-HA candidate vaccines

The encoding HA sequences from IAV subtypes A/Ruddy/Turnstone/Delaware/374/2019(H2N9), A/Singapore/1/1957 (H2N2) and A/seal/Germany-SH/AI05379/2021(H5N8) were used to construct the recombinant MVA-IAV-HA candidate vaccines MVA-IAV-H2R (MVA-H2R), MVA-IAV-H2S (MVA-H2S) and MVA-IAV-H5G (MVA-H5G), respectively. Codon-optimization of the sequences was done, including the removal of G/C runs and TTTTTNT regions on the genomic level. Furthermore, enzyme restrictions sites for enzymes NotI/BamHI and XhoI/HindIII (H2N9) SalI/HindIII (H2N2) or NotI/BamHI (H5N8) were added at the 5´ and 3´end of the sequences, respectively, for cloning into the MVA vector plasmid pIIIsynIIred. The cDNAs were placed under the transcriptional control of the Vaccinia virus-specific late PSynII promoter. The new generated plasmids, pSynIIred-H2R, pSynIIred-H2S and pSynIIred-H5G contain a resistance gene (AmpR), flank regions (flank-1 and flank-2) of MVA genomic DNA and the reporter gene mCherry (see **Figure 9**). Correct insertion of the HA sequences was confirmed by enzyme restriction digestions.

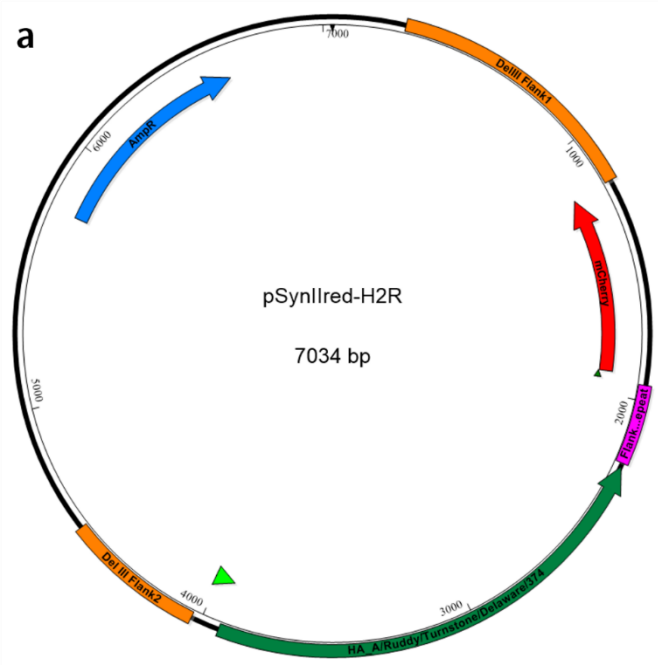

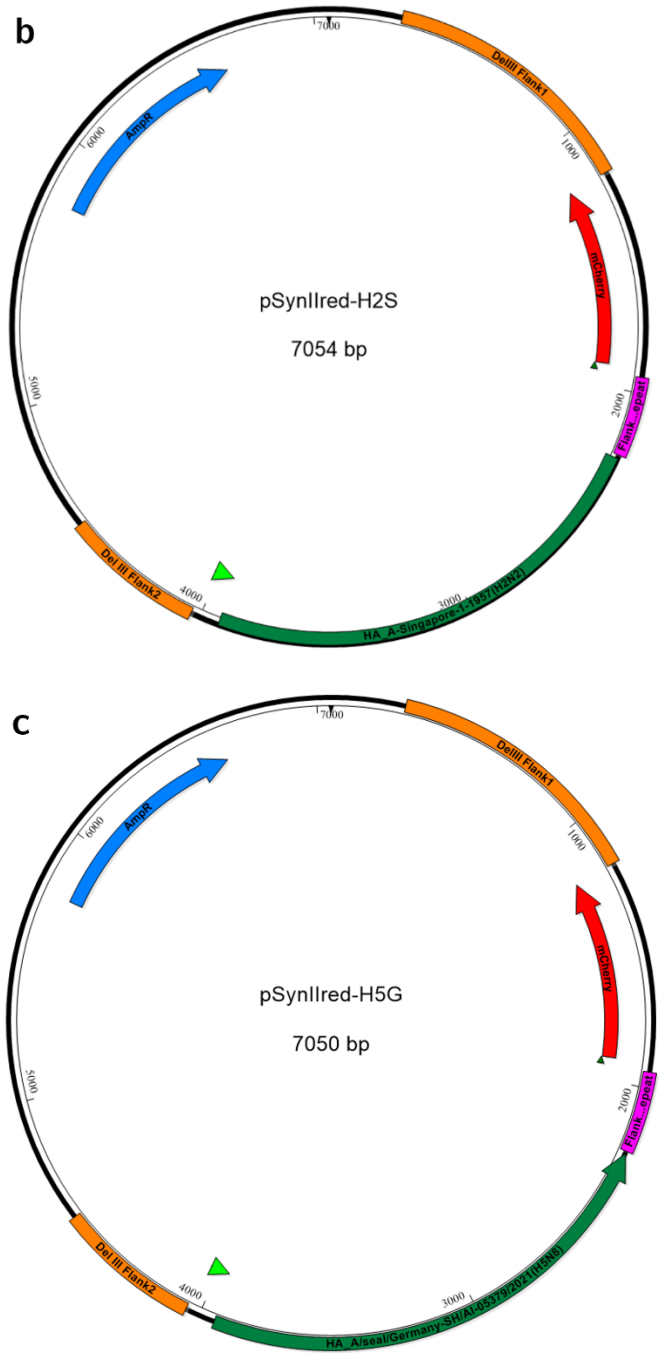

Figure 9: Plasmid map of MVA transfer plasmids pSynIIred-H2R **(a)**, pSynIIred-H2S **(b)**, and pSynIIred-H5G **(c)**. The marker gene mCherry is depicted as red arrow and is under transcriptional control of the p11 promoter. The AmpR resistance gene (AmpR) is depicted in blue. The corresponding HA sequences are flanked by deletion site III (Del-III)-specific repeats for homologous recombination (depicted in orange) and are placed under the transcriptional control of PsynII promoter (small arrow depicted in light green). An additional flanking region (pink) allows for removal of mCherry by intragenomic recombination.

Subsequent infection of DF-1 cells with MVA-p11GFP, followed by transfection with either pSynIIred-H2R, pSynIIred-H2S or pSynIIred-H5G yielded in recombinant MVA-H2R, MVA-H2S and MVA-H5G, respectively.

The HA sequences were inserted into the MVA genome of non-recombinant MVA by homologous recombination, based on homologous flanking regions in both the plasmids and non-recombinant MVA (see **Figure 10**). The red marker gene mCherry was used to identify recombinant viruses and allowed discrimination from non-recombinant MVA-p11GFP, which expressed the green fluorescent protein (GFP) as marker. After several passages on DF-1 cells, mCherry was removed from the MVA genomes by intragenomic recombination, enabled by repeats of the flanking region. Recombinant MVA-IAV-HA candidate vaccines were amplified to high-titer virus stocks for *in vitro* and *in vivo* characterization.

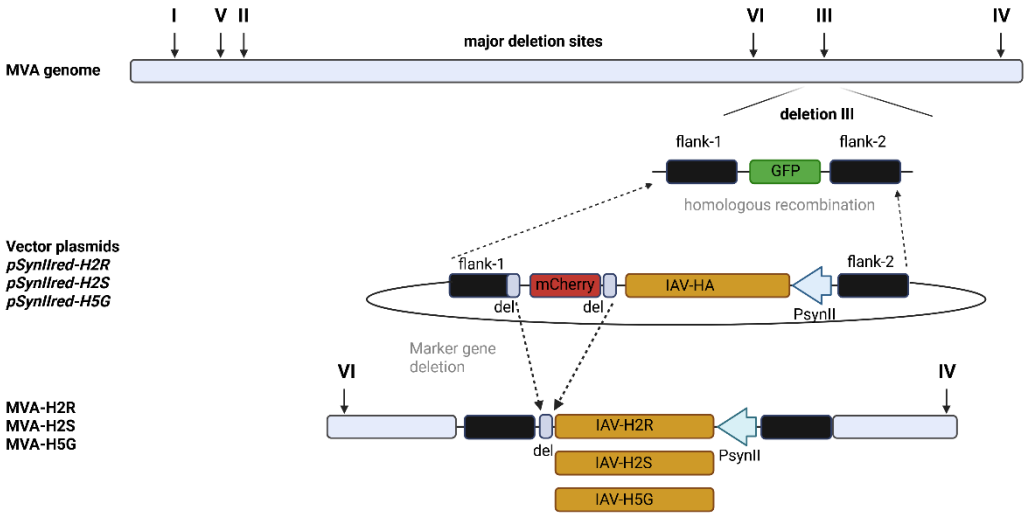

Figure 10: Construction of recombinant MVA-IAV-HA viruses. Schematic diagram of the MVA genome with the major deletion site I to VI. The coding sequence of IAV-HA (subtypes H2N2, H2N9 or H5N8) were inserted into deletion III by homologous recombination, under transcriptional control of the VACV-specific late PsynII promoter. Repetitive sequences were designed to remove the marker gene mCherry during plaque purification by intragenomic recombination. Created with BioRender.com

2. *In vitro* characterization of recombinant MVA viruses delivering IAV-HA antigens

2.1. Genetic characterization and stability of recombinant MVA-IAV-HA

PCR analysis of isolated viral DNA was conducted using oligonucleotide primers targeting deletion site III within the MVA genome (see **Figure 11**, **Table 2**) to confirm genetic stability and integrity of the newly generated

MVA-IAV-HA candidate vaccines. Correct insertion of the target HA antigens was confirmed by detecting one prominent band of about 2.8 kb (**Figure 11 a-c**; first lanes). In addition, correct removal of the marker gene mCherry during plaque passages and virus amplification was confirmed by comparing amplicon sizes obtained for the MVA transfer plasmids pSynII-IAV-HA (pSynIIred-H2R, pSynIIred-H2S, pSynIIred-H5G) (**Figure 11 a-c**; second lanes) and the recombinant MVA-IAV-HA constructs. In the transfer plasmids the mCherry marker gene is still present, resulting in an amplified size of ~3.5 kb compared to the ~2.8 kb obtained for the MVA-IAV-HA constructs (MVA-H2R, MVA-H2S, MVA-H5G). Furthermore, the absence of non-recombinant MVA in the MVA-IAV-HA vaccines was confirmed by the absence of the empty MVA backbone specific 0.762 kb PCR product (**Figure 11 a-c**; lanes 1 vs 3).

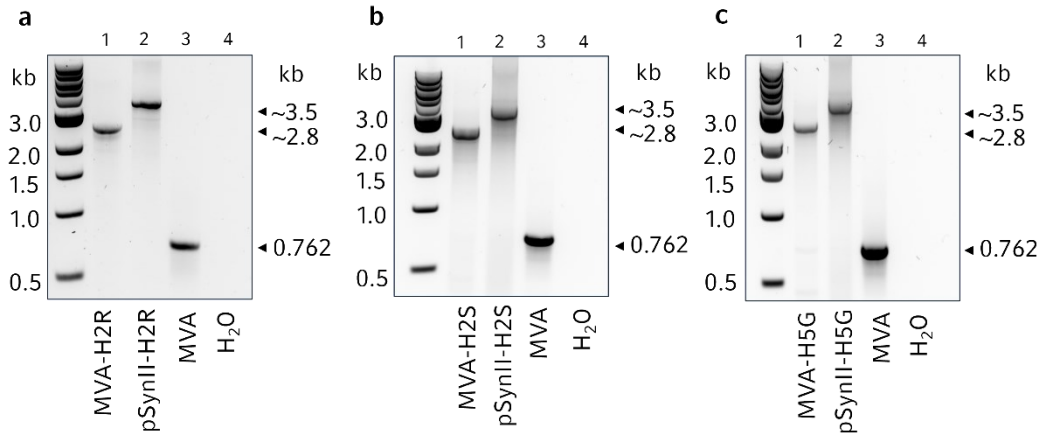

Figure 11: Genetic integrity of recombinant MVA-H2R **(a)**, MVA-H2S **(b)** and MVA-H5G **(c)**. Genomic viral DNA was analyzed by PCR using oligonucleotide primers specific for deletion site III of MVA. A 1 kb DNA ladder served as size reference.

Genetic stability of the MVA backbone genome was confirmed by performing a PCR with oligonucleotide sequences targeting all six major deletion sites (see **Figure 12**, **Table 2**). Primer pairs were designed to bind to regions within deletion sites I to VI, yielding a ladder pattern specific for MVA (**Figure 12 a-c**; lanes 1, 2, 4 – 6). Specifically, PCR products migrated with sizes of 0.291 kb for Del-I, ~ 0.354 kb for Del-II, ~ 0.447 kb for Del-IV, ~ 0.502 kb for Del-V, ~ 0.702 kb for Del-VI. PCR products which migrated at sizes ~ 2.5 kb were observed for deletion III (**Figure 12 a-c**; lanes 3), suggesting incorporation of the HA target sequences into the MVA genome.

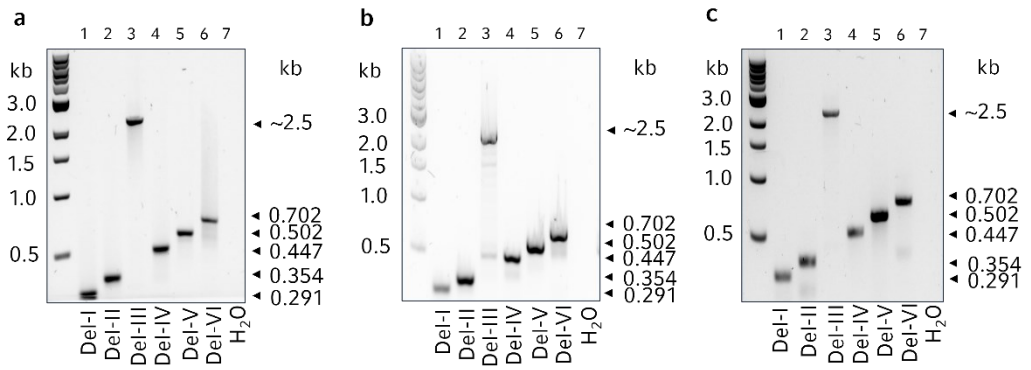

Figure 12: Genetic integrity of the six major deletions sites of recombinant MVA-H2R **(a)**, MVA-H2S **(b)** and MVA-H5G **(c)**. Primer pairs targeted specific regions within deletion sites I-VI. A 1 kb DNA ladder serves as size reference. An MVA-specific ladder pattern was observed except for deletion III, where the corresponding HA sequence was incorporated.

Identity of the inserted HA sequences was evaluated by PCR with designed primer pairs, which bound to a specific part of the HA inserts (see **Figure 13**, **Table 2**). A specific band at 1.029 kb for MVA-H2R, 1.076 kb for MVA-H2S and 0.421 kb for MVA-H5G (**Figure 13 a-c**; lane 1) was observed. The same sizes of amplicons were detected for the corresponding MVA transfer plasmids pSynII-H2R, pSynII-H2S and pSynII-H5G. While PCR analysis with Del-III specific primer pairs detected only the presence of a foreign sequence, the here shown results confirm integration of the HA sequences specific for each subtype into the MVA genome. No band was detected for non-recombinant MVA (**Figure 13 a-c**; lane 3).

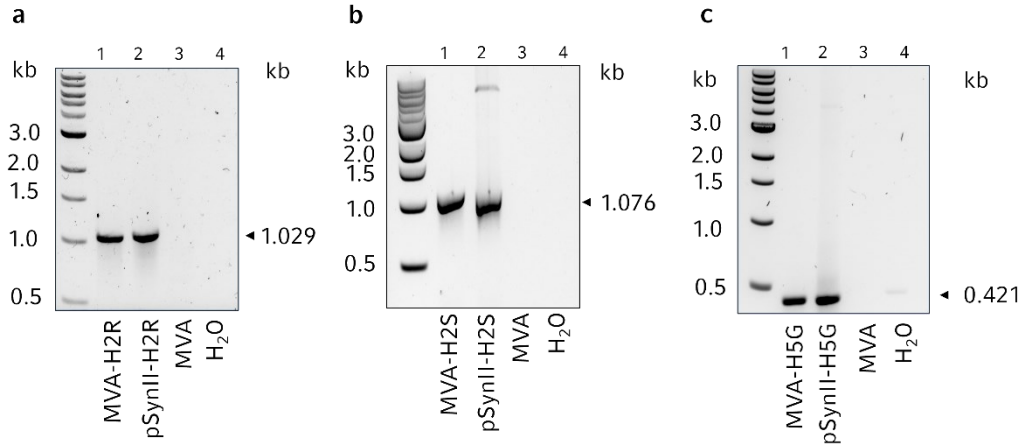

Figure 13: PCR analysis confirming identity of inserted target genes. A 1 kb DNA ladder served as size reference. Expected sizes (indicated with an arrow) according to the plasmid maps were observed for the corresponding recombinant candidate vaccines MVA-H2R **(a)**, MVA-H2S **(b)**, MVA-H5G **(c)**.

The presence of the *C7L* gene, which is required for unimpaired late viral gene expression (Backes et al., 2010), was examined using PCR analysis with primer pairs targeting the *C7L* gene locus (see **Figure 14**, **Table 2**). A band with ~ 0.447 kb in size was observed for all candidate vaccines (**Figure 14 a-c**; lanes 1), which matched the size of the amplified region for non-recombinant MVA (**Figure 14 a-c**; lane 2), thus, confirming stability of the C7L gene during plaque purification and virus amplification.

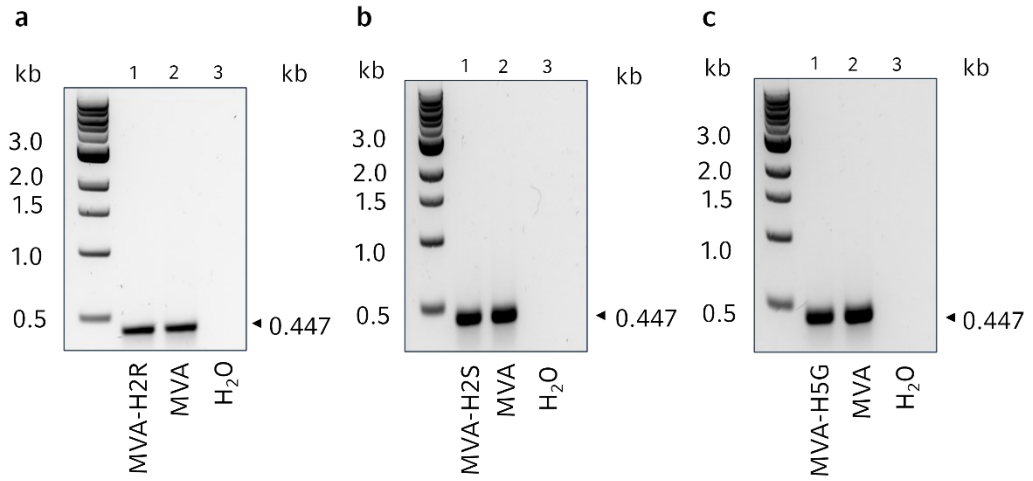

Figure 14: Genetic stability of the *C7L* gene was confirmed with specific oligonucleotide sequences targeting the *C7L* gene locus. A 1 kb DNA ladder served as size reference. The VACV-specific gene was detected for the candidate vaccines MVA-H2R **(a)**, MVA-H2S **(b)**, MVA-H5G **(c)**, confirming stability of the *C7L* gene locus.

Maintained genetic stability of the inserted sequences and identity of the MVA backbone was examined by a PCR targeting the six major deletion sites (see **Table 2**) after five passages of the recombinant MVA-IAV-HA viruses on DF-1 cells at a low MOI (see **Figure 15**). Low MOI allowed for extensive replication during the passages. Cell cultures were collected after passages 1 and 5 and PCR of isolated DNA was conducted, using the same primer pairs as described before. An MVA-specific ladder pattern (**Figure 15 a-f**; lanes 1, 2, 4 – 6) and a band with 2.5 kb in size (**Figure 15 a-f**; lane 3) was detected for both passages 1 (**Figure 15 a–c**) and 5 (see **Figure 15 d–f**) for MVA-H2R (**Figure 15 a, d**), MVA-H2S (**Figure 15 b, e**) and MVA-H5G (**Figure 15 c, f**). This confirmed stability of the incorporated sequences and the MVA backbone even after five passages at a low MOI, which is relevant for production of recombinant MVA-IAV-HA viruses at industrial scale.

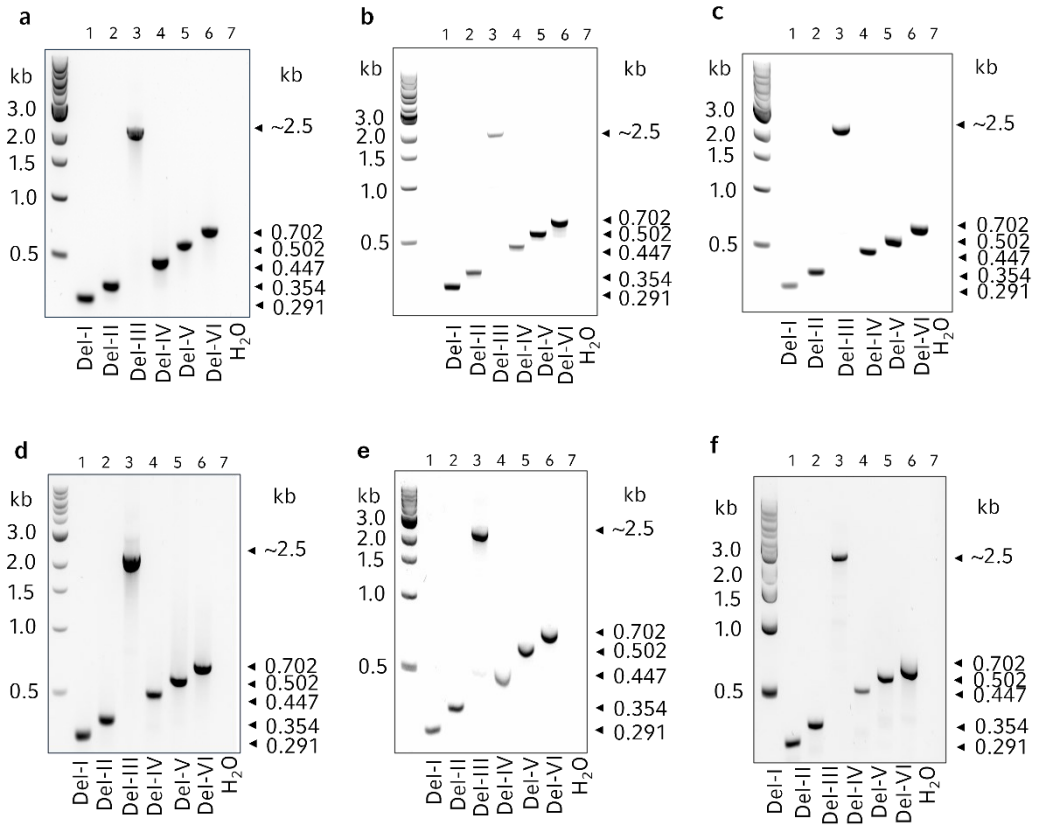

Figure 15: Genetic stability of MVA-H2R **(a, d)**, MVA-H2S **(b, e)** and MVA-H5G **(c, f)** candidate vaccines following serial passages at low MOI. DF-1 cells were inoculated at MOI of 0.05 and cell cultures were collected 48 hpi. Then, virus was used to re-infect DF-1 cells at MOI of 0.05 and the same procedure was repeated another 4 passages. PCR analysis with primers targeting all six major deletion sites of MVA was carried out from passages 1 **(a-c)** and 5 **(d-f)**. A 1 kb DNA ladder served as size reference. A band at ~2.5 kb in size was observed for deletion site III, which served as insertion site for the HA sequences. In addition, a characteristic ladder pattern was observed after passages 1 and 5 for deletion sites I, II, IV, V and VI with amplicon sizes of 0.291 kb, 0.354 kb, 0.447 kb, 0.502 kb and 0.702 kb, respectively.

2.2. Characterization of recombinant HA proteins

To examine the unimpaired expression of recombinant IAV-HA, staining of MVA-IAV-HA -infected Vero cells was performed with H2 or H5-subtype specific primary antibodies, and a secondary antibody conjugated with Alexa 488 (green fluorescent signal) (see **Figure 16**). Green foci were observed in cells infected with recombinant MVA-H2R (**Figure 16 a**; first row), MVA-H2S (**Figure 16 b**; first row) and MVA-H5G (**Figure 16 c**; first row) but no signal was detected in neither non-recombinant MVA infected (**Figure 16 a-c**; second row) nor uninfected cells (**Figure 16 a-c**; third row) (negative controls). Cell nuclei were counterstained with DAPI.

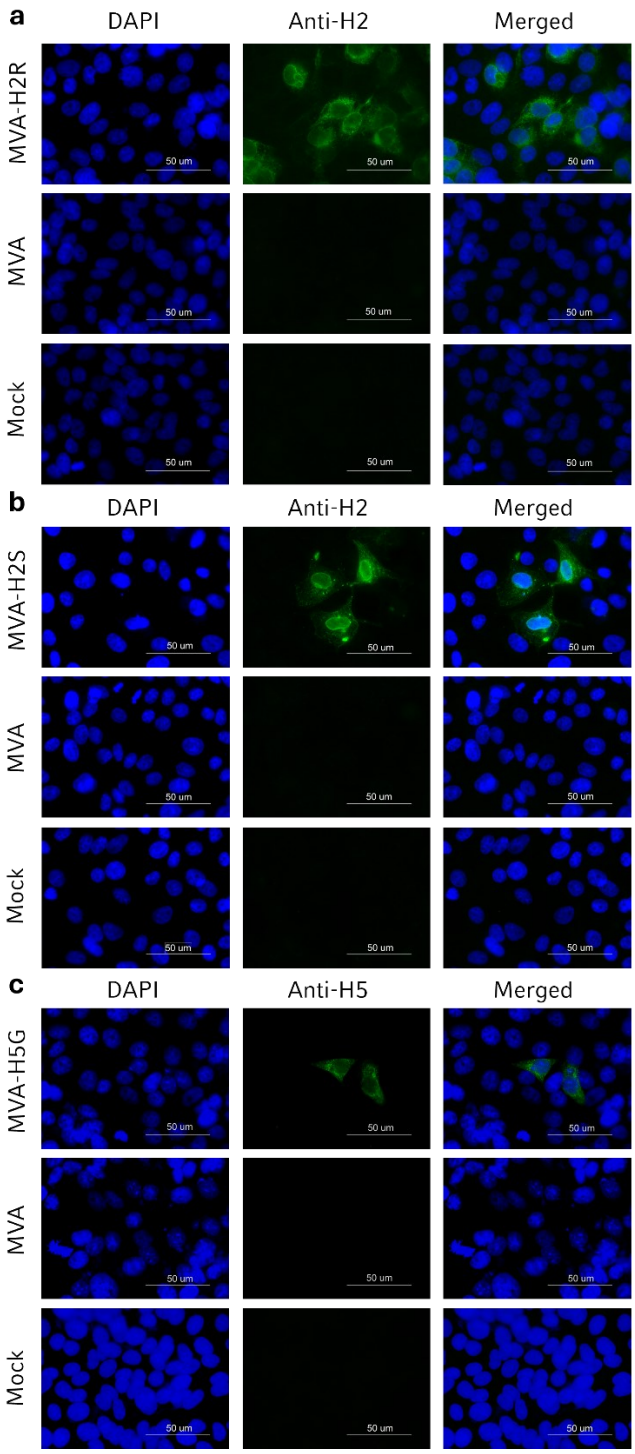

Figure 16: Detection of recombinant IAV-HA expressed by MVA-H2R **(a)**, MVA-H2S **(b)** and MVA-H5G **(c)** using immunofluorescence analysis. Vero cells were infected at MOI of 0.5 and incubated for 16-24 h. Permeabilized cells were stained with H2 or H5 subtype-specific antibodies and a secondary antibody which was conjugated with Alexa-Fluor 488. DAPI was used to counterstain cell nuclei. The Figure depicts green-fluorescent staining for the MVA-H2R, MVA-H2S and MVA-H5G candidate vaccine, but neither for MVA-infected (MVA) nor for uninfected cells (Mock).

Additionally, unimpaired expression of HA was detected by Western blot analysis. Lysates from MVA-H2R, MVA-H2S or MVA-H5G-infected Vero

cells were analyzed 24 hpi (see **Figure 17**). The highly glycosylated HA revealed one prominent band which migrated with a molecular mass of ~ 76 kDa (**Figure 17 a–c**; first lane).Treatment of the HA proteins with peptide-N-glycosidase F (PNGase F) revealed the deglycosylated form which migrated at ~63 kDa for IAV-H2R (**Figure 17 a**; second lane) and IAV-H2S (**Figure 17 b**; second lane) and ~64 kDa for IAV-H5G (**Figure 17 c**; second lane). No H2 or H5 specific staining was observed in MVA-infected and uninfected cells. In the next approach, MVA-IAV-HA infected cells were harvested at 0, 4, 8, 24, and 48 hpi (see **Figure 18**) and analyzed using Western blotting. As crude stock material was used for infection, protein was already detectable at 0 hpi, however, the amount of HA proteins increased over time in MVA-H2R, MVA-H2S and MVA-H5G infected cells.

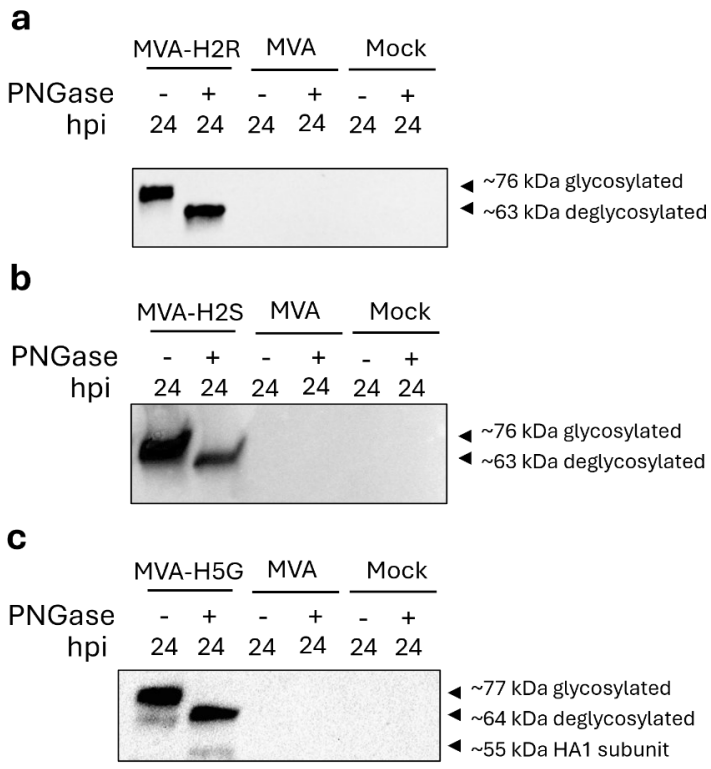

Figure 17: Detection of recombinant IAV-HA expressed by MVA-H2R **(a)**, MVA-H2S **(b)** and MVA-H5G **(c)** using Western blot analysis. Vero cells were infected at a MOI of 5 and cell cultures were collected at 24 hpi. Non-infected cells (Mock) and cells infected with non-recombinant MVA (MVA) served as controls. Furthermore, PNGase F was used for deglycosylation. Polypeptides in cell lysates were separated by SDS-PAGE and stained with H2 or H5 subtype- specific antibodies, revealing prominent bands that migrated with molecular masses of ~76 kDa (glycosylated) or ~63 and ~64 kDa (deglycosylated).

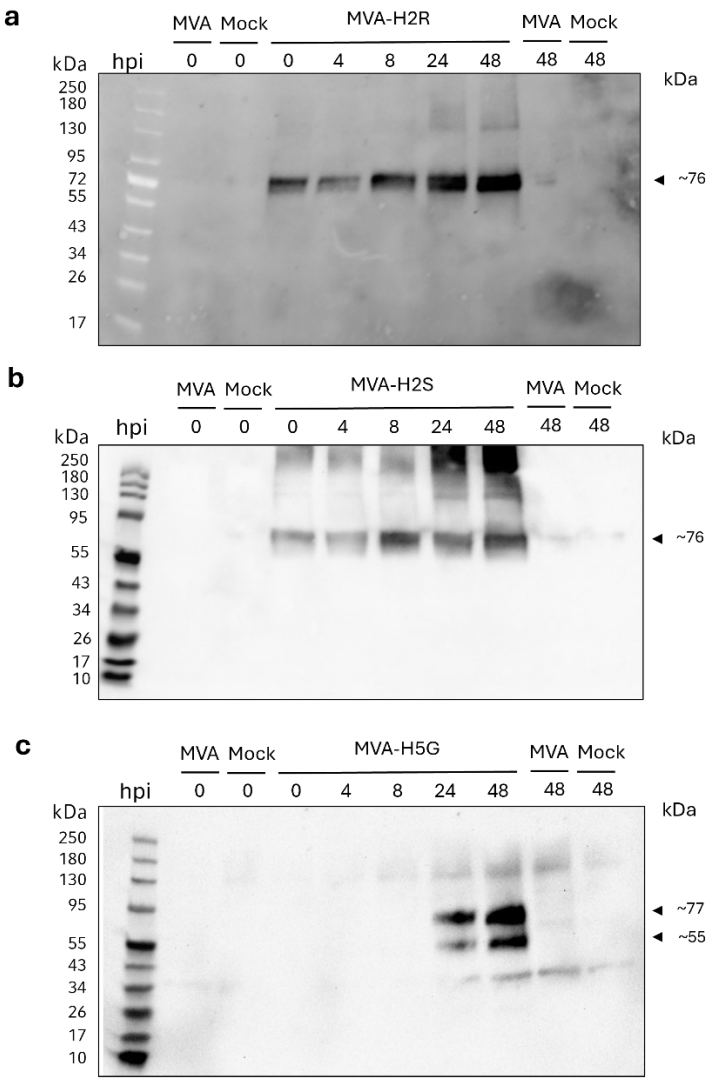

Figure 18: Protein expression over time was examined by Western blot analysis. Vero cells were infected at MOI of 5 with recombinant MVA-H2R **(a)**, MVA-H2S **(b)** or MVA-H5G **(c)** and cell cultures were collected at 0, 4, 8, 24 and 48 hpi. Non-infected cells (Mock) and cells infected with non-recombinant MVA (MVA) served as controls. Polypeptides in cell lysates were separated by SDS-PAGE and stained with H2 or H5 specific antibodies confirming increased protein expression over time. A protein standard for kDa served as size reference.

2.3. Replicative capacity of recombinant MVA-IAV-HA viruses

Importantly, MVA and MVA-based vaccines are attenuated to chicken cells and are not replicating in cells of human origin. To proof, whether the insertion of the HA gene sequences negatively impact the replicative deficiency on human cells, a multi-step growth curve analysis was performed on human HaCaT cells. Furthermore, to proof the suitability of the recombinant MVA-IAV-HA vaccines for clinical use, replicative capacity on DF-1 producer cells was evaluated in comparison to non-recombinant

MVA. DF-1 and HaCaT cell lines were infected with recombinant MVA or non-recombinant MVA and cell cultures were collected at 0, 4, 8, 24, 48 and 72 hpi (see **Figure 19**). Infectivity in the collected cell cultures were determined by counting plaque-forming units, which confirmed the replicative capacity of recombinant MVA-H2R (**Figure 19 a**), MVA-H2S (**Figure 19 b**) and MVA-H5G (**Figure 19 c**) in DF-1 cells and the replicative deficiency in human cells. Viral titers were comparable to non-recombinant MVA (black dashed lines) for both cell lines.

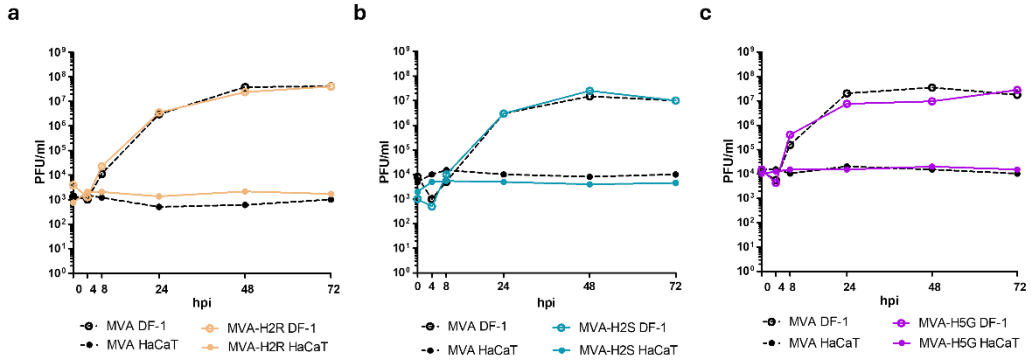

Figure 19: Multi-step growth curve analysis of MVA-H2R **(a,** beige**)**, MVA-H2S **(b**, cyan**)** and MVA-H5G **(c**, purple**)** relative to non-recombinant MVA (MVA, black) in DF-1 and HaCaT cells. Cells were infected at a MOI of 0.05 and cell cultures were collected at 0, 4, 8, 24, 48 and 72 hpi. Re-titration was done on CEF cells using an anti-VACV specific antibody for staining plaques. Plaque-forming units (PFU) per ml are plotted against indicated timepoints. All three experimental vaccines replicated efficiently in chicken DF-1 cell line but failed to replicate in the human HaCaT cell line.

3. Immunogenicity testing of the candidate vaccines MVA-H2R, MVA-H2S and MVA-H5G

3.1. Immunization schedule

In vitro quality control procedures verified identity, stability and replicative capacity of recombinant MVA-IAV-HA vaccines. Next, *in vivo* characterization was carried out in a mouse model to study the immune responses of the candidate vaccines. For immunogenicity testing of our candidate vaccines, *HLA-A2.1-/HLA-DR1-transgenic H-2 class I-/class II-knockout* mice, which possess HLA molecules of a human phenotype, were chosen to extrapolate results for future testing in humans. A prime-boost immunization scheme was chosen as depicted in **Figure 20** using 10^7 PFU

for MVA-H2R, MVA-H2S or MVA-H5G for both prime and booster immunization. The booster immunization was carried out 21 days after the prime immunization. Blood samples were taken on days 18 and 35, while spleens were isolated on day 35.

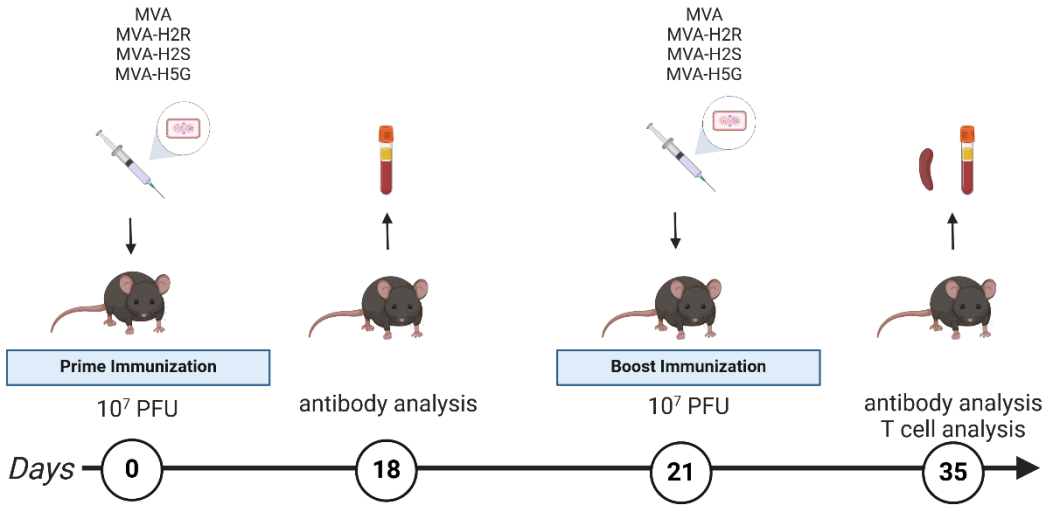

Figure 20: Prime-boost immunization scheme. Groups *of HLA-A2.1-/HLA-DR1-transgenic H-2 class I-/class II-knockout* mice (n=5-6) were IM immunized with 10^7 PFU of recombinant MVA-H2R, MVA-H2S, MVA-H5G or non-recombinant MVA (MVA) over a 21-day interval. Mice were euthanized on day 35 post prime immunization and splenocytes were isolated to assess IAV-HA specific cellular immune responses. Blood samples were taken on days 18 and 35 to assess IAV-HA specific binding antibody responses. Created with BioRender.com,

To explore safety and tolerability of the recombinant MVA-IAV-HA vaccines, immunized mice were monitored daily over the course of the experiment for body weight changes and signs of illnesses (see **Figure 21**). No abnormalities were observed, suggesting that all three candidate vaccines were well-tolerated. Additionally, mice were scored using predefined parameters for physical appearance, behavior and clinical evaluation to assess their well-being. No signs of side effects or disease were detected.

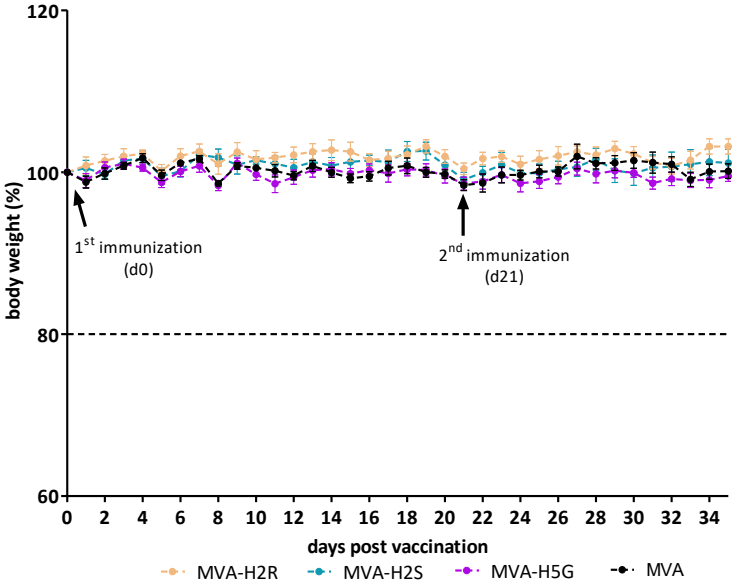

Figure 21: Representation of percentual daily body weight changes of mice after prime-boost vaccination with MVA-H2R (beige), MVA-H2S (cyan) and MVA–H5G (purple). Mice vaccinated with non-recombinant MVA (MVA, black) served as control. Body weights were measured daily as represented by each datapoint. The dashed line at 80% body weight change represents the maximum tolerated body weight loss of 20%. When body weight decreased below this limit, the mice had to be euthanized. Overall, body weights remained constant over the course of the trial. None of the mice showed neither side effects nor signs of illness.

3.2. Determination of cellular immune responses

3.2.1. Peptide prediction

As only limited information of T cell epitope specificities for all three HA sequences were available, *in silico* analysis was performed to predict potential binding epitope regions within the HA sequences.

The *in silico* analysis yielded in a list of potential epitope regions specific for MHC-I and MHC-II binding (see **Table 5, 6** and **8**). The procedure is specified in the methods section (chapter *4.2.*). To narrow down the list, binding peptides were further sorted according to parameters influencing binding affinity and antigen processing. Those peptides shared sequences for both experiments and are shown in **Table 12** and **13**. For MHC-I alleles, median percentile values ranged between 0.09% and 0.76%. Values between 0.61% and 7.2%. IC_{50} values between 4.49 nM and 115.68 nM. For MHC-II alleles, MHC-II binding rank values ranged between 0.11% and

7.2%. IC_{50} values between 5.37 nM and 25.96 nM. The smaller the values, the better the predicted binding.

Table 12: Shared peptide sequences between ELISpot and ICS analysis used for epitope prediction of IAV-H2 and IAV-H5. For MHC-I epitopes the median percentile and IC_{50} are listed. The smaller the values, the better the predicted binding.

Name	Amino acid sequence	Pool	Median percentile [%]	IC_{50} [nM]
HA H2-S p1	YLILLFTAV	H2S-P6	0.28	16.26
HA H2-S p2	TLLDMWDTI	H2S-P6	0.54	57.35
HA H2-S p3	VLMENERTL	H2S-P6	0.47	115.68
HA H2-S p4	MMAGISFWM	H2S-P6	0.3	5.23
HA H2-R p5	FLILLFTVV	H2R-P6	0.76	66.88
HA H2-R p6	ILMENERTL	H2R-P6	0.31	67.7
HA H2-R p7	QILAIYATV	H2R-P6	0.76	68.28
HA H2-S+R p8	TILERNVTV	H2S-P7, H2R-P7	0.35	80.89
HA H2-S+R p9	VLATGLRNV	H2S-P7, H2R-P7	0.17	28.17
HA H2-S+R p10	KMNTQFEAV	H2S-P7, H2R-P7	0.24	29.95
HA H2-S+R p11	KMEDGFLDV	H2S-P7, H2R-P7	0.43	66.84
HA H2-S+R p12	FLDVWTYNA	H2S-P7, H2R-P7	0.09	4.49
HA H2-S+R p13	NLYDKVRMQL	H2S-P7, H2R-P7	0.39	91.8
HA H2-S+R p14	QILAIYATV	H2S-P7, H2R-P7	0.76	68.28
HA H5-G p1	VLLLAIVSL	H5G-P6	0.35	62.16
HA H5-G p2	LLLAIVSLV	H5G-P6	0.16	8.03
HA H5-G p3	TIMEKNVTV	H5G-P6	0.12	24.28
HA H5-G p4	KMNTQFEAV	H5G-P6	0.24	29.95
HA H5-G p5	FLDVWTYNA	H5G-P6	0.09	4.49
HA H5-G p6	SMPFHNIHPL	H5G-P7	0.88	40.37
HA H5-G p7	KMEDGFLDV	H5G-P7	0.43	66.84
HA H5-G p8	VLMENERTL	H5G-P7	0.47	115.68
HA H5-G p9	SLALAIMMA	H5G-P7	0.65	90.24
HA H5-G p10	ALAIMMAGL	H5G-P7	0.63	51.01

Table 13: Shared peptide sequences between ELISpot and ICS analysis used for epitope prediction of IAV-H2 and IAV-H5. For MHC-II epitopes the binding rank and IC_{50} are listed. The smaller the values, the better the predicted binding.

Name	Amino acid sequence	Pool	IC_{50} [nM]	MHC-II binding rank [%]
HA H2-S p15	ILLFTAVRGDQICIG	H2S-P8, H2R-P8	10.41	7.1
HA H2-S p16	VGTYVSVGTSTLNKR	H2S-P8, H2R-P8	9.92	0.92
HA H2-S p17	GNLIAPEYGFKISKR	H2S-P8, H2R-P8	17.39	0.61
HA H2-S p18	TTLPFHNVHPLTIGE	H2S-P8, H2R-P8	18.83	1.7
HA H2-S p19	SEKLVLATGLRNVPQ	H2S-P8, H2R-P8	9.43	2.5
HA H2-S p20	AELLVLMENERTLDF	H2S-P8, H2R-P8	-	7.2
HA H2-S-R p21	GVYQILAIYATVAGS	H2S-P9, H2R-P9	-	4.3
HA H5-G p11	WSYIVERANPANDLC	H5G-P8	5.37	0.11
HA H5-G p12	TTYISVGTSTLNQRL	H5G-P8	11.29	4.9
HA H5-G p13	GNFIAPEYAYKIVKK	H5G-P8	12.32	0.48
HA H5-G p14	SSMPFHNIHPLTIGE	H5G-P8	13.75	0.87
HA H5-G p15	SNKLVLATGLRNSPL	H5G-P8	8.86	3.4
HA H5-G p16	REDLLILWGIHHSNN	H5G-P9	25.96	5.5
HA H5-G p17	IGTYQILSIYSTAAS	H5G-P9	11.14	5.5

3.2.2. HA-specific $CD4^+$ and $CD8^+$ T cell responses

HA-antigen specific cellular immune responses ($CD8^+$ and $CD4^+$) after prime-boost immunization were tested with the recombinant MVA candidate vaccines (MVA-H2R, MVA-H2S, MVA-H5G) in *HLA-A2.1-/HLA-DR1-transgenic H-2 class I-/class II-knockout* mice. Subsequently, splenocytes from MVA-H2R, MVA-H2S and MVA-H5G immunized mice were collected for restimulation with nine pools of overlapping or predicted peptides (see **Table 5–10**), followed by ELISpot and ICS analysis (see **Figure 22–24**). For IAV-H2R and IAV-H2S, which both are based on IAV subtype H2, four out of nine pools contained shared peptide sequences.

Stimulation of anti-HA specific IFN-γ^+ T cells was observed (H2R-P8) for MVA-H2R with pool 8 (H2R-P8) with mean numbers of 21.04 ± 5.71 IFN-γ spot-forming cells (SFC) in splenocytes (**Figure 22 a**). This result was confirmed by ICS following flow cytometry analysis. A robust $CD4^+$, but not $CD8^+$, T cell response was observed with mean values of 0.508 ± 0.075% IFN-γ^+ T cells (**Figure 22 b**) after re-stimulation with pool 8 (H2R-P8). When

screening for $CD8^+$ T cell responses following re-stimulation with selected peptide pools (H2R+S-P4, H2R+S-P5, H2R+S-P7, H2R+S-P9), containing peptide sequences shared between H2N9 and H2N2 HAs, only low levels of IFN-γ^+ $CD8^+$ T cells were observed after re-stimulation with pool H2R+S-P7, with mean values of 0.087 ± 0.027% IFN-γ^+ $CD8^+$ T cells (**Figure 22 c**). In addition, an upregulation of anti-HA specific IFN-γ^+ and TNF-α^+ T cells was identified by ICS following flow cytometry after re-stimulation of splenocytes with pool 8 (H2R-P8) (**Figure 22 d-f**). Substantial numbers of IFN-γ^+ $CD4^+$ T cells showed a co-expression of TNF-α, with mean values of 80.908 ± 3.047%.

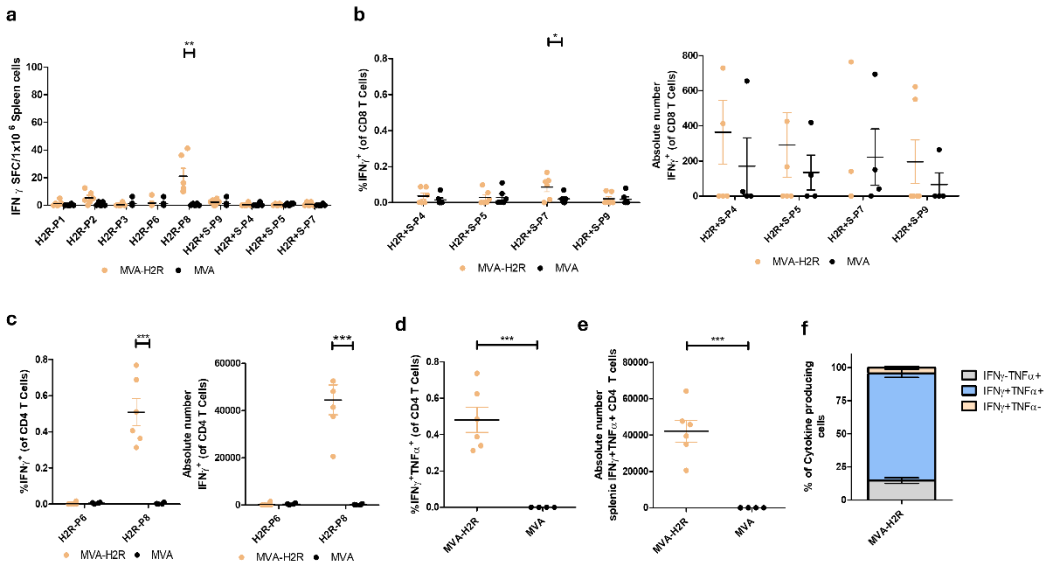

Figure 22: Activation of IAV specific CD4⁺ and CD8⁺ T cell response after prime-boost immunization with MVA-H2R. Groups of *HLA-A2.1-/HLA-DR1-transgenic H-2 class I-/class II-knockout* mice (n=6) were immunized twice over a 21-day interval with 10^7 PFU MVA-H2R (beige) using the IM route. Mice vaccinated with non-recombinant MVA (black) served as controls. Splenocytes were isolated on day 35 post prime immunization (14 days after the boost immunization) and stimulated with pools of peptides and T cell activation was measured by ELISpot **(a)** and IFN-ɣ and TNF-α ICS plus FACS analysis **(b - f)**. **(a)** IFN-γ SFCs measured by ELISPOT assay. Graph shows the IFN-γ SFCs in splenocytes. **(b)** IFN-γ producing CD8⁺ T cells measured by FACS analysis. Graphs show the frequency and absolute number of IFN-γ CD4⁺ T cells. **(c)** IFN-γ producing CD4⁺ T cells measured by FACS analysis. Graphs show the frequency and absolute number of IFN-γ CD4⁺ T cells. **(d, e)** IFN-γ and TNF-α producing CD4⁺ T cells measured by FACS analysis. Graphs show the frequency and absolute number of IFN-γ⁺ TNF-α⁺ CD4⁺ T cells. **(f)** Cytokine profile of H2R-P8 stimulated CD4⁺ T cells. Graph shows the mean frequency of IFN-γ⁻TNF-α⁺ (grey), IFN-γ⁺TNF-α⁻ (beige), and IFN-γ⁺TNF-α⁺ (blue) cells within the positive CD4⁺ T cell population. Mean values with standard error are displayed. Statistical analysis was performed with an unpaired two-tailed t-test. * $p < 0.05$.

Stimulation of anti-HA specific IFN-ɣ⁺ T cells was observed for pool 8 (H2S-P8) for MVA-HSR with mean numbers of 13.75 ± 4.793 IFN-ɣ spot-forming cells (SFC) in splenocytes (**Figure 23 a**). This result was confirmed by ICS. A robust CD4⁺ skewed T cell response was observed with mean values of 0.196 ± 0.065% IFN-ɣ⁺ T cells (**Figure 23 b**) after restimulation with pool 8 (H2S-P8). When screening for CD8⁺ T cell responses following selected peptide pools (H2R+S-P4, H2R+S-P5, H2R+S-P7, H2R+S-P9), only low levels of IFN-ɣ⁺ CD8⁺ T cells were observed after re-stimulation with pool H2R+S-P7, with mean values of 0.048 ± 0.015% IFN-ɣ⁺ CD8⁺ T

cells (**Figure 23 c**). In addition, an upregulation of anti-HA specific IFN-γ$^+$ and TNF-α$^+$ T cells was identified by ICS (**Figure 23 d-f**). Substantial numbers of IFN-γ$^+$ CD4$^+$ T cells showed a co-expression of TNF-α, with mean values of 90.370 ± 2.747%.

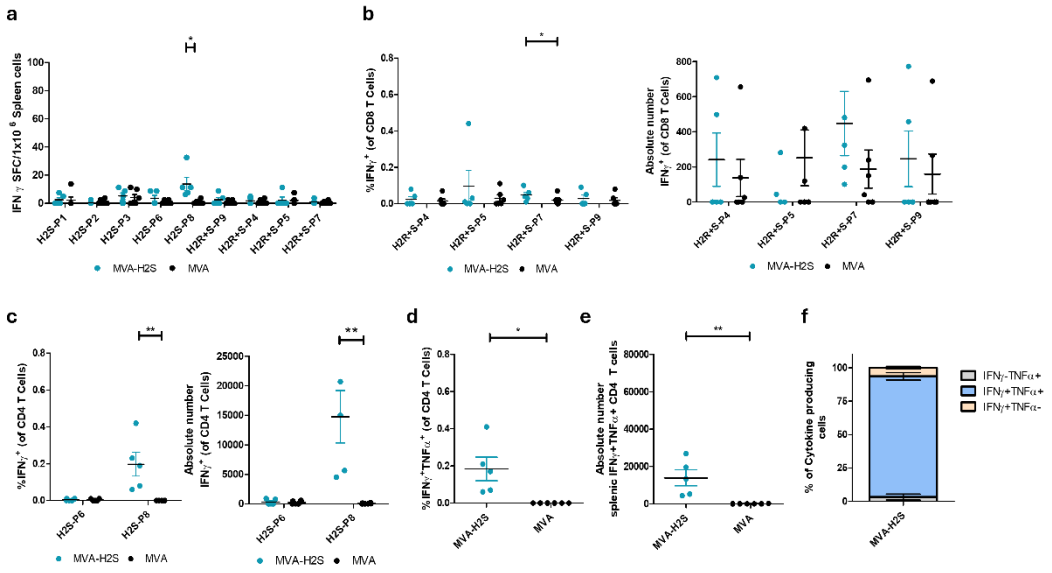

Figure 23: Activation of IAV specific CD4$^+$ and CD8$^+$ T cell response after prime-boost immunization with MVA-H2S. Groups of *HLA-A2.1-/HLA-DR1-transgenic H-2 class I-/class II-knockout* mice (n=5) were immunized twice over a 21-day interval with 10^7 PFU MVA-H2S (cyan) using the IM route. Mice vaccinated with non-recombinant MVA (black) served as controls. Splenocytes were isolated on day 35 post prime immunization (14 days after the boost immunization) and stimulated with pools of peptides and T cell activation was measured by ELISpot **(a)** and IFN-γ and TNF-α ICS plus FACS analysis **(b - f)**. **(a)** IFN-γ SFCs measured by ELISPOT assay. Graph shows the IFN-γ SFCs in splenocytes. **(b)** IFN-γ producing CD8$^+$ T cells measured by FACS analysis. Graphs show the frequency and absolute number of IFN-γ CD4$^+$ T cells. **(c)** IFN-γ producing CD4$^+$ T cells measured by FACS analysis. Graphs show the frequency and absolute number of IFN-γ CD4$^+$ T cells. **(d, e)** IFN-γ and TNF-α producing CD4$^+$ T cells measured by FACS analysis. Graphs show the frequency and absolute number of IFN-γ$^+$ TNF-α$^+$ CD4$^+$ T cells. **(f)** Cytokine profile of H2S-P8 stimulated CD4$^+$ T cells. Graph shows the mean frequency of IFN-γ$^-$TNF-α$^+$ (grey), IFN-γ$^+$TNF-α$^-$ (beige), and IFN-γ$^+$TNF-α$^+$ (blue) cells within the positive CD4$^+$ T cell population. Mean values with standard error are displayed. Statistical analysis was performed with an unpaired two-tailed t-test. * $p < 0.05$.

Stimulation of anti-HA specific IFN-γ$^+$ T cells was observed for pool 8 (H5G-P8) for MVA-H5G with mean numbers of 145.6 ± 37.78 IFN-γ spot-forming cells (SFC) in splenocytes (**Figure 24 a**). This result was confirmed by ICS. A robust CD4$^+$ skewed T cell response was observed with mean values of 0.135 ± 0.026% IFN-γ$^+$ T cells (**Figure 24 b**) after restimulation

with pool 8 (H5G-P8) with mean values of 0.064 ± 0.026% IFN-γ$^+$ CD8$^+$ T cells (**Figure 24 c**). When screening for CD8$^+$ T cell responses following selected peptide pools (H5G-P6, H5G-P7, H5G-P8, H5G-P9), only low levels of IFN-γ$^+$ CD8$^+$ T cells were observed after re-stimulation (**Figure 24 c**). In addition, an upregulation of anti-HA specific IFN-γ$^+$ and TNF-α$^+$ T cells were identified by ICS (**Figure 24 d-f**). Substantial numbers of IFN-γ$^+$ CD4$^+$ T cells showed a co-expression of TNF-α, with mean values of 73.170 ± 4.793%.

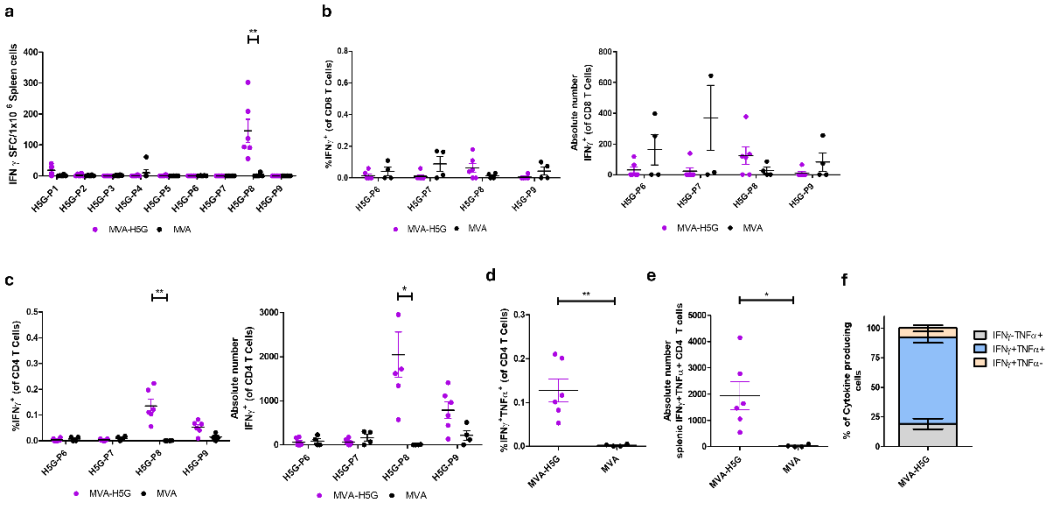

Figure 24: Activation of IAV specific CD4$^+$ and CD8$^+$ T cell response after prime-boost immunization with MVA-H5G. Groups of *HLA-A2.1-/HLA-DR1-transgenic H-2 class I-/class II-knockout* mice (n=6) were immunized twice over a 21-day interval with 10^7 PFU MVA-H5G (purple) using the IM route. Mice vaccinated with non-recombinant MVA (black) served as controls. Splenocytes were isolated on day 35 post prime immunization (14 days after the boost immunization) and stimulated with pools of peptides and T cell activation was measured by ELISpot **(a)** and IFN-γ and TNF-α ICS plus FACS analysis **(b - f)**. **(a)** IFN-γ SFCs measured by ELISPOT assay. Graph shows the IFN-γ SFCs in splenocytes. **(b)** IFN-γ producing CD8$^+$ T cells measured by FACS analysis. Graphs show the frequency and absolute number of IFN-γ CD4$^+$ T cells. **(c)** IFN-γ producing CD4$^+$ T cells measured by FACS analysis. Graphs show the frequency and absolute number of IFN-γ CD4$^+$ T cells. **(d, e)** IFN-γ and TNF-α producing CD4$^+$ T cells measured by FACS analysis. Graphs show the frequency and absolute number of IFN-γ$^+$ TNF-α$^+$ CD4$^+$ T cells. **(f)** Cytokine profile of H5G-P8 stimulated CD4$^+$ T cells. Graph shows the mean frequency of IFN-γ$^-$TNF-α$^+$ (grey), IFN-γ$^+$TNF-α$^-$ (beige), and IFN-γ$^+$TNF-α$^+$ (blue) cells within the positive CD4$^+$ T cell population. Mean values with standard error are displayed. Statistical analysis was performed with an unpaired two-tailed t-test. * $p < 0.05$.

3.2.3. MVA specific CD8$^+$ T cell responses

In addition, we determined the MVA vector-specific T cell response using the MVA-specific immunodominant CD8$^+$ T cell epitope A6(L)$_{6-14}$ (see **Figure 25**). A6L is a virion core protein required for membrane formation (Meng et al., 2012; Meng et al., 2007). Prime-boost immunizations with MVA-H2R, MVA-H2S and MVA-H5G induced substantial levels of A6(L)$_{6-14}$ epitope-specific T cells with mean values of 22.708 ± 8.976 IFN-ɣ SFC, 28.0 ± 13.945 IFN-ɣ SFC and 146.667 ± 43.294 IFN-ɣ SFC (**Figure 25 a-c**). Mice immunized with non-recombinant MVA showed mean values of 26.250 ± 7.115 IFN-ɣ SFC, 41.042 ± 15.477 IFN-ɣ SFC and 122.500 ± 39.879 IFN-ɣ SFC. ICS revealed values of 0.570 ± 0.222% IFN-γ$^+$, 0.204 ± 0.051% IFN-γ$^+$ and 0.200 ± 0.045% IFN-γ$^+$ CD8$^+$ T cells in the spleen (**Figure 25 d–f**). Mice immunized with non-recombinant MVA showed mean values of 0.252 ± 0.084% IFN-γ$^+$, 0.257 ± 0.055% IFN-γ$^+$ and 0.111 ± 0.063% IFN-γ$^+$ CD8$^+$ T cells. A high proportion of IFN-γ$^+$ CD8$^+$ T cells also co-expressed TNF-α (**Figure 25 j–l**) with 85.314 ± 5.416% for MVA-H2R, 85.710 ± 9.676% for MVA-H2S and 69.299 ± 4.128% for MVA-H5G. Values for non-recombinant MVA amounted to 67.115 ± 12.520%, 67.895 ± 7.933% and 74.630 ± 9.884% IFN-γ$^+$ TNF-α$^+$ CD8$^+$ T cells.

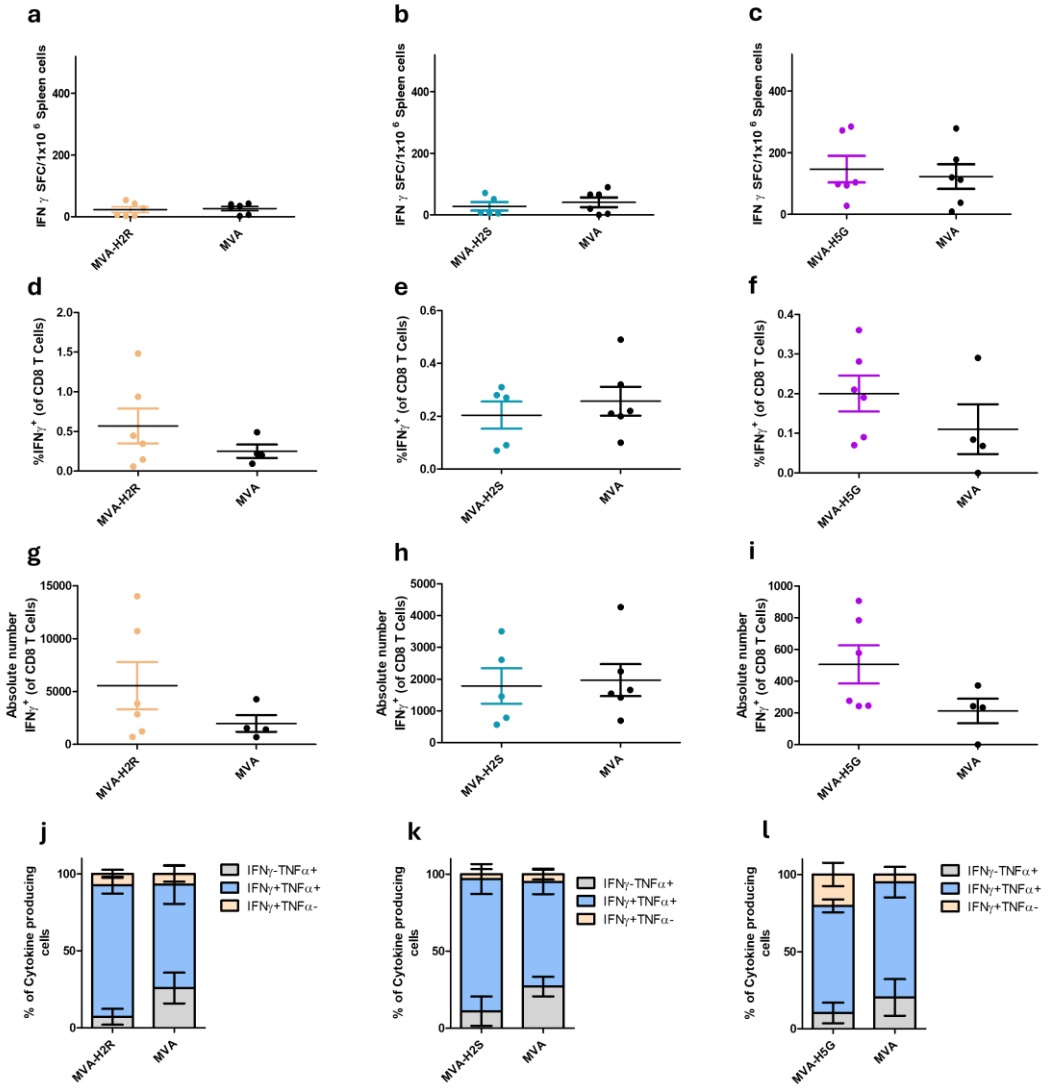

Figure 25: Induction of MVA-specific CD8⁺ T cell responses upon prime-boost immunization with MVA-H2R, MVA-H2S and MVA-H5G. Groups of *HLA-A2.1-/HLA-DR1-transgenic H-2 class I-/class II-knockout* mice were immunized twice over a 21-day interval with 10^7 PFU MVA-H2R (beige), MVA-H2S (cyan) and MVA-H5G (purple) using the IM route. Mice immunized with non-recombinant MVA served as control. Splenocytes were isolated on day 35 post prime immunization (14 days post boost immunization) and re-stimulated with the HLA-I restricted MVA-specific peptide $A6(L)_{6\text{-}14}$. Measurement was performed by IFN-γ ELISPOT assay **(a-c)** and IFN-γ and TNF-α ICS plus FACS analysis **(d–l)**. **(a-c)** IFN-γ SFCs measured by ELISPOT assay. Graphs show the IFN-γ SFCs in splenocytes. **(d-f)** IFN-γ producing CD8⁺ T cells measured by FACS analysis. Graphs show the frequency of IFN-γ CD8⁺ T cells. **(g-i)** IFN-γ producing CD8⁺ T cells measured by FACS analysis. Graphs show the absolute number of IFN-γ CD8⁺ T cells. **(j-l)** Cytokine profile of CD8⁺ T cells co-expressing IFN-γ and TNF-α. Mean values with standard error are displayed. Statistical analysis was performed with an unpaired two-tailed t-test. * $p < 0.05$.

3.3. HA-specific antibody responses

To evaluate the HA-antigen specific humoral immune response upon immunizations with MVA-H2R, MVA-H2S and MVA-H5G, *HLA-A2.1-/HLA-DR1-transgenic H-2 class I-/class II-knockout* mice were immunized twice with 10^7 PFU of the candidate vaccines over a 21-day interval. On day 18 post prime immunization and 14 days after the booster immunization, serum was collected and subsequently analyzed by ELISA (see **Figure 26**). Serum samples from vaccinated mice were tested for serum IgG antibodies using full-length HA proteins as antigen. The recombinant protein used for MVA-H2R and MVA-H2S was based on the A/Guiyang/1/1957 (H2N2) subtype, while the protein for MVA-H5G was based on the A/Astrakhan/3212/2020 (H5N8) subtype. A single immunization led to seroconversion in 1/6 MVA-H2R immunized, 4/4 MVA-H2S immunized and 5/6 MVA-H5G immunized mice, with mean titers of <1:100 (**Figure 26 a**), <1:200 (**Figure 26 a**) and <1:784 (**Figure 26 b**), respectively. The booster immunization led to the seroconversion in all MVA-H2S immunized and MVA-H5G immunized mice with mean titers of <1:1380 and <1:1900 respectively, whereas only 4/6 MVA-H2R immunized mice seroconverted with a mean titer of <1:100.

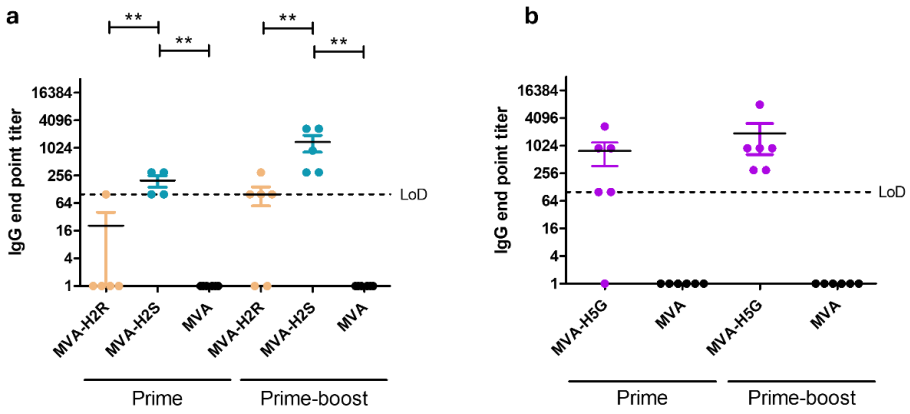

Figure 26: HA-antigen specific humoral immune response induced upon prime-boost immunization of *HLA-A2.1-/HLA-DR1-transgenic H-2 class I-/class II-knockout* with MVA-H2R, MVA-H2S and MVA-H5G. Groups of mice (n=5-6) were immunized twice with 10^7 PFU of MVA-H2R (beige), MVA-H2S (cyan) and MVA-H5G (purple) over a 21-day interval using the IM route. Mice immunized with non-recombinant MVA (black) served as controls. Serum samples were collected on day 18 post prime immunization (prime) and day 14 post booster immunization (prime-boost) and tested for HA-specific IgG titers by ELISA. Titers are displayed in 2-log scale and the limit of detection (LoD) is indicated as dotted line. Mean values with standard error are displayed. Statistical analysis was performed with a one-way ANOVA Tukey test. * $p < 0.05$.

To evaluate the HA-antigen cross-reactive humoral immune response upon immunizations with MVA-H2R, MVA-H2S and MVA-H5G, *HLA-A2.1-/HLA-DR1-transgenic H-2 class I-/class II-knockout* mice were immunized twice with 10^7 PFU of the candidate vaccines over a 21-day interval. 14 days after the booster immunization, serum was collected and subsequently analyzed by ELISA (see **Figure 27**). Serum samples from vaccinated mice were tested for serum IgG antibodies using full-length HA proteins as coating antigen. Sera from MVA-H2R and MVA-H2S vaccinated mice were probed against the A/Astrakhan/3212/2020 (H5N8) HA recombinant protein, while sera from MVA-H5G vaccinated mice were probed against the A/Guiyang/1/1957 (H2N2) HA recombinant protein. Cross-reactive antibodies were observed in 0/6 MVA-H2R immunized, 4/5 MVA-H2S immunized and 0/6 MVA-H5G immunized mice, with mean titers of <1:100 (**Figure 27 a**), <1:120 (**Figure 27 a**) and <1:100 (**Figure 27 b**), respectively. Additionally, sera from all three candidate vaccines were probed against the A/Puerto Rico/8/1934 (H1N1) HA recombinant protein. For the H1N1 recombinant protein, no cross-reactivity was observed for any candidate vaccine (**Figure 27 c**).

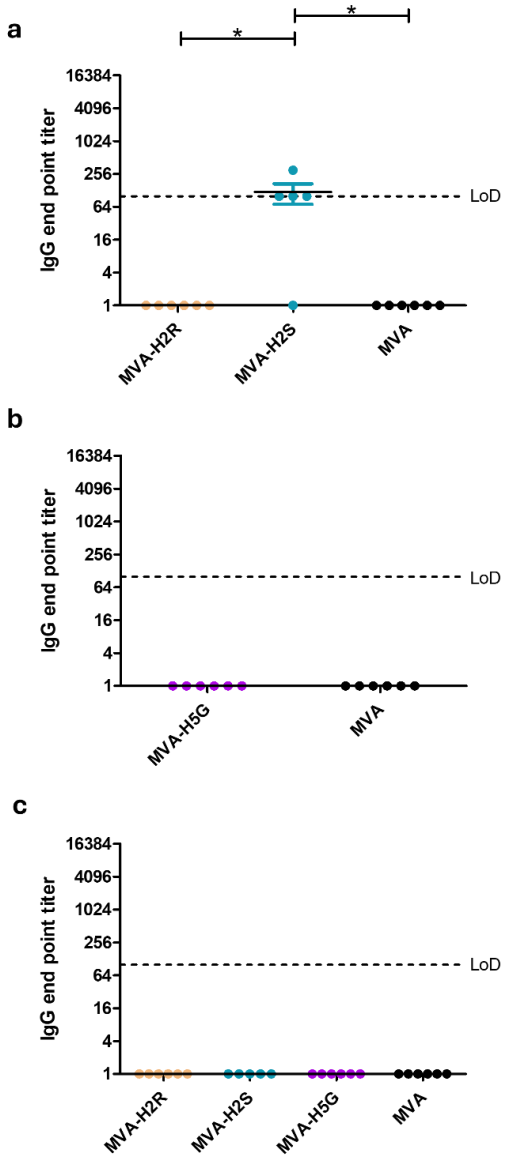

Figure 27: Cross-reactive HA-antigen humoral immune response induced upon prime-boost immunization of *HLA-A2.1-/HLA-DR1-transgenic H-2 class I-/class II-knockout* with MVA-H2R, MVA-H2S and MVA-H5G. Groups of mice (n=5-6) were immunized twice with 10^7 PFU MVA-H2R (beige), MVA-H2S (cyan) and MVA-H5G (purple) over a 21-day interval using the IM route. Mice immunized with non-recombinant MVA (black) served as controls. Serum samples were collected on day 14 post booster immunization (prime-boost) and tested for HA-cross-reactive IgG titers by ELISA. **(a)** Cross-reactivity against the H5N8 recombinant protein. **(b)** Cross-reactivity against the H2N2 recombinant protein. **(c)** Cross-reactivity against the H1N1 recombinant protein. Titers are displayed in 2-log scale and the limit of detection (LoD) is indicated as dotted line. Mean values with standard error are displayed. Statistical analysis was performed with a one-way ANOVA Tukey test. * $p < 0.05$.

VIII. DISCUSSION

History has shown that the H2 subtype was involved in major pandemics, and it still circulates in wildlife. This highlights the importance of considering effective countermeasures against this subtype for pandemic preparedness (Jones et al., 2014; Kessler et al., 2021). Furthermore, outbreaks from the past including both human and avian cases highlight the concern for the H5N1, H5N5, H5N6 and H5N8 subtypes (Beigel et al., 2005; Globig et al., 2018; He et al., 2020; Kessler et al., 2021; King et al., 2021; Kuiken et al., 2023; Li et al., 2019; Postel et al., 2022; The Lancet Infectious, 2014; Ungchusak et al., 2005; Wang et al., 2012). Latest cases of global H5N1 infections as reported by the CDC (CDC, February 2025), emphasize our efforts to generate a safe and effective vaccine. Although the risk of a pandemic scenario involving the current circulating H5N1 strain is estimated as low by the RKI (RKI, November 2024) and WHO (WHO, March 2025), these events of transmission and cases should act as an example of how probable a future influenza pandemic is. Due to the high mutation rate, it is unlikely to precisely determine which IAV strain will cause the next influenza pandemic. Thus, broadly reactive and rationally designed vaccines are necessary for pandemic preparedness.

We successfully generated and characterized MVA-IAV candidate vaccines targeting the HA protein of different circulating IAV subtypes. On the genetic level, correct insertion of the genes of interest was confirmed by PCRs targeting deletion site III of the MVA backbone genome and the inserted genes themselves. Beyond that, stable insertion was demonstrated by multiple passages at low MOI on DF-1 cells. On the protein level, unimpaired expression of the antigens was confirmed by Western blot analysis and immunofluorescence staining. Replication deficiency was demonstrated in human cells, while comparable titers to non-recombinant MVA were observed for cells of avian origin. In humanized *HLA-A2.1-/HLA-DR1-transgenic H-2 class I-/class II-knockout* mice, all three candidate vaccines elicited a strong systemic cellular and humoral immune response using a prime-boost immunization schedule. Furthermore, the vaccines were well-tolerated in mice. All of which support their suitability for further

clinical testing in humans.

MVA as vaccine platform against influenza

MVA is utilized as a tool for basic research, e.g., studying VACV host regulators K1L and C7L (Gillard et al., 1986; Perkus et al., 1990) or the importance of the VACV interleukin-1β receptor protein to dampen host defense mechanisms (Alcamí & Smith, 1992; Spriggs et al., 1992). MVA can be also used to target cancers such as melanoma (Drexler et al., 1999) or nasopharyngeal carcinoma (Sun et al., 2025). Furthermore, MVA can be exploited as vaccine platform, entailing favorable characteristics. One important feature is its use under BSL-1 conditions (Altenburg et al., 2014). Its genetic stability, high immunogenicity and safe use in immunocompromised are further features for the MVA vaccine (Volz & Sutter, 2017).

Considering MVA as vaccine platform against IAV, the feasibility to incorporate multiple antigens of interest is another advantage (Altenburg et al., 2014; Powell et al., 2013; Volz & Sutter, 2017). For example, a combination of HA, NA and M1 might be of interest. All these proteins play a significant role in the life cycle of IAV as highlighted in the literature review, and a vaccine targeting several important proteins at once would most likely increase its efficacy. One could also think of inserting HA sequences from different influenza virus strains into one MVA backbone virus, thus, enhancing protection against multiple strains by using only one vaccine preparation. This application would be feasible for both seasonal vaccination and pandemic events.

Regarding pandemic vaccines, MVA offers suitability of large-scale manufacturing in both developed and developing countries. Compared to mRNA-based vaccines, it simplifies vaccine supply as higher temperatures do not harm the integrity and stability of the viral vector vaccine and no adjuvants are required (Crommelin et al., 2021; Robert-Guroff, 2007; Uddin & Roni, 2021; Volz & Sutter, 2017; Wadhwa et al., 2020). An advantage over adenoviral vectors is that vaccine efficacy is largely not diminished by vector immunity as outlined in the literature review (Altenburg et al., 2018). However, MVA-based vaccination regimens usually require a second immunization to establish sufficient titers of neutralizing antibodies

(Raadsen et al., 2025). Another drawback is the labor-extensive *in vitro* characterization required as some foreign gene products can suppress MVA's replication which may cause outgrowth of non-expressing mutants (Wyatt et al., 2009).

Several examples in the vaccine landscape strengthen the use of MVA as platform. For instance, the MVA-based vaccine Jynneos/Imvanex against Mpox underpin its safety and efficacy with real-world data (EMA, 2013; Duffy et al., 2022; Nave et al., 2023). Furthermore, there is an MVA-based vaccine licensed for human use against Ebola (Mvabea) which is used as booster immunization after a prime immunization with an adenoviral based vaccine (Zabdeno). For this vaccine, MVA delivers proteins of four different virus strains of the *Filoviridae* family (Zaire ebolavirus, Sudan ebolavirus, Taï Forest ebolavirus, Marburg marburgvirus) and both in preclinical and clinical studies, robust humoral and cellular immunity was elicited (EMA, 2020; Choi et al., 2024; Rostad et al., 2024; Valayer et al., 2025; Wiedemann et al., 2024). The pipeline of MVA-based vaccines is supplied by experimental vaccines in preclinical evaluation. Examples include experimental MVA-based vaccines designated against Nipah virus (Kalodimou et al., 2019) and SARS-CoV-2 (Tscherne et al., 2021).

Around 15 MVA-based candidate vaccines have entered clinical trials (ClinicalTrials.gov), after confirming their immunogenicity in preclinical small animal models and non-human primates. For instance, a HIV vaccine (MVA/HIV62B) was evaluated in a phase 1 clinical study (NCT02852005). The induction of both a cellular and humoral immune response was observed, while no severe adverse events were reported. In one phase 2a clinical study with recombinant MVA-NP+M1, T cell responses increased significantly, and duration of virus shedding was reduced among study participants who developed influenza upon infection with IAV (NCT00993083). An MVA-based booster vaccine against hepatitis C (MVA-NSmut) has also been tested in a phase 1 clinical study (NCT01296451). Recent entries indicate that an MVA vaccine (Triplex) will be clinically assessed to cure acute lymphoblastic leukemia in a phase 1b/2a clinical trial (NCT06735690), hepatitis B (TherVacB) in a phase 1b/2a clinical trial (NCT06513286) or cytomegalovirus in transplantations (CMV-

MVA Triplex) in a phase 2 clinical trial (NCT06075745).

Until recently, licensed vaccines against seasonal flu were quadrivalent vaccines comprising the two lineages A(H1N1) and A(H3N2) plus the two lineages B/Victoria and B/Yamagata which were updated annually with seasonal strains (CDC, September 2024). Notably, transition to trivalent vaccines is pursued as the Yamagata strain displays no longer a public health threat as COVID-19 pandemic measures ceased its circulation (EMA, March 2024; CDC, March 2024). By now, seven vaccines against IAV intended for pandemic response use received marketing authorization. Although different technologies are used for these licensed vaccines, all of them are targeted against the H5N1 or the H5N8 subtypes (PEI, March 2025). This demonstrates the need of vaccines targeting H5Nx for the pandemic repository and simultaneously the lack of vaccines against other subtypes on the market such as H2Nx.

Influenza A virus host interactions and implications for vaccine induced immune response

HA of IAV binds via sialic acid residues to the host cell as outlined in the introduction (Bouvier & Palese, 2008; Cheung & Poon, 2007). As this step is critical for infectivity, inhibition of this process is desired to avoid infection and therefore, HA is preferentially used for vaccine design.

Although NA also plays a role in endocytosis of virions, NA mainly cleaves the HA-sialic acid interaction at the release stage, which is the very last step in the life cycle of the virus (McAuley et al., 2019). The M2 ion channel is required to generate pH-dependent uncoating of viral particles involving M1 matrix protein (Cheung & Poon, 2007). Thus, all these viral proteins are interesting targets for vaccine development as interference with processes in the replication cycle of IAV would render the virus ineffective to infect host cells. Choosing M2 or M1 as antigen in vaccination would also diminish challenges resulting from antigenic drift, as these proteins are highly conserved (Chan et al., 2021; Goneau et al., 2018).

In our approach, we delivered the HA antigen of the three IAV subtypes H2N2, H2N8 and H5N8 by MVA. HA in particular is known to be a major target for neutralizing antibodies, which implicates that vaccination should

result in eliciting a humoral immune response (Cheung & Poon, 2007). Furthermore, after IAV infection, B cells are activated for antibody secretion (Chan et al., 2021; Crowe, 2017). Consequently, establishment of humoral immune response is substantial for vaccine development. Immunization experiments with our candidate vaccines yielded in upregulation of binding antibody responses, which was confirmed by elevated levels of IgG antibodies directed against the HA. The increase of antibody titers after the second immunization suggests a prime-boost regimen for further clinical evaluation. In addition, T cell memory is expected to be boosted by a second dose (Capone et al., 2020). Furthermore, emergence of novel strains leads to immune incompetence due to a lack of pre-existing immunity and consequently, vaccine efficacy is reduced (Krammer et al., 2018). Thus, immunological memory is also crucial to benefit from strong and long-lasting protection in terms of humoral and cellular immunity. Investigation of memory cells including memory B cells could reveal insights for long lasting immunity but would have gone beyond the scope of our study. This will become interesting when universal protection is plausible as it would also reduce vaccination frequency of seasonal influenza.

Ideally, vaccines should be able to induce not only a humoral, but also a cellular mediated immune response. T cells play a significant role in immune response upon IAV infection and could contribute to universal influenza vaccines due to recognition of more conserved regions of HA or NA (Grant et al., 2014; Terrier et al., 2021). Both cytotoxic T cells and T helper cells, which support B cell responses, are involved in elimination of influenza infections (Mosmann et al., 2024). We confirmed this in our preclinical study, identifying at least one pool of overlapping or predicted peptides for each vaccine, which stimulated cellular immune responses above the background. $CD4^+$ cells, rather than $CD8^+$ T cells, were preferably activated, indicating establishment of a complex immune response involving helper T cells, which are as well required for B cell activation and priming of $CD8^+$ cells. Interestingly, the peptide pool 8 for HA-H2R and HA-H2S, which induced a strong T cell response after re-stimulation of splenocytes, contained six peptides (HA H2-S p15, HA H2-S p16, HA H2-S p17, HA H2-S p18, HA H2-S p19, HA H2-S p20), all of which presented via MHC-II

correlating with a $CD4^+$ T cell response. Compared to other peptides with IC_{50} values even above 100 nM, IC_{50} values for those peptides were lower (< 20 nM), which demonstrates a high binding affinity for the MHC-II allele. For the identified peptide pool 8 comprising HA-H5G epitopes all the included peptides (HA H5-G p11, HA H5-G p12, HA H5-G p13, HA H5-G p14, HA H5-G p15) correspond to MHC-II alleles and IC_{50} values were even lower with the maximum of 13.75 nM. Again, our prediction parameters aligned with the observed immune response. One could speculate that the frequency of $CD4^+$ T cells was higher to initiate B cell proliferation and amplifying $CD8^+$ population as fast as possible, which would align with the literature (Chan et al., 2021). One could attempt to enhance CD8+ T cell response by co-delivery of the cytokines IFN-γ or IL-12 as shown in another study (Abaitua et al., 2006). In this study BALB/c mice were immunized with a recombinant MVA-based vaccine, delivering the envelope antigen of HIV-1 and either IFN-γ or IL-12, which led to an improved $CD8^+$ T cell response. In the next step, single peptide identification could be carried out by ELISpot to determine specific epitopes which elicit immune response.

Upon IAV infection, the human innate immune response is activated as a first line of defense. Toll-like receptors (TLR) recognize foreign viral components, which are called pathogen associated molecular patterns (PAMPs), and upon activation, important pathways, including the type-I interferon pathways are activated to eliminate the pathogen. Double-stranded RNA (dsRNA) may serve as PAMP, leading to the activation of downstream factors of the type-I interferon pathway, resulting in the transcription of cytokines, such as type I and type III interferons. Consequently, leukocytes such as neutrophils, which are activated by the cytokines, limit IAV infection (Chan et al., 2021; Guillot et al., 2005). Interestingly, breast-fed infants suffering from influenza have elevated production of interferons which causes activation of innate antiviral mechanisms (Crowe, 1998). It was also shown that proinflammatory interleukins are released by activation of the NOD-like receptor family pyrin domain containing 3 (NLRP3) inflammasome. Most important interleukins involved are TNF-α, IL-6, IL-1β and interferons (Chan et al., 2021; Guillot et al., 2005). Thus, an upregulation of proinflammatory cytokines by vaccines

is a desired feature. We observed elevated levels of TNF-α and IFN-ɣ at 14 days after the booster immunization. Co-secretion of IFN-ɣ and TNF-α highlights the robust induction of antiviral mechanisms of the immune system, which can act directly as apoptotic signal against infected cells or indirectly as stimuli for T cell immune responses, orchestrating the T cell pool and recruitment of other immune cells (A. K. Mehta et al., 2018). Furthermore, TNF-α plays a substantial role in battling influenza infections (Seo & Webster, 2002). Influenza viruses can prevent IFN synthesis by production of a nonstructural protein. Interferons have anti-viral activity, recruit and activate natural killer cells, dendritic cells and alveolar macrophages. Influenza viruses have the capability to directly infect dendritic cells. Those cells play a substantial role in IAV infection by presentation of antigens to B- and T cells within the lymph node and hence priming of immune cells (Chan et al., 2021; Crowe, 2017).

Upon infection with IAV, T cells are activated by dendritic cells. Among them are cytotoxic T cells, but also $CD4^+$ T cells, which can be subdivided into Th1 and Th2 cells. Th1 cells act proinflammatory, enhance phagocytosis and activate $CD8^+$ T cells, while Th2 cells regulate B cells. Th1 response is favored for vaccine development against influenza viruses but accomplishing that depends on the vaccine technology (Chan et al., 2021). The induction of a robust cellular immunity is therefore a considerable correlate for vaccine immunogenicity and protection. Another factor which influences IAV vaccines is the concept of antigenic imprinting, which means that antibody responses tend towards the first antigen encountered, dampening vaccine efficacy. This should be considered for vaccination of immunological immature young children since it could alter immune responses against IAV for future exposure (Chan et al., 2021). Additionally, immunocompromised individuals, risk factors and comorbidities are factors which should be considered for vaccine development.

Differences in immune responses due to sex, (e.g., men develop fewer neutralizing antibodies to modern vaccines) and individuum (HLA polymorphism) further complicate efforts to improve vaccines against influenza (Chan et al., 2021). Another issue which should be taken into consideration is immunosenescence, the gradual deterioration of the

immune system when aging, which reduces both vaccine efficacy (Goodwin et al., 2006) and duration of protection (Castilla et al., 2013; Kang et al., 2004; Young et al., 2017). Remarkably, innate immunity can be trained which addresses vulnerable individuals like the elderly (Chan et al., 2021). In this respect, a better outcome was observed for COVID-19 patients, when they were previously vaccinated against influenza (Fink et al., 2020). Similarly, Bacillus Calmette-Guérin (BCG) vaccination against tuberculosis proved beneficial in patients with influenza (Leentjens et al., 2015). Further research needs to be conducted on this topic. Altogether, virus-host interactions should spur the development of future vaccines against influenza.

Challenges of making effective influenza vaccines

As recently reported, the numbers of influenza cases in poultry farms in Europe and cattle stock in the US have increased, indicating increased risk of zoonotic transmission in the long term (EFSA, December 2024). Globalization and increasing world population facilitate evolution and spread of the virus. Additionally, reports showed that more and more wild birds are infected with highly pathogenic avian influenza throughout the summer period in Europe (EFSA, October 2022). Surveillance of migratory birds is hence of significance (King et al., 2021). Hygiene standards and veterinary measures alone will certainly not be sufficient to avoid a future influenza outbreak. Reports indicate that there is an increased risk of a future swine flu pandemic, as pre-existing immunity is lacking and a certain H1N1 strain replicates efficiently in human airway cells (Le Sage et al., 2024). Data collected from China highlighted high risk of infection with influenza virus among swine workers (Borkenhagen et al., 2020). Taken together, findings propose the necessity of effective influenza vaccines and cross-protection. In addition, farming regulations, public health efforts and not only therapeutic but also prophylactic efforts by industry and academia are indispensable to address pandemic influenza.

The efficacy of influenza vaccines and how to increase it, is an unresolved issue. A systematic review and meta-analysis found a vaccine effectiveness among 15- to 64-year-old individuals of 39.3 to 55.4% in randomized-controlled trials, depending on the match between the vaccine and

circulating strain (Martins et al., 2023). Values for test-negative study designs, were even lower (35.1 – 45.1%), urging the development of next-generational vaccines. Another study examined data from 14 flu seasons and found vaccine effectiveness values ranging from 19 to 60% (CDC, August 2024). A further meta-analysis revealed a pooled vaccine effectiveness of only 41.4% with higher or lower values for specific influenza strains (Guo et al., 2024). Notably, vaccine effectiveness decreased with age, suggesting higher vaccine effectiveness is required especially for risk groups like the elderly. Another study calculated a vaccine effectiveness of 44% among hospitalizations due to influenza A of the 2022/23 season in the US (Tenforde et al., 2024).

IAV is a respiratory virus with the upper airways being the main side of infection. To generate effective vaccines, one might to consider the induction of a strong and robust mucosal and sterilizing immunity, associated with the upregulation of secretory IgA antibody responses and the maturation of tissue-resident T and B cells. (van Riet et al., 2012). Sterilizing immunity for optimal protection from disease would be desirable, preventing the virus from infecting epithelial cells in the upper and lower airways. This could be achieved by intranasal vaccine formulations. The FDA has already approved a live-attenuated flu vaccine, which is administered intranasally via spray formulation. However, as it is a live-attenuated vaccine, pregnant women cannot receive this vaccine (Heida et al., 2023). Our candidate vaccines were administered only via the IM route, so we did not measure mucosal immune responses. Apart from that, IgG is essential for neutralizing the virus after infection, and therefore, vaccination aims to increase the IgG titers for a more rapid response upon viral entry (Pollard & Bijker, 2021; van Riet et al., 2012). However, further studies might include the administration via the intranasal route, as other studies confirmed the capability of MVA-based vaccines to induce a strong mucosal immune response when administered via the mucosal route (Bošnjak et al., 2021; Endt et al., 2022).

Vaccine effectiveness could be further addressed with a universal vaccine, which protects against a broad spectrum of influenza strains. However, rapid mutation of the virus due to high error rate and no proof-reading ability

of the viral RNA-dependent RNA-polymerase contradicts the development of universal flu vaccines (Goneau et al., 2018). Our cross-reactivity studies propose a higher chance of cross-reactive antibody responses the closer related the strains are. H2N9 was isolated in 2019, whereas H2N2 and the recombinant H2 protein used for ELISA are based on sequences from 1957. In fact, sequence alignment showed 99% identity of the H2N2 strain with the H2 recombinant protein, whereas H2N9 shared 84% of its sequence with the recombinant protein. H5N8 and recombinant H5 protein used for ELISA aligned with a percentage of 99%. The positive signal of sera from MVA-H2S immunized mice for IAV-H5 protein suggests a similar sequence to the IAV-H5 protein. Alignment resulted in homology of both IAV-H2 strains with the H5 protein of 73%. A mutated antibody binding site in the H2N9 hemagglutinin could explain the positive signal of the sera from MVA-H2S immunized mice. Hence, a universal vaccine against influenza A remains a challenge. Further rational approaches should be pursued by trial and error. Multivalent vaccines beyond HA - as supported by the literature (Nachbagauer & Palese, 2020), adjuvants and alternative routes of administration could be of interest. Internal proteins do not induce neutralizing antibodies. However, integration of those could establish cellular immunity which might be beneficial for universal coverage (Wiersma et al., 2015). MVA as a platform offers optimal prerequisites for the incorporation of multiple antigens (Altenburg et al., 2014). Universal vaccines should ideally also target the stalk region of HA, as the stalk region is highly conserved among different subtypes (Lim et al., 2024; Wu & Wilson, 2020). Interestingly, the pools tested for HA-H2R and HA-H2S comprised peptides with sequences majorly aligning with the head region of HA (HA_{8-21}, $HA_{208-222}$, $HA_{259-273}$, $HA_{301-315}$, $HA_{321-336}$). We suggest that multivalent vaccines should comprise of epitopes from both head and stalk region of hemagglutinin as described in the literature (Wiersma et al., 2015; Wu & Wilson, 2020). Focusing on the conserved stalk region alone, should be avoided as this would result in detriments of antibody titers (Steel et al., 2010). In this respect, vaccines which also elicit T cell responses are the preferential choice. One possibility to increase immunogenicity of stalk directed antibodies is to incorporate chimeric HA, which nonetheless requires further investigation (Isakova-Sivak & Rudenko, 2022). Finally,

studies of novel vaccine technologies like nanotechnology and microneedle patches await a complete evaluation compared to conventional vaccine technologies (Pollard & Bijker, 2021; Rouphael et al., 2017). A meta-analysis could shed more light on the consensus of different vaccine technologies regarding a universal flu vaccine (Wang et al., 2022).

Another hurdle for influenza vaccines is the production in embryonated eggs, which is not only expensive, but also more labor intensive compared to production on cell lines (Buckland, 2015). As shown in the literature, Madin-Darby Canine Kidney (MDCK) cells are superior for vaccine production in a pandemic scenario (Hamamoto et al., 2013; Kim et al., 2018). A benefit of our MVA-based vaccines is that they can be manufactured in bioreactors with cell suspension of the avian cell lines, e.g., AGE1.CR.pIX or EB66® (Gränicher et al., 2021) (Cottingham & Carroll, 2013; Jordan et al., 2009) (Léon et al., 2016). Furthermore, influenza strain isolation and propagation for subsequent vaccine production is time-consuming in a pandemic scenario. Especially, if the strain is highly pathogenic, consuming manufacturing capacity or adding complications due to biosafety (Harrington et al., 2021). This is fully circumvented with our MVA platform.

The study here described faced limitations. In fact, we did not measure the capability of our recombinant MVA-IAV vaccines to induce neutralizing antibody responses as work with live influenza viruses were not feasible in our BSL-2 facility. In natural infection, antibodies neutralize the virus in various mechanisms of action (Crowe, 1998). Aggregation of viral particles before attachment is one of them. Antibodies can also block the receptor-binding domain hindering attachment. Binding of antibodies to other parts of HA conveys block in entry. Post-attachment inhibition of viral uncoating is also feasible. Binding to viral proteins of newly formed virions is another possible mechanism which inhibits budding from host cells. Neutralization can be aided by other molecules and cells, e.g., by the complement. For example, phagocytic cells can take up Fc receptor ɣ-mediated antigen-antibody immune complexes. Antibody-dependent cell-mediated cytotoxicity, where, e.g., natural killer cells, guided by antibodies, destroy the infected cell, is a further mechanism of neutralization (Crowe, 1998).

Moreover, there is multiple evidence that maternal antibodies have an inhibitory effect on immune responses to influenza infection and influenza candidate vaccines by suppressing antibody responses (Crowe, 1998). The use of nucleoside-modified mRNA encapsulated in lipid nanoparticles is a promising strategy to avoid inhibitory effects of maternal antibodies on vaccination as explored in one study (Willis et al., 2020). In this study, BALB/c and C57BL/6 mice pups had long-lived germinal centers and a strong antibody response after vaccination. The second limitation of this study was the lack of protective activity investigation. Therefore, animal models are immunized with the candidate vaccines and subsequently inoculated with the live IAV virus to verify if animals were protected from disease. Finally, determination of mucosal IgA was not pursued as this would have gone beyond the scope of our study. This can be achieved by intranasal application of the candidate vaccines for subsequent detection of secretory IgA as previously outlined.

Future perspective

Influenza A virus is still a challenge as it needs to be addressed by seasonal vaccination. Moreover, circulation of IAV in animals and human population gives rise to zoonotic transmission and future pandemics. Hence, influenza A virus is a global public health issue causing disease and deaths. Additionally, it is a burden to national healthcare systems and causes economic damage to our society. Efforts need to be undertaken by various stakeholders to diminish the overall impact of influenza A.

The here described recombinant MVA viruses expressing HA from subtypes H2N9, H2N2 and H5N8 show promise as candidate vaccines against IAV, as the vaccines were genetically stable, and were well-tolerated upon vaccination. All three vaccines induced strong $CD4^+$ and / or $CD8^+$ T cell responses as well as high antibody responses after two immunizations. Future work would include a detailed analysis of the vaccines in a suitable challenge model to assess the protective capacity of the vaccines.

IX. ZUSAMMENFASSUNG

Das Influenza-A-Virus stellt eine große Bedrohung für den Menschen dar und verursacht jährlich eine enorme Anzahl von Krankenhausaufenthalten und Todesfällen. Endemische und pandemische Ereignisse haben schwerwiegende Auswirkungen auf das Gesundheitssystem und führen gleichzeitig zu wirtschaftlichen Verlusten. Das wiederkehrende Auftreten von Influenza-A-Viren in Tierbeständen sowie die steigende Zahl humaner Fälle unterstreichen zudem die Bedeutung der Entwicklung wirksamer Impfstoffe und antiviraler Medikamente gegen das Influenza-A-Virus. Die schnelle Anpassungsfähigkeit von Influenza-A-Viren erschwert jedoch die Entwicklung wirksamer medizinischer Gegenmaßnahmen.

In dieser Studie wird die Erzeugung und präklinische Charakterisierung von rekombinantem MVA beschrieben, welches das vollständige HA-Protein der IAV-Subtypen A/Ruddy/Turnstone/Delaware/374/-2019 (H2N9), A/Singapore/1/-1957 (H2N2) und A/seal/Germany-SH/AI05379/2021 (H5N8) exprimiert. Die In-vitro-Charakterisierung der drei rekombinanten MVA-Impfstoffkandidaten nach etablierten Qualitätskontrollverfahren, einschließlich genetischer Integrität und Stabilität, Replikationsdefizit in humanen Zellen und unbeeinträchtigter Expression der HA-Antigene, lieferte vielversprechende Daten für präklinische Tests an Mäusen. *HLA-A2.1-/HLA-DR1-transgene H-2-Klasse-I-/Klasse-II-Knockout* Mäuse lösten eine robuste HA-Antigen-spezifische $CD4^+$- oder $CD8^+$-T-Zell-Antwort aus. Darüber hinaus induzierten immunisierte Mäuse bereits nach einmaliger Immunisierung HA-Antigen-spezifische Serum-IgG-Antikörper, die nach der Auffrischungsimpfung erhöht werden konnten. Darüber hinaus wurden in den Seren H2N2-immunisierter Mäuse subtypübergreifende Serum-IgG-Antikörper nachgewiesen.

X. SUMMARY

Influenza A virus is a major threat for humans, causing a tremendous number of hospitalizations and deaths each year. Endemic and pandemic events have severe impact on the healthcare system and simultaneously lead to economic loss. Furthermore, recurring emergence of influenza A viruses in animal stocks, in addition to the increasing number of human cases, highlight the importance to develop efficacious vaccines and antivirals against influenza A virus. However, the fast-adapting nature of influenza A viruses hampers the development of effective medical countermeasures.

In this study, the generation and preclinical characterization of recombinant MVA expressing the full-length HA protein of IAV subtypes A/Ruddy/Turnstone/Delaware/374/-2019(H2N9), A/Singapore/1/-1957(H2N2) and A/seal/Germany-SH/AI05379/2021(H5N8), is described. *In vitro* characterization of the three recombinant MVA candidate vaccines following well-established quality control procedures, including genetic integrity and stability, replicative deficiency in human cells, in combination with an unimpaired expression of the HA-antigens, revealed promising data for preclinical testing in mice. *HLA-A2.1-/HLA-DR1-transgenic H-2 class I-/class II-knockout* mice elicited a robust HA-antigen specific $CD4^+$ or $CD8^+$ T cell response. Furthermore, immunized mice induced HA-antigen specific serum IgG antibodies even after a single immunization, which could be increased after the booster immunization. In addition, cross-subtype specific serum IgG antibodies were detected in the sera of H2N2 immunized mice.

XI. REFERENCES

A revision of the system of nomenclature for influenza viruses: a WHO memorandum. (1980). *Bull World Health Organ*, *58*(4), 585-591. https://www.ncbi.nlm.nih.gov/pubmed/6969132

Abaitua, F., Rodríguez, J. R., Garzón, A., Rodríguez, D., & Esteban, M. (2006). Improving recombinant MVA immune responses: Potentiation of the immune responses to HIV-1 with MVA and DNA vectors expressing Env and the cytokines IL-12 and IFN-gamma. *Virus Research*, *116*(1), 11-20. https://doi.org/10.1016/j.virusres.2005.08.008

Alcamí, A., & Smith, G. L. (1992). A soluble receptor for interleukin-1 beta encoded by vaccinia virus: a novel mechanism of virus modulation of the host response to infection. *Cell*, *71*(1), 153-167. https://doi.org/10.10-16/0092-8674(92)90274-g

Alharbi, N. K., Aljamaan, F., Aljami, H. A., Alenazi, M. W., Albalawi, H., Almasoud, A., Alharthi, F. J., Azhar, E. I., Barhoumi, T., Bosaeed, M., Gilbert, S. C., & Hashem, A. M. (2022). Immunogenicity of High-Dose MVA-Based MERS Vaccine Candidate in Mice and Camels. *Vaccines*, *10*(8), 1330. https://www.mdpi.com/2076-393X/10/8/1330

Altenburg, A. F., Kreijtz, J. H., de Vries, R. D., Song, F., Fux, R., Rimmelzwaan, G. F., Sutter, G., & Volz, A. (2014). Modified vaccinia virus ankara (MVA) as production platform for vaccines against influenza and other viral respiratory diseases. *Viruses*, *6*(7), 2735-2761. https://doi.org/10.3390/v6072735

Altenburg, A. F., van de Sandt, C. E., Li, B. W. S., MacLoughlin, R. J., Fouchier, R. A. M., van Amerongen, G., Volz, A., Hendriks, R. W., de Swart, R. L., Sutter, G., Rimmelzwaan, G. F., & de Vries, R. D. (2017). Modified Vaccinia Virus Ankara Preferentially Targets Antigen Presenting Cells In Vitro, Ex Vivo and In Vivo. *Scientific Reports*, *7*(1), 8580. https://doi.org/10.1038/s41598-017-08719-y

Altenburg, A. F., van Trierum, S. E., de Bruin, E., de Meulder, D., van de Sandt, C. E., van der Klis, F. R. M., Fouchier, R. A. M., Koopmans, M. P. G., Rimmelzwaan, G. F., & de Vries, R. D. (2018). Effects of pre-existing orthopoxvirus-specific immunity on the performance of Modified Vaccinia virus Ankara-based influenza vaccines. *Sci Rep*, *8*(1), 6474. https://doi.org/10.1038/s41598-018-24820-2

Antoine, G., Scheiflinger, F., Dorner, F., & Falkner, F. G. (1998). The Complete Genomic Sequence of the Modified Vaccinia Ankara Strain: Comparison with Other Orthopoxviruses. *Virology*, *244*(2), 365-396. https://doi.org/10.1006/viro.1998.9123

Backes, S., Sperling, K. M., Zwilling, J., Gasteiger, G., Ludwig, H., Kremmer, E., Schwantes, A., Staib, C., & Sutter, G. (2010). Viral host-range factor C7 or K1 is essential for modified vaccinia virus Ankara late gene expression in human and murine cells, irrespective of their capacity to inhibit protein kinase R-mediated phosphorylation of eukaryotic translation initiation factor 2alpha. *J Gen Virol*, *91*(Pt 2), 470-482. https://doi.org/10.1099/vir.0.015347-0

Beigel, J. H., Farrar, J., Han, A. M., Hayden, F. G., Hyer, R., de Jong, M. D., Lochindarat, S., Nguyen, T. K., Nguyen, T. H., Tran, T. H., Nicoll, A., Touch, S., & Yuen, K. Y. (2005). Avian influenza A (H5N1) infection in humans. *N Engl J Med*, *353*(13), 1374-1385. https://doi.org/10.10-56/NEJMra052211

Bertram, S., Glowacka, I., Steffen, I., Kühl, A., & Pöhlmann, S. (2010). Novel insights into proteolytic cleavage of influenza virus hemagglutinin. *Reviews in Medical Virology*, *20*(5), 298-310. https://doi.org/ /10.1002/rmv.657

Bisht, H., Roberts, A., Vogel, L., Bukreyev, A., Collins, P. L., Murphy, B. R., Subbarao, K., & Moss, B. (2004). Severe acute respiratory syndrome coronavirus spike protein expressed by attenuated vaccinia virus protectively immunizes mice. *Proc Natl Acad Sci U S A*, *101*(17), 6641-6646. https://doi.org/10.1073/pnas.0401939101

Borkenhagen, L. K., Wang, G. L., Simmons, R. A., Bi, Z. Q., Lu, B., Wang, X. J., Wang, C. X., Chen, S. H., Song, S. X., Li, M., Zhao, T., Wu, M. N., Park, L. P., Cao, W. C., Ma, M. J., & Gray, G. C. (2020). High Risk of Influenza Virus Infection Among Swine Workers: Examining a Dynamic Cohort in China. *Clin Infect Dis*, *71*(3), 622-629. https://doi.org/10.1093/cid/ciz865

Bošnjak, B., Odak, I., Barros-Martins, J., Sandrock, I., Hammerschmidt, S. I., Permanyer, M., Patzer, G. E., Greorgiev, H., Gutierrez Jauregui, R., Tscherne, A., Schwarz, J. H., Kalodimou, G., Ssebyatika, G., Ciurkiewicz, M., Willenzon, S., Bubke, A., Ristenpart, J., Ritter, C., Tuchel, T., . . . Förster, R. (2021). Intranasal Delivery of MVA Vector Vaccine Induces Effective Pulmonary Immunity Against SARS-CoV-2 in Rodents. Front Immunol, 12, 772240. https://doi.org/10.3389/fimmu.2021.772240

Bouvier, N. M., & Palese, P. (2008). The biology of influenza viruses. *Vaccine*, *26 Suppl 4*(Suppl 4), D49-53. https://doi.org/10.1016/j.vaccine.2008.07.039

Brüssow, H. (2024). The Arrival of Highly Pathogenic Avian Influenza Viruses in North America, Ensuing Epizootics in Poultry and Dairy Farms and Difficulties in Scientific Naming. *Microb Biotechnol*, *17*(12), e70062. https://doi.org/10.1111/1751-7915.70062

Buckland, B. C. (2015). The development and manufacture of influenza vaccines. Human Vaccines & Immunotherapeutics, 11(6), 1357-1360. https://doi.org/10.1080/21645515.2015.1026497

Burrough, E. R., Magstadt, D. R., Petersen, B., Timmermans, S. J., Gauger, P. C., Zhang, J., Siepker, C., Mainenti, M., Li, G., Thompson, A. C., Gorden, P. J., Plummer, P. J., & Main, R. (2024). Highly Pathogenic Avian Influenza A(H5N1) Clade 2.3.4.4b Virus Infection in Domestic Dairy Cattle and Cats, United States, 2024. *Emerg Infect Dis*, *30*(7), 1335-1343. https://doi.org/10.3201/eid3007.240508

Capelle, M. A. H., Babich, L., van Deventer-Troost, J. P. E., Salerno, D., Krijgsman, K., Dirmeier, U., Raaby, B., & Adriaansen, J. (2018). Stability and suitability for storage and distribution of Ad26.ZEBOV/MVA-BN®-Filo heterologous prime-boost Ebola vaccine. *Eur J Pharm Biopharm*, *129*, 215-221. https://doi.org/10.1016/j.ejpb.2018.06.001

Capone, S., Brown, A., Hartnell, F., Sorbo, M. D., Traboni, C., Vassilev, V., Colloca, S., Nicosia, A., Cortese, R., Folgori, A., Klenerman, P., Barnes, E., & Swadling, L. (2020). Optimising T cell (re)boosting strategies for adenoviral and modified vaccinia Ankara vaccine regimens in humans. *npj Vaccines*, *5*(1), 94. https://doi.org/10.1038/s41541-020-00240-0

Castilla, J., Martínez-Baz, I., Martínez-Artola, V., Reina, G., Pozo, F., Cenoz, M. G., Guevara, M., Moran, J., Irisarri, F., & Arriazu, M. (2013). Decline in influenza vaccine effectiveness with time after vaccination, Navarre, Spain, season 2011/12. *Eurosurveillance*, *18*(5), 20388.

CDC, CDC Seasonal Flu Vaccine Effectiveness, August 2024. https://www.cdc.gov/flu-vaccines-work/php/effectiveness-studies/index.html

CDC, Trivalent Influenza Vaccines, September 2024. https://www.cdc.gov/flu/vaccine-types/trivalent.html

CDC, US Will Transition to Trivalent Flu Vaccines for 2024-2025, March 2024. https://www.cdc.gov/flu/whats-new/trivalent-vaccines-2024-2025.html

CDC., CDC A(H5N1) Bird Flu Response Update, February 2025. https://www.cdc.gov/bird-flu/spotlights/h5n1-response-02262025.html

Chan, L., Alizadeh, K., Alizadeh, K., Fazel, F., Kakish, J. E., Karimi, N., Knapp, J. P., Mehrani, Y., Minott, J. A., Morovati, S., Rghei, A., Stegelmeier, A. A., Vanderkamp, S., Karimi, K., & Bridle, B. W. (2021). Review of Influenza Virus Vaccines: The Qualitative Nature of Immune Responses to Infection and Vaccination Is a Critical Consideration. *Vaccines*, *9*(9), 979. https://www.mdpi.com/2076-393X/9/9/979

Chen, Z., Zhang, L., Qin, C., Ba, L., Yi, C. E., Zhang, F., Wei, Q., He, T., Yu, W., Yu, J., Gao, H., Tu, X., Gettie, A., Farzan, M., Yuen, K. Y., & Ho, D. D. (2005). Recombinant modified vaccinia virus Ankara expressing the spike glycoprotein of severe acute respiratory syndrome coronavirus induces protective neutralizing antibodies primarily targeting the receptor binding region. *J Virol*, *79*(5), 2678-2688. https://doi.org/10.1128/jvi.79.5.2678-2688.2005

Cheung, T. K., & Poon, L. L. (2007). Biology of influenza a virus. *Ann N Y Acad Sci*, *1102*, 1-25. https://doi.org/10.1196/annals.1408.001

Choi, E. M., Kasonia, K., Kavunga-Membo, H., Mukadi-Bamuleka, D., Soumah, A., Mossoko, Z., Edwards, T., Tetsa-Tata, D., Makarimi, R., Toure, O., Mambula, G., Brindle, H., Camacho, A., Connor, N. E., Mukadi, P., McLean, C., Keshinro, B., Gaddah, A., Robinson, C., . . . Muyembe-Tamfum, J. J. (2024). Immunogenicity of an Extended Dose Interval for the Ad26.ZEBOV, MVA-BN-Filo Ebola Vaccine Regimen in Adults and Children in the Democratic Republic of the Congo. *Vaccines (Basel)*, *12*(8). https://doi.org/10.3390/vaccines12080828

Cottingham, M. G., & Carroll, M. W. (2013). Recombinant MVA vaccines: dispelling the myths. *Vaccine*, *31*(39), 4247-4251. https://doi.org/10.1016/j.vaccine.2013.03.021

Crommelin, D. J. A., Anchordoquy, T. J., Volkin, D. B., Jiskoot, W., & Mastrobattista, E. (2021). Addressing the Cold Reality of mRNA Vaccine Stability. *J Pharm Sci*, *110*(3), 997-1001. https://doi.org/10.1016/j.xphs.2020.12.006

Cross, K. J., Langley, W. A., Russell, R. J., Skehel, J. J., & Steinhauer, D. A. (2009). Composition and functions of the influenza fusion peptide. *Protein Pept Lett*, *16*(7), 766-778. https://doi.org/10.2174/092986609788681715

Crowe, J. E. (1998). Immune responses of infants to infection with respiratory viruses and live attenuated respiratory virus candidate vaccines. *Vaccine*, *16*(14), 1423-1432. https://doi.org/10.1016/S0264-410X(98)00103-0

Crowe, J. E. (2017). 122 - Host Defense Mechanisms Against Viruses. In R. A. Polin, S. H. Abman, D. H. Rowitch, W. E. Benitz, & W. W. Fox (Eds.), *Fetal and Neonatal Physiology (Fifth Edition)* (pp. 1175-1197.e1177). Elsevier. https://doi.org/10.1016/B978-0-323-35214-7.00122-0

Damon, I. K. (2011). Poxviruses. In *Manual of Clinical Microbiology* (pp. 1647-1658). https://doi.org/10.1128/9781555816728.ch105

Dhanda, S. K., Mahajan, S., Paul, S., Yan, Z., Kim, H., Jespersen, M. C., Jurtz, V., Andreatta, M., Greenbaum, J. A., Marcatili, P., Sette, A., Nielsen, M., & Peters, B. (2019). IEDB-AR: immune epitope database—analysis resource in 2019. Nucleic Acids Research, 47(W1), W502-W506. https://doi.org/10.1093/nar/gkz452

Dönnes, P., & Kohlbacher, O. (2005). Integrated modeling of the major events in the MHC class I antigen processing pathway. *Protein Science*, *14*(8), 2132-2140. https://doi.org/10.1110/ps.051352405

Döring, M., De Azevedo, K., Blanco-Rodriguez, G., Nadalin, F., Satoh, T., Gentili, M., Lahaye, X., De Silva, N. S., Conrad, C., Jouve, M., Centlivre, M., Lévy, Y., & Manel, N. (2021). Single-cell analysis reveals divergent responses of human dendritic cells to the MVA vaccine. *Sci Signal*, *14*(697). https://doi.org/10.1126/scisignal.abd9720

Drexler, I., Antunes, E., Schmitz, M., Wölfel, T., Huber, C., Erfle, V., Rieber, P., Theobald, M., & Sutter, G. (1999). Modified vaccinia virus Ankara for delivery of human tyrosinase as melanoma-associated antigen: induction of tyrosinase- and melanoma-specific human leukocyte antigen A*0201-restricted cytotoxic T cells in vitro and in vivo. *Cancer Res*, *59*(19), 4955-4963.

Duffy, J., Marquez, P., Moro, P., Weintraub, E., Yu, Y., Boersma, P., Donahue, J. G., Glanz, J. M., Goddard, K., Hambidge, S. J., Lewin, B., Lewis, N., Rouse, D., & Shimabukuro, T. (2022). Safety Monitoring of JYNNEOS Vaccine During the 2022 Mpox Outbreak - United States, May 22-October 21, 2022. *MMWR Morb Mortal Wkly Rep*, *71*(49), 1555-1559. https://doi.org/10.15585/mmwr.mm7149a4

Durbin, A. P., Cho, C. J., Elkins, W. R., Wyatt, L. S., Moss, B., & Murphy, B. R. (1999). Comparison of the immunogenicity and efficacy of a replication-defective vaccinia virus expressing antigens of human parainfluenza virus type 3 (HPIV3) with those of a live attenuated HPIV3 vaccine candidate in rhesus monkeys passively immunized with PIV3 antibodies. *J Infect Dis*, *179*(6), 1345-1351. https://doi.org/10.1086/314769

Durbin, A. P., Wyatt, L. S., Siew, J., Moss, B., & Murphy, B. R. (1998). The immunogenicity and efficacy of intranasally or parenterally administered replication-deficient vaccinia-parainfluenza virus type 3 recombinants in rhesus monkeys. *Vaccine*, *16*(13), 1324-1330. https://doi.org/10.10-16/s0264-410x(98)00010-3

ECDC, Testing and detection of zoonotic influenza virus infections in humans in the EU/EEA, and occupational safety and health measures for those exposed at work, October 2022. https://www.ecdc.europa.eu/en/publications-data/zoonotic-influenza-virus-infections-humans-testing-and-detection

EFSA, Avian influenza: increased spread in poultry-dense areas at end 2024, December 2024. https://www.efsa.europa.eu/en/news/avian-influenza-increased-spread-poultry-dense-areas-end-2024

EFSA, Avian influenza: unprecedented number of summer cases in Europe, October 2022. https://www.efsa.europa.eu/en/news/avian-influenza-unprecedented-number-summer-cases-europe

Eisfeld, A. J., Neumann, G., & Kawaoka, Y. (2014). Influenza A virus isolation, culture and identification. *Nature Protocols*, *9*(11), 2663-2681. https://doi.org/10.1038/nprot.2014.180

EMA, EU recommendations for 2024/2025 seasonal flu vaccine composition, March 2024. https://www.ema.europa.eu/en/news/eu-recommendations-2024-2025-seasonal-flu-vaccine-composition

EMA, Imvanex: EPAR – Product information, 2013. https://www.ema.europa.eu/en/medicin-es/human/EPAR/imvanex

EMA, Mvabea: EPAR – Product information, 2020. https://www.ema.eur-opa.eu/en/medicin-es/human/EPAR/mvabea

Endt, K., Wollmann, Y., Haug, J., Bernig, C., Feigl, M., Heiseke, A., Kalla, M., Hochrein, H., Suter, M., Chaplin, P., & Volkmann, A. (2022). A Recombinant MVA-Based RSV Vaccine Induces T-Cell and Antibody Responses That Cooperate in the Protection Against RSV Infection. Front Immunol, 13, 841471. https://doi.org/10.3389/fimmu.2022.841471

Erbs, P., Findeli, A., Kintz, J., Cordier, P., Hoffmann, C., Geist, M., & Balloul, J. M. (2008). Modified vaccinia virus Ankara as a vector for suicide gene therapy. *Cancer Gene Ther*, *15*(1), 18-28. https://doi.org/10.1038/sj.cgt.7701098

Escalante, G. M., Reidel, I. G., Mutsvunguma, L. Z., Cua, S., Tello, B. A., Rodriguez, E., Farelo, M. A., Zimmerman, C., Muniraju, M., Li, H., Govindan, A. N., Axthelm, M. K., Wong, S. W., & Ogembo, J. G. (2024). Multivalent MVA-vectored vaccine elicits EBV neutralizing antibodies in rhesus macaques that reduce EBV infection in humanized mice. *Front Immunol*, *15*, 1445209. https://doi.org/10.3389/fimmu.2024.1445209

Fink, G., Orlova-Fink, N., Schindler, T., Grisi, S., Ferrer, A. P. S., Daubenberger, C., & Brentani, A. (2020). Inactivated trivalent influenza vaccination is associated with lower mortality among patients with COVID-19 in Brazil. BMJ Evid Based Med. https://doi.org/10.1136/bmjebm-2020-111549

Gilbert, S. C. (2013). Clinical development of Modified Vaccinia virus Ankara vaccines. *Vaccine*, *31*(39), 4241-4246. https://doi.org/10.1016/j.vaccine.2013.03.020

Gillard, S., Spehner, D., Drillien, R., & Kirn, A. (1986). Localization and sequence of a vaccinia virus gene required for multiplication in human cells. *Proceedings of the National Academy of Sciences*, *83*(15), 5573-5577. https://doi.org/doi:10.1073/pnas.83.15.5573

Globig, A., Staubach, C., Sauter-Louis, C., Dietze, K., Homeier-Bachmann, T., Probst, C., Gethmann, J., Depner, K. R., Grund, C., Harder, T. C., Starick, E., Pohlmann, A., Höper, D., Beer, M., Mettenleiter, T. C., & Conraths, F. J. (2018). Highly Pathogenic Avian Influenza H5N8 Clade 2.3.4.4b in Germany in 2016/2017 [Original Research]. *Frontiers in Veterinary Science*, *4*. https://doi.org/10.3389/fvets.2017.00240

Goneau, L. W., Mehta, K., Wong, J., L'Huillier, A. G., & Gubbay, J. B. (2018). Zoonotic Influenza and Human Health-Part 1: Virology and Epidemiology of Zoonotic Influenzas. *Curr Infect Dis Rep*, *20*(10), 37. https://doi.org/10.10-07/s11908-018-0642-9

Goodwin, K., Viboud, C., & Simonsen, L. (2006). Antibody response to influenza vaccination in the elderly: a quantitative review. *Vaccine*, *24*(8), 1159-1169. https://doi.org/10.1016/j.vaccine.2005.08.105

Goonetilleke, N. P., McShane, H., Hannan, C. M., Anderson, R. J., Brookes, R. H., & Hill, A. V. (2003). Enhanced immunogenicity and protective efficacy against Mycobacterium tuberculosis of bacille Calmette-Guérin vaccine using mucosal administration and boosting with a recombinant modified vaccinia virus Ankara. *J Immunol*, *171*(3), 1602-1609. https://doi.org/10.40-49/jimmunol.171.3.1602

Gränicher, G., Tapia, F., Behrendt, I., Jordan, I., Genzel, Y., & Reichl, U. (2021). Production of Modified Vaccinia Ankara Virus by Intensified Cell Cultures: A Comparison of Platform Technologies for Viral Vector Production. *Biotechnol J*, *16*(1), e2000024. https://doi.org/10.1002/biot.20-2000024

Grant, E. J., Chen, L., Quiñones-Parra, S., Pang, K., Kedzierska, K., & Chen, W. (2014). T-cell immunity to influenza A viruses. *Crit Rev Immunol*, *34*(1), 15-39. https://doi.org/10.1615/critrevimmunol.2013010019

Greseth, M. D., & Traktman, P. (2022). The Life Cycle of the Vaccinia Virus Genome. *Annual Review of Virology*, *9*(Volume 9, 2022), 239-259. https://doi.org/10.1146/annurev-virology-091919-104752

Guillot, L., Le Goffic, R., Bloch, S., Escriou, N., Akira, S., Chignard, M., & Si-Tahar, M. (2005). Involvement of toll-like receptor 3 in the immune response of lung epithelial cells to double-stranded RNA and influenza A virus. *J Biol Chem*, *280*(7), 5571-5580. https://doi.org/10.1074/jbc.M41059-2200

Guo, J., Chen, X., Guo, Y., Liu, M., Li, P., Tao, Y., Liu, Z., Yang, Z., Zhan, S., & Sun, F. (2024). Real-world effectiveness of seasonal influenza vaccination and age as effect modifier: A systematic review, meta-analysis and meta-regression of test-negative design studies. *Vaccine*, *42*(8), 1883-1891. https://doi.org/10.1016/j.vaccine.2024.02.059

Hamamoto, I., Takaku, H., Tashiro, M., & Yamamoto, N. (2013). High yield production of influenza virus in Madin Darby canine kidney (MDCK) cells with stabletable knockdown of IRF7. *PLoS One*, *8*(3), e59892. https://doi.org/10.1371/journal.pone.0059892

Harrington, W. N., Kackos, C. M., & Webby, R. J. (2021). The evolution and future of influenza pandemic preparedness. *Exp Mol Med*, *53*(5), 737-749. https://doi.org/10.1038/s12276-021-00603-0

He, W.-T., Wang, L., Zhao, Y., Wang, N., Li, G., Veit, M., Bi, Y., Gao, G. F., & Su, S. (2020). Adaption and parallel evolution of human-isolated H5 avian influenza viruses. *Journal of Infection*, *80*(6), 630-638. https://doi.org/10.1016/j.jinf.2020.01.012

Heida, R., Frijlink, H. W., & Hinrichs, W. L. J. (2023). Inhalation of vaccines and antiviral drugs to fight respiratory virus infections: reasons to prioritize the pulmonary route of administration. *mBio*, *14*(5), e0129523. https://doi.org/10.1128/mbio.01295-23

Henderson, D. A., Inglesby, T. V., Bartlett, J. G., Ascher, M. S., Eitzen, E., Jahrling, P. B., Hauer, J., Layton, M., McDade, J., Osterholm, M. T., O'Toole, T., Parker, G., Perl, T., Russell, P. K., & Tonat, K. (1999). Smallpox as a biological weapon: medical and public health management. Working Group on Civilian Biodefense. *Jama*, *281*(22), 2127-2137. https://doi.org/10.1001/jama.281.22.2127

Herrlich, A., & Mayr, A. (1954). [Comparative experimental works on cow pox virus vaccines]. *Arch Hyg Bakteriol*, *138*(7), 479-504. (Vergleichende experimentelle Arbeiten über die Vaccine-Kuhpocken-Viren.)

Husain, M., & Moss, B. (2002). Similarities in the induction of post-Golgi vesicles by the vaccinia virus F13L protein and phospholipase D. J Virol, 76(15), 7777-7789. https://doi.org/10.1128/jvi.76.15.7777-7789.2002

ICTV, 2024. https://ictv.global/taxonomy

Isakova-Sivak, I., & Rudenko, L. (2022). The future of haemagglutinin stalk-based universal influenza vaccines. *The Lancet Infectious Diseases*, *22*(7), 926-928. https://doi.org/10.1016/S1473-3099(22)00056-1

Javanian, M., Barary, M., Ghebrehewet, S., Koppolu, V., Vasigala, V., & Ebrahimpour, S. (2021). A brief review of influenza virus infection. *J Med Virol*, *93*(8), 4638-4646. https://doi.org/10.1002/jmv.26990

Jones, J. C., Baranovich, T., Marathe, B. M., Danner, A. F., Seiler, J. P., Franks, J., Govorkova, E. A., Krauss, S., & Webster, R. G. (2014). Risk assessment of H2N2 influenza viruses from the avian reservoir. *J Virol*, *88*(2), 1175-1188. https://doi.org/10.1128/jvi.02526-13

Jordan, I., Vos, A., Beilfuss, S., Neubert, A., Breul, S., & Sandig, V. (2009). An avian cell line designed for production of highly attenuated viruses. *Vaccine*, *27*(5), 748-756. https://doi.org/10.1016/j.vaccine.2008.11.066

Kalodimou, G., Veit, S., Jany, S., Kalinke, U., Broder, C. C., Sutter, G., & Volz, A. (2019). A Soluble Version of Nipah Virus Glycoprotein G Delivered by Vaccinia Virus MVA Activates Specific CD8 and CD4 T Cells in Mice. *Viruses*, *12*(1). https://doi.org/10.3390/v12010026

Kang, I., Hong, M. S., Nolasco, H., Park, S. H., Dan, J. M., Choi, J.-Y., & Craft, J. (2004). Age-associated change in the frequency of memory CD4+ T cells impairs long term CD4+ T cell responses to influenza vaccine. *The Journal of Immunology*, *173*(1), 673-681.

Kennedy, J. S., & Greenberg, R. N. (2009). IMVAMUNE: modified vaccinia Ankara strain as an attenuated smallpox vaccine. *Expert Rev Vaccines*, *8*(1), 13-24. https://doi.org/10.1586/14760584.8.1.13

Kessler, S., Harder, T. C., Schwemmle, M., & Ciminski, K. (2021). Influenza A Viruses and Zoonotic Events-Are We Creating Our Own Reservoirs? *Viruses*, *13*(11). https://doi.org/10.3390/v13112250

Khmer Times, 2 year old child dies from bird flu in Cambodia, February 2025. https://www.khmertimeskh.com/501645670/2-year-child-dies-from-bird-flu-in-cambodia/

Kim, E. H., Kwon, H. I., Park, S. J., Kim, Y. I., Si, Y. J., Lee, I. W., Kim, S. M., Kim, S. I., Ahn, D. H., & Choi, Y. K. (2018). Generation of a High-Growth Influenza Vaccine Strain in MDCK Cells for Vaccine Preparedness. *J Microbiol Biotechnol*, *28*(6), 997-1006. https://doi.org/10.4014/jmb.17-12.12007

King, J., Harder, T., Conraths, F. J., Beer, M., & Pohlmann, A. (2021). The genetics of highly pathogenic avian influenza viruses of subtype H5 in Germany, 2006-2020. *Transbound Emerg Dis*, *68*(3), 1136-1150. https://doi.org/10.1111/tbed.13843

Koch, T., Dahlke, C., Fathi, A., Kupke, A., Krähling, V., Okba, N. M. A., Halwe, S., Rohde, C., Eickmann, M., Volz, A., Hesterkamp, T., Jambrecina, A., Borregaard, S., Ly, M. L., Zinser, M. E., Bartels, E., Poetsch, J. S. H., Neumann, R., Fux, R., . . . Addo, M. M. (2020). Safety and immunogenicity of a modified vaccinia virus Ankara vector vaccine candidate for Middle East respiratory syndrome: an open-label, phase 1 trial. *Lancet Infect Dis*, *20*(7), 827-838. https://doi.org/10.1016/s1473-3099(20)30248-6

Krammer, F., Smith, G. J. D., Fouchier, R. A. M., Peiris, M., Kedzierska, K., Doherty, P. C., Palese, P., Shaw, M. L., Treanor, J., Webster, R. G., & García-Sastre, A. (2018). Influenza. *Nature Reviews Disease Primers*, *4*(1), 3. https://doi.org/10.1038/s41572-018-0002-y

Kreijtz, J. H., Goeijenbier, M., Moesker, F. M., van den Dries, L., Goeijenbier, S., De Gruyter, H. L., Lehmann, M. H., Mutsert, G., van de Vijver, D. A., Volz, A., Fouchier, R. A., van Gorp, E. C., Rimmelzwaan, G. F., Sutter, G., & Osterhaus, A. D. (2014). Safety and immunogenicity of a modified-vaccinia-virus-Ankara-based influenza A H5N1 vaccine: a randomised, double-blind phase 1/2a clinical trial. *Lancet Infect Dis*, *14*(12), 1196-1207. https://doi.org/10.1016/s1473-3099(14)70963-6

Kremer, M., Volz, A., Kreijtz, J. H., Fux, R., Lehmann, M. H., & Sutter, G. (2012). Easy and efficient protocols for working with recombinant vaccinia virus MVA. *Methods Mol Biol*, *890*, 59-92. https://doi.org/10.1007/978-1-61779-876-4_4

Kubinski, M., Beicht, J., Zdora, I., Biermann, J., Puff, C., Gerlach, T., Tscherne, A., Baumgärtner, W., Osterhaus, A., Sutter, G., Prajeeth, C. K., & Rimmelzwaan, G. F. (2023). A recombinant Modified Vaccinia virus Ankara expressing prME of tick-borne encephalitis virus affords mice full protection against TBEV infection. *Front Immunol*, *14*, 1182963. https://doi.org/10.3389/fimmu.2023.1182963

Kuiken, T., Fouchier, R. A. M., & Koopmans, M. P. G. (2023). Being ready for the next influenza pandemic? *Lancet Infect Dis*, *23*(4), 398-399. https://doi.org/10.1016/s1473-3099(23)00117-2

Langenmayer, M. C., Luelf-Averhoff, A. T., Marr, L., Jany, S., Freudenstein, A., Adam-Neumair, S., Tscherne, A., Fux, R., Rojas, J. J., Blutke, A., Sutter, G., & Volz, A. (2023). Newly Designed Poxviral Promoters to Improve Immunogenicity and Efficacy of MVA-NP Candidate Vaccines against Lethal Influenza Virus Infection in Mice. *Pathogens*, *12*(7). https://doi.org/10.3390/pathogens12070867

Laurie, K. L., & Rockman, S. (2021). Which influenza viruses will emerge following the SARS-CoV-2 pandemic? *Influenza Other Respir Viruses*, *15*(5), 573-576. https://doi.org/10.1111/irv.12866

Le Sage, V., Rockey, N. C., French, A. J., McBride, R., McCarthy, K. R., Rigatti, L. H., Shephard, M. J., Jones, J. E., Walter, S. G., Doyle, J. D., Xu, L., Barbeau, D. J., Wang, S., Frizzell, S. A., Myerburg, M. M., Paulson, J. C., McElroy, A. K., Anderson, T. K., Vincent Baker, A. L., & Lakdawala, S. S. (2024). Potential pandemic risk of circulating swine H1N2 influenza viruses. *Nat Commun*, *15*(1), 5025. https://doi.org/10.1038/s41467-024-49117-z

Leentjens, J., Kox, M., Stokman, R., Gerretsen, J., Diavatopoulos, D. A., van Crevel, R., Rimmelzwaan, G. F., Pickkers, P., & Netea, M. G. (2015). BCG Vaccination Enhances the Immunogenicity of Subsequent Influenza Vaccination in Healthy Volunteers: A Randomized, Placebo-Controlled Pilot Study. J Infect Dis, 212(12), 1930-1938. https://doi.org/10.1093/infdis/jiv332

Lehmann, M. H., Kastenmuller, W., Kandemir, J. D., Brandt, F., Suezer, Y., & Sutter, G. (2009). Modified vaccinia virus ankara triggers chemotaxis of monocytes and early respiratory immigration of leukocytes by induction of CCL2 expression. *J Virol*, *83*(6), 2540-2552. https://doi.org/10.1128/jvi.018-84-08

Léon, A., David, A.-L., Madeline, B., Guianvarc'h, L., Dureau, E., Champion-Arnaud, P., Hebben, M., Huss, T., Chatrenet, B., & Schwamborn, K. (2016). The EB66® cell line as a valuable cell substrate for MVA-based vaccines production. *Vaccine*, *34*(48), 5878-5885. https://doi.org/10.1016/j.vaccine.2016.10.043

Li, H., Zhu, J., Qin, W., Wang, Z., Xie, S., Zhang, Z., Wang, J., Song, B., Wu, W., & Peng, C. (2025). Modified Vaccinia Virus Ankara Selectively Targets Human Cancer Cells With Low Expression of the Zinc-Finger Antiviral Protein. *J Med Virol*, *97*(1), e70131. https://doi.org/10.1002/jmv.70131

Li, Y.-T., Linster, M., Mendenhall, I. H., Su, Y. C. F., & Smith, G. J. D. (2019). Avian influenza viruses in humans: lessons from past outbreaks. *British Medical Bulletin*, *132*(1), 81-95. https://doi.org/10.1093/bmb/ldz036

Lim, C. M. L., Komarasamy, T. V., Adnan, N., Radhakrishnan, A. K., & Balasubramaniam, V. (2024). Recent Advances, Approaches and Challenges in the Development of Universal Influenza Vaccines. *Influenza Other Respir Viruses*, *18*(3), e13276. https://doi.org/10.1111/irv.13276

Lycett, S. J., Duchatel, F., & Digard, P. (2019). A brief history of bird flu. *Philos Trans R Soc Lond B Biol Sci*, *374*(1775), 20180257. https://doi.org/10.1098/rstb.2018.0257

Mahnel, H., & Mayr, A. (1994). [Experiences with immunization against orthopox viruses of humans and animals using vaccine strain MVA]. *Berl Munch Tierarztl Wochenschr*, *107*(8), 253-256. (Erfahrungen bei der Schutzimpfung gegen Orthopocken von Mensch und Tier mit dem Impfstamm MVA.)

Martins, J. P., Santos, M., Martins, A., Felgueiras, M., & Santos, R. (2023). Seasonal Influenza Vaccine Effectiveness in Persons Aged 15-64 Years: A Systematic Review and Meta-Analysis. *Vaccines (Basel)*, *11*(8). https://doi.org/10.3390/vaccines11081322

Mason, L. M. K., Betancur, E., Riera-Montes, M., Lienert, F., & Scheele, S. (2024). MVA-BN vaccine effectiveness: A systematic review of real-world evidence in outbreak settings. *Vaccine*, *42*(26), 126409. https://doi.org/10.1016/j.vaccine.2024.126409

Mayr, A., Hochstein-Mintzel, V., & Stickl, H. (1975). Abstammung, eigenschaften und verwendung des attenuierten vaccinia-stammes MVA. Infection, 3(1), 6-14.

McArthur, D. B. (2019). Emerging Infectious Diseases. *Nurs Clin North Am*, *54*(2), 297-311. https://doi.org/10.1016/j.cnur.2019.02.006

McAuley, J. L., Gilbertson, B. P., Trifkovic, S., Brown, L. E., & McKimm-Breschkin, J. L. (2019). Influenza Virus Neuraminidase Structure and Functions [Review]. *Frontiers in Microbiology*, *10*. https://doi.org/10.33-89/fmicb.2019.00039

Mehta, A. K., Gracias, D. T., & Croft, M. (2018). TNF activity and T cells. *Cytokine*, *101*, 14-18. https://doi.org/10.1016/j.cyto.2016.08.003

Mehta, K., Goneau, L. W., Wong, J., L'Huillier, A. G., & Gubbay, J. B. (2018). Zoonotic Influenza and Human Health-Part 2: Clinical Features, Diagnosis, Treatment, and Prevention Strategies. *Curr Infect Dis Rep*, *20*(10), 38. https://doi.org/10.1007/s11908-018-0643-8

Meng, X., Embry, A., Rose, L., Yan, B., Xu, C., & Xiang, Y. (2012). Vaccinia virus A6 is essential for virion membrane biogenesis and localization of virion membrane proteins to sites of virion assembly. *J Virol*, *86*(10), 5603-5613. https://doi.org/10.1128/jvi.00330-12

Meng, X., Embry, A., Sochia, D., & Xiang, Y. (2007). Vaccinia virus A6L encodes a virion core protein required for formation of mature virion. *J Virol*, *81*(3), 1433-1443. https://doi.org/10.1128/jvi.02206-06

Meyer, H., Sutter, G., & Mayr, A. (1991). Mapping of deletions in the genome of the highly attenuated vaccinia virus MVA and their influence on virulence. *Journal of General Virology*, *72*(5), 1031-1038. https://doi.org/10.10-99/0022-1317-72-5-1031

Modrow S. et al., Molekulare Virologie, *Spektrum*, 2021. ISBN 978-3-8274-1833-3

Moghadami, M. (2017). A Narrative Review of Influenza: A Seasonal and Pandemic Disease. *Iran J Med Sci*, *42*(1), 2-13. https://pmc.ncbi.nlm.nih.gov/articles/PMC5337761/pdf/IJMS-42-2.pdf

Mosmann, T. R., McMichael, A. J., LeVert, A., McCauley, J. W., & Almond, J. W. (2024). Opportunities and challenges for T cell-based influenza vaccines. *Nat Rev Immunol*, *24*(10), 736-752. https://doi.org/10.1038/s415-77-024-01030-8

Moss, B. (2006). Poxvirus entry and membrane fusion. *Virology*, *344*(1), 48-54. https://doi.org/10.1016/j.virol.2005.09.037

Moussatche, N., & Condit, R. C. (2015). Fine structure of the vaccinia virion determined by controlled degradation and immunolocalization. *Virology*, *475*, 204-218. https://doi.org/10.1016/j.virol.2014.11.020

Nachbagauer, R., & Palese, P. (2020). Is a Universal Influenza Virus Vaccine Possible? *Annual Review of Medicine*, *71*(Volume 71, 2020), 315-327. https://doi.org/10.1146/annurev-med-120617-041310

Nave, L., Margalit, I., Tau, N., Cohen, I., Yelin, D., Lienert, F., & Yahav, D. (2023). Immunogenicity and Safety of Modified Vaccinia Ankara (MVA) Vaccine-A Systematic Review and Meta-Analysis of Randomized Controlled Trials. *Vaccines (Basel)*, *11*(9). https://doi.org/10.3390/vaccines11091410

Nelson, M. I., & Vincent, A. L. (2015). Reverse zoonosis of influenza to swine: new perspectives on the human–animal interface. *Trends in Microbiology*, *23*(3), 142-153. https://doi.org/10.1016/j.tim.2014.12.002

Nilsson, J. B., Kaabinejadian, S., Yari, H., Kester, M. G. D., van Balen, P., Hildebrand, W. H., & Nielsen, M. (2023). Accurate prediction of HLA class II antigen presentation across all loci using tailored data acquisition and refined machine learning. *Science Advances*, *9*(47), eadj6367. https://doi.org/doi:10.1126/sciadv.adj6367

Nuwarda, R. F., Alharbi, A. A., & Kayser, V. (2021). An Overview of Influenza Viruses and Vaccines. Vaccines (Basel), 9(9). https://doi.org/10.3390/vaccines9091032

Pajot, A., Michel, M. L., Fazilleau, N., Pancre, V., Auriault, C., Ojcius, D. M., Lemonnier, F. A., & Lone, Y. C. (2004). A mouse model of human adaptive immune functions: HLA-A2.1-/HLA-DR1-transgenic H-2 class I-/class II-knockout mice. *Eur J Immunol*, *34*(11), 3060-3069. https://doi.org/10.1002/eji.200425463

PEI, Influenza (Flu) Vaccines, accessed March 2025. https://www.pei.de/EN/medicinal-products/vaccines-human/influenza-flu/influenza-flu-node.html

Perkus, M. E., Goebel, S. J., Davis, S. W., Johnson, G. P., Limbach, K., Norton, E. K., & Paoletti, E. (1990). Vaccinia virus host range genes. *Virology*, *179*(1), 276-286. https://doi.org/10.1016/0042-6822(90)90296-4

Pollard, A. J., & Bijker, E. M. (2021). A guide to vaccinology: from basic principles to new developments. *Nature Reviews Immunology*, *21*(2), 83-100. https://doi.org/10.1038/s41577-020-00479-7

Postel, A., King, J., Kaiser, F. K., Kennedy, J., Lombardo, M. S., Reineking, W., de le Roi, M., Harder, T., Pohlmann, A., Gerlach, T., Rimmelzwaan, G., Rohner, S., Striewe, L. C., Gross, S., Schick, L. A., Klink, J. C., Kramer, K., Osterhaus, A., Beer, M., . . . Becher, P. (2022). Infections with highly pathogenic avian influenza A virus (HPAIV) H5N8 in harbor seals at the German North Sea coast, 2021. *Emerg Microbes Infect*, *11*(1), 725-729. https://doi.org/10.1080/22221751.2022.2043726

Powell, T. J., Peng, Y., Berthoud, T. K., Blais, M.-E., Lillie, P. J., Hill, A. V. S., Rowland-Jones, S. L., McMichael, A. J., Gilbert, S. C., & Dong, T. (2013). Examination of Influenza Specific T Cell Responses after Influenza Virus Challenge in Individuals Vaccinated with MVA-NP+M1 Vaccine. *PLoS One*, *8*(5), e62778. https://doi.org/10.1371/journal.pone.0062778

Raadsen, M. P., Dahlke, C., Fathi, A., Hardtke, S., Klüver, M., Krähling, V., Gerresheim, G. K., Mayer, L., Mykytyn, A. Z., Weskamm, L. M., Zoran, T., van Gorp, E. C. M., Sutter, G., Becker, S., Haagmans, B. L., Addo, M. M., Borregaard, S., Kaltenberg, L., Kelidou, A., . . . Kupke, A. (2025). Safety, immunogenicity, and optimal dosing of a modified vaccinia Ankara-based vaccine against MERS-CoV in healthy adults: a phase 1b, double-blind, randomised placebo-controlled clinical trial. *The Lancet Infectious Diseases*, *25*(2), 231-242. https://doi.org/10.1016/S1473-3099(24)00423-7

Ramírez, J. C., Gherardi, M. M., & Esteban, M. (2000). Biology of Attenuated Modified Vaccinia Virus Ankara Recombinant Vector in Mice: Virus Fate and Activation of B- and T-Cell Immune Responses in Comparison with the Western Reserve Strain and Advantages as a Vaccine. *Journal of Virology*, *74*(2), 923-933. https://doi.org/doi:10.11-28/jvi.74.2.923-933.2000

Raza, M. A., & Ashraf, M. A. (2024). Drug resistance and possible therapeutic options against influenza A virus infection over past years. *Arch Microbiol*, *206*(12), 458. https://doi.org/10.1007/s00203-024-04181-3

Reynisson, B., Alvarez, B., Paul, S., Peters, B., & Nielsen, M. (2020). NetMHCpan-4.1 and NetMHCIIpan-4.0: improved predictions of MHC antigen presentation by concurrent motif deconvolution and integration of MS MHC eluted ligand data. *Nucleic Acids Res*, *48*(W1), W449-w454. https://doi.org/10.1093/nar/gkaa379

Rheinbaben, F. v., Gebel, J., Exner, M., & Schmidt, A. (2007). Environmental resistance, disinfection, and sterilization of poxviruses. *Poxviruses*, 397-405.

RKI, RKI zu humanen Erkrankungen mit aviärer Influenza (Vogelgrippe), November 2024. https://www.rki.de/DE/Themen/Infektions-krankheiten/Infektionskrankheiten-A-Z/Z/ZoonotischeInfluenza/Vogel-grippe.html?nn=16904306

Robert-Guroff, M. (2007). Replicating and non-replicating viral vectors for vaccine development. *Current Opinion in Biotechnology*, *18*(6), 546-556. https://doi.org/10.1016/j.copbio.2007.10.010

Roberts, K. L., & Smith, G. L. (2008). Vaccinia virus morphogenesis and dissemination. *Trends Microbiol*, *16*(10), 472-479. https://doi.org/10.10-16/j.tim.2008.07.009

Rostad, C. A., Yildirim, I., Kao, C., Yi, J., Kamidani, S., Peters, E., Stephens, K., Gibson, T., Hsiao, H. M., Singh, K., Spearman, P., McCracken, C., Agbakoba, V., Tomashek, K. M., Goll, J. B., Gelber, C. E., Johnson, R. A., Lee, S., Maner-Smith, K., . . . Anderson, E. J. (2024). A Phase 1 randomized trial of homologous and heterologous filovirus vaccines with a late booster dose. *npj Vaccines*, *9*(1), 255. https://doi.org/10.1038/s41541-024-01042-4

Rotz, L. D., Khan, A. S., Lillibridge, S. R., Ostroff, S. M., & Hughes, J. M. (2002). Public health assessment of potential biological terrorism agents. *Emerg Infect Dis*, *8*(2), 225-230. https://doi.org/10.3201/eid0802.010164

Rouphael, N. G., Paine, M., Mosley, R., Henry, S., McAllister, D. V., Kalluri, H., Pewin, W., Frew, P. M., Yu, T., Thornburg, N. J., Kabbani, S., Lai, L., Vassilieva, E. V., Skountzou, I., Compans, R. W., Mulligan, M. J., & Prausnitz, M. R. (2017). The safety, immunogenicity, and acceptability of inactivated influenza vaccine delivered by microneedle patch (TIV-MNP 2015): a randomised, partly blinded, placebo-controlled, phase 1 trial. *Lancet*, *390*(10095), 649-658. https://doi.org/10.1016/s0140-6736(17)30575-5

Sakurai, F., Tachibana, M., & Mizuguchi, H. (2022). Adenovirus vector-based vaccine for infectious diseases. *Drug Metab Pharmacokinet*, *42*, 100432. https://doi.org/10.1016/j.dmpk.2021.100432

Schneider, J., Gilbert, S. C., Blanchard, T. J., Hanke, T., Robson, K. J., Hannan, C. M., Becker, M., Sinden, R., Smith, G. L., & Hill, A. V. (1998). Enhanced immunogenicity for CD8+ T cell induction and complete protective efficacy of malaria DNA vaccination by boosting with modified vaccinia virus Ankara. Nat Med, 4(4), 397-402. https://doi.org/10.1038/nm0498-397

Seo, S. H., & Webster, R. G. (2002). Tumor necrosis factor alpha exerts powerful anti-influenza virus effects in lung epithelial cells. *J Virol*, *76*(3), 1071-1076. https://doi.org/10.1128/jvi.76.3.1071-1076.2002

Sharma, L., Rebaza, A., & Dela Cruz, C. S. (2019). When “B” becomes “A”: the emerging threat of influenza B virus. *European Respiratory Journal*, *54*(2), 1901325. https://doi.org/10.1183/13993003.01325-2019

Skehel, J. J., & Wiley, D. C. (2000). Receptor binding and membrane fusion in virus entry: the influenza hemagglutinin. *Annu Rev Biochem*, *69*, 531-569. https://doi.org/10.1146/annurev.biochem.69.1.531

Song, F., Fux, R., Provacia, L. B., Volz, A., Eickmann, M., Becker, S., Osterhaus, A. D., Haagmans, B. L., & Sutter, G. (2013). Middle East respiratory syndrome coronavirus spike protein delivered by modified vaccinia virus Ankara efficiently induces virus-neutralizing antibodies. *J Virol*, *87*(21), 11950-11954. https://doi.org/10.1128/jvi.01672-13

Soo, R. J. J., Chiew, C. J., Ma, S., Pung, R., & Lee, V. (2020). Decreased Influenza Incidence under COVID-19 Control Measures, Singapore. Emerg Infect Dis, 26(8), 1933-1935. https://doi.org/10.3201/eid2608.201229

Spriggs, M. K., Hruby, D. E., Maliszewski, C. R., Pickup, D. J., Sims, J. E., Buller, R. M., & VanSlyke, J. (1992). Vaccinia and cowpox viruses encode a novel secreted interleukin-1-binding protein. *Cell*, *71*(1), 145-152. https://doi.org/10.1016/0092-8674(92)90273-f

Steel, J., Lowen, A. C., Wang, T. T., Yondola, M., Gao, Q., Haye, K., García-Sastre, A., & Palese, P. (2010). Influenza virus vaccine based on the conserved hemagglutinin stalk domain. *mBio*, *1*(1). https://doi.org/10.11-28/mBio.00018-10

Stickl, H., & Hochstein-Mintzel, V. (1971). [Intracutaneous smallpox vaccination with a weak pathogenic vaccinia virus ("MVA virus")]. *Munch Med Wochenschr*, *113*(35), 1149-1153. (Die intrakutane Pockenimpfung mit einem schwach virulenten Vakzinia-Virus ("MVA-Virus".)

Stickl, H., Hochstein-Mintzel, V., Mayr, A., Huber, H. C., Schäfer, H., & Holzner, A. (1974). [MVA vaccination against smallpox: clinical tests with an attenuated live vaccinia virus strain (MVA) (author's transl)]. Dtsch Med Wochenschr, 99(47), 2386-2392. https://doi.org/10.1055/s-0028-1108143 (MVA-Stufenimpfung gegen Pocken. Klinische Erprobung des attenuierten Pocken-Lebendimpfstoffes, Stamm MVA.)

Sun, L., Liu, C., & Peng, J. (2025). Specific Immune Responses and Oncolytic Effects Induced by EBV LMP2A-Armed Modified Ankara-Vaccinia Virus Vectored Vaccines in Nasopharyngeal Cancer. *Pharmaceutics*, *17*(1). https://doi.org/10.3390/pharmaceutics17010052

Sutter, G., & Moss, B. (1992). Nonreplicating vaccinia vector efficiently expresses recombinant genes. *Proceedings of the National Academy of Sciences of the United States of America*, *89*(22), 10847-10851. https://www.unboundmedicine.com/medline/citation/1438287/Nonreplicating_vaccinia_vector_efficiently_expresses_recombinant_genes_

Sutter, G., Wyatt, L. S., Foley, P. L., Bennink, J. R., & Moss, B. (1994). A recombinant vector derived from the host range-restricted and highly attenuated MVA strain of vaccinia virus stimulates protective immunity in mice to influenza virus. *Vaccine*, *12*(11), 1032-1040. https://doi.org/10.10-16/0264-410x(94)90341-7

SWISS-MODEL, Biozentrum of the University of Basel and Swiss Institute of Bioinformatics, accessed March 2025. https://swissmodel.expasy.org/repository/uniprot/P03436?temp-late=7zj7.1.A&range=30-515

Talic, S., Shah, S., Wild, H., Gasevic, D., Maharaj, A., Ademi, Z., Li, X., Xu, W., Mesa-Eguiagaray, I., Rostron, J., Theodoratou, E., Zhang, X., Motee, A., Liew, D., & Ilic, D. (2021). Effectiveness of public health measures in reducing the incidence of covid-19, SARS-CoV-2 transmission, and covid-19 mortality: systematic review and meta-analysis. *BMJ*, *375*, e068302. https://doi.org/10.1136/bmj-2021-068302

Tapia, M. D., Sow, S. O., Lyke, K. E., Haidara, F. C., Diallo, F., Doumbia, M., Traore, A., Coulibaly, F., Kodio, M., Onwuchekwa, U., Sztein, M. B., Wahid, R., Campbell, J. D., Kieny, M.-P., Moorthy, V., Imoukhuede, E. B., Rampling, T., Roman, F., De Ryck, I., . . . Levine, M. M. (2016). Use of ChAd3-EBO-Z Ebola virus vaccine in Malian and US adults, and boosting of Malian adults with MVA-BN-Filo: a phase 1, single-blind, randomised trial, a phase 1b, open-label and double-blind, dose-escalation trial, and a nested, randomised, double-blind, placebo-controlled trial. *The Lancet Infectious Diseases*, *16*(1), 31-42. https://doi.org/10.1016/S1473-3099(15)00362-X

Tenforde, M. W., Weber, Z. A., Yang, D. H., DeSilva, M. B., Dascomb, K., Irving, S. A., Naleway, A. L., Gaglani, M., Fireman, B., Lewis, N., Zerbo, O., Goddard, K., Timbol, J., Hansen, J. R., Grisel, N., Arndorfer, J., McEvoy, C. E., Essien, I. J., Rao, S., . . . Klein, N. P. (2024). Influenza Vaccine Effectiveness Against Influenza A-Associated Emergency Department, Urgent Care, and Hospitalization Encounters Among US Adults, 2022-2023. *J Infect Dis*, *230*(1), 141-151. https://doi.org/10.1093/infdis/jiad542

Terrier, O., Si-Tahar, M., Ducatez, M., Chevalier, C., Pizzorno, A., Le Goffic, R., Crépin, T., Simon, G., & Naffakh, N. (2021). Influenza viruses and coronaviruses: Knowns, unknowns, and common research challenges. *PLoS Pathog*, *17*(12), e1010106. https://doi.org/10.1371/journal.ppat.10-10106

The Lancet Infectious, D. (2014). Pandemic potential of emerging influenza. *The Lancet Infectious Diseases*, *14*(3), 173. https://doi.org/10.1016/S1473-3099(14)70072-6

The Lancet Infectious, D. (2018). How to be ready for the next influenza pandemic. *Lancet Infect Dis*, *18*(7), 697. https://doi.org/10.1016/s1473-3099(18)30364-5

Tscherne, A., Kalodimou, G., Kupke, A., Rohde, C., Freudenstein, A., Jany, S., Kumar, S., Sutter, G., Krähling, V., Becker, S., & Volz, A. (2024). Rapid Development of Modified Vaccinia Virus Ankara (MVA)-Based Vaccine Candidates Against Marburg Virus Suitabletable for Clinical Use in Humans. *Vaccines (Basel)*, *12*(12). https://doi.org/10.3390/vaccines12121316

Tscherne, A., Meyer Zu Natrup, C., Kalodimou, G., & Volz, A. (2025). Generating MVA-Vector Vaccine Candidates and Testing Them in Animal Models. *Methods Mol Biol*, *2860*, 297-340. https://doi.org/10.1007/978-1-0716-4160-6_20

Tscherne, A., Schwarz, J. H., Rohde, C., Kupke, A., Kalodimou, G., Limpinsel, L., Okba, N. M. A., Bošnjak, B., Sandrock, I., Odak, I., Halwe, S., Sauerhering, L., Brosinski, K., Liangliang, N., Duell, E., Jany, S., Freudenstein, A., Schmidt, J., Werner, A., . . . Volz, A. (2021). Immunogenicity and efficacy of the COVID-19 candidate vector vaccine MVA-SARS-2-S in preclinical vaccination. *Proc Natl Acad Sci U S A*, *118*(28). https://doi.org/10.1073/pnas.2026207118

Uddin, M. N., & Roni, M. A. (2021). Challenges of Storage and Stability of mRNA-Based COVID-19 Vaccines. *Vaccines (Basel)*, *9*(9). https://doi.org/10.3390/vaccines9091033

Ungchusak, K., Auewarakul, P., Dowell, S. F., Kitphati, R., Auwanit, W., Puthavathana, P., Uiprasertkul, M., Boonnak, K., Pittayawonganon, C., Cox, N. J., Zaki, S. R., Thawatsupha, P., Chittaganpitch, M., Khontong, R., Simmerman, J. M., & Chunsutthiwat, S. (2005). Probable person-to-person transmission of avian influenza A (H5N1). *N Engl J Med*, *352*(4), 333-340. https://doi.org/10.1056/NEJMoa044021

United Nations, Avian flu reported in 108 countries across five continents, says UN health agency, December 2024. https://news.un.org/en/story/2024/12/1158286

Valayer, S., Alexandre, M., Prague, M., Beavogui, A. H., Doumbia, S., Kieh, M., Greenwood, B., Leigh, B., Poupelin, M., Schwimmer, C., Sow, S. O., Berry, I. M., Kuhn, J. H., Fusco, D., Cauwelaert, N. D., Watson-Jones, D., Thiébaut, R., Lévy, Y., Yazdanpanah, Y., . . . Zhou, H. B. (2025). Evaluation of waning of IgG antibody responses after rVSVΔG-ZEBOV-GP and Ad26.ZEBOV, MVA-BN-Filo Ebola virus disease vaccines: a modelling study from the PREVAC randomized trial. *Emerg Microbes Infect*, *14*(1), 2432353. https://doi.org/10.1080/22221751.2024.2432353

van Riet, E., Ainai, A., Suzuki, T., & Hasegawa, H. (2012). Mucosal IgA responses in influenza virus infections; thoughts for vaccine design. *Vaccine*, *30*(40), 5893-5900. https://doi.org/10.1016/j.vaccine.2012.04.109

Veit, S., Jany, S., Fux, R., Sutter, G., & Volz, A. (2018). CD8+ T Cells Responding to the Middle East Respiratory Syndrome Coronavirus Nucleocapsid Protein Delivered by Vaccinia Virus MVA in Mice. *Viruses*, *10*(12). https://doi.org/10.3390/v10120718

ViralZone, Poxvirus replication cycle, Swiss Institute of Bioinformatics, accessed March 2025. https://viralzone.expasy.org/4399

Vollmar, J., Arndtz, N., Eckl, K. M., Thomsen, T., Petzold, B., Mateo, L., Schlereth, B., Handley, A., King, L., Hülsemann, V., Tzatzaris, M., Merkl, K., Wulff, N., & Chaplin, P. (2006). Safety and immunogenicity of IMVAMUNE, a promising candidate as a third generation smallpox vaccine. *Vaccine*, *24*(12), 2065-2070. https://doi.org/10.1016/j.vaccine.2005.11.022

Volz, A., & Sutter, G. (2017). Modified Vaccinia Virus Ankara: History, Value in Basic Research, and Current Perspectives for Vaccine Development. *Adv Virus Res*, *97*, 187-243. https://doi.org/10.1016/bs.aivir.2016.07.001

Volz, A., Lim, S., Kaserer, M., Lülf, A., Marr, L., Jany, S., Deeg, C. A., Pijlman, G. P., Koraka, P., Osterhaus, A. D., Martina, B. E., & Sutter, G. (2016). Immunogenicity and protective efficacy of recombinant Modified Vaccinia virus Ankara candidate vaccines delivering West Nile virus envelope antigens. *Vaccine*, *34*(16), 1915-1926. https://doi.org/10.10-16/j.vaccine.2016.02.042

von Krempelhuber, A., Vollmar, J., Pokorny, R., Rapp, P., Wulff, N., Petzold, B., Handley, A., Mateo, L., Siersbol, H., Kollaritsch, H., & Chaplin, P. (2010). A randomized, double-blind, dose-finding Phase II study to evaluate immunogenicity and safety of the third generation smallpox vaccine candidate IMVAMUNE®. *Vaccine*, *28*(5), 1209-1216. https://doi.org/10.10-16/j.vaccine.2009.11.030

Wadhwa, A., Aljabbari, A., Lokras, A., Foged, C., & Thakur, A. (2020). Opportunities and Challenges in the Delivery of mRNA-based Vaccines. *Pharmaceutics*, *12*(2). https://doi.org/10.3390/pharmaceutics12020102

Wang, T. T., Parides, M. K., & Palese, P. (2012). Seroevidence for H5N1 influenza infections in humans: meta-analysis. *Science*, *335*(6075), 1463. https://doi.org/10.1126/science.1218888

Wang, W. C., Sayedahmed, E. E., Sambhara, S., & Mittal, S. K. (2022). Progress towards the Development of a Universal Influenza Vaccine. *Viruses*, *14*(8). https://doi.org/10.3390/v14081684

Wang, W., DeFeo, C. J., Alvarado-Facundo, E., Vassell, R., & Weiss, C. D. (2015). Intermonomer Interactions in Hemagglutinin Subunits HA1 and HA2 Affecting Hemagglutinin Stability and Influenza Virus Infectivity. *J Virol*, *89*(20), 10602-10611. https://doi.org/10.1128/jvi.00939-15

Werden, S. J., Rahman, M. M., & McFadden, G. (2008). Poxvirus host range genes. *Adv Virus Res*, *71*, 135-171. https://doi.org/10.1016/s0065-3527(08)00003-1

WHO, Avian Influenza Weekly Update #988: 7 March 2025, March 2025. https://www.who.int/westernpacific/publications/m/i-tem/avian-influenza-weekly-update---988--7-march-2025

WHO, Influenza (seasonal), February 2025. https://www.who.int/news-room/fact-sheets/detail/influenza-(seasonal)

WHO, Non-pharmaceutical public health measures for mitigating the risk and impact of epidemic and pandemic influenza, September 2019. https://www.who.int/publications/i/item/non-pharmaceutical-public-health-measuresfor-mitigating-the-risk-and-impact-of-epidemic-and-pandemic-influenza

WHO, Pathogens prioritization: a scientific framework for epidemic and pandemic research preparedness, July 2024. https://www.who.int/publications/m/item/pathogens-prioritization-a-scientific-framework-for-epidemic-and-pandemic-research-preparedness

WHO, The burden of Influenza, March 2024. https://www.who.int/news-room/feature-stories/detail/the-burden-of-influenza

WHO, Updated joint FAO/WHO/WOAH assessment of recent influenza A(H5N1) virus events in animals and people, August 2024. https://www.who.int/publications/m/item/updated-joint-fao-who-woah-assessment-of-recent-influenza-a(h5n1)-virus-events-in-animals-and-people

WHO, WHO study lists top endemic pathogens for which new vaccines are urgently needed, November 2024. https://www.who.int/news/item/05-11-2024-who-study-lists-top-endemic-pathogens-for-which-new-vaccines-are-urgently-needed

Wiedemann, A., Lhomme, E., Huchon, M., Foucat, E., Bérerd-Camara, M., Guillaumat, L., Yaradouno, M., Tambalou, J., Rodrigues, C., Ribeiro, A., Béavogui, A. H., Lacabaratz, C., Thiébaut, R., Richert, L., & Lévy, Y. (2024). Long-term cellular immunity of vaccines for Zaire Ebola Virus Diseases. *Nat Commun*, *15*(1), 7666. https://doi.org/10.1038/s41467-024-51453-z

Wiersma, L. C., Rimmelzwaan, G. F., & de Vries, R. D. (2015). Developing Universal Influenza Vaccines: Hitting the Nail, Not Just on the Head. *Vaccines (Basel)*, *3*(2), 239-262. https://doi.org/10.3390/vaccines3020239

Wilks, S., de Graaf, M., Smith, D. J., & Burke, D. F. (2012). A review of influenza haemagglutinin receptor binding as it relates to pandemic properties. *Vaccine*, *30*(29), 4369-4376. https://doi.org/10.1016/j.vaccine.2012.02.076

Willis, E., Pardi, N., Parkhouse, K., Mui, B. L., Tam, Y. K., Weissman, D., & Hensley, S. E. (2020). Nucleoside-modified mRNA vaccination partially overcomes maternal antibody inhibition of de novo immune responses in mice. *Sci Transl Med*, *12*(525). https://doi.org/10.1126/scitranslmed.aav5701

Wilson, I. A., Skehel, J. J., & Wiley, D. C. (1981). Structure of the haemagglutinin membrane glycoprotein of influenza virus at 3 A resolution. *Nature*, *289*(5796), 366-373. https://doi.org/10.1038/289366a0

Wold, W. S., & Toth, K. (2013). Adenovirus vectors for gene therapy, vaccination and cancer gene therapy. *Curr Gene Ther*, *13*(6), 421-433. https://doi.org/10.2174/15665232133666131125095046

Wu, N. C., & Wilson, I. A. (2020). Structural Biology of Influenza Hemagglutinin: An Amaranthine Adventure. *Viruses*, *12*(9). https://doi.org/10.3390/v12091053

Wu, Y., Wu, Y., Tefsen, B., Shi, Y., & Gao, G. F. (2014). Bat-derived influenza-like viruses H17N10 and H18N11. *Trends Microbiol*, *22*(4), 183-191. https://doi.org/10.1016/j.tim.2014.01.010

Wyatt, L. S., Earl, P. L., Xiao, W., Americo, J. L., Cotter, C. A., Vogt, J., & Moss, B. (2009). Elucidating and minimizing the loss by recombinant vaccinia virus of human immunodeficiency virus gene expression resulting from spontaneous mutations and positive selection. *J Virol*, *83*(14), 7176-7184. https://doi.org/10.1128/jvi.00687-09

Wyatt, L. S., Shors, S. T., Murphy, B. R., & Moss, B. (1996). Development of a replication-deficient recombinant vaccinia virus vaccine effective against parainfluenza virus 3 infection in an animal model. Vaccine, 14(15), 1451-1458. https://doi.org/10.1016/s0264-410x(96)00072-2

Yan, Z., Kim, K., Kim, H., Ha, B., Gambiez, A., Bennett, J., de Almeida Mendes, Marcus F., Trevizani, R., Mahita, J., Richardson, E., Marrama, D., Blazeska, N., Koşaloğlu-Yalçın, Z., Nielsen, M., Sette, A., Peters, B., & Greenbaum, Jason A. (2024). Next-generation IEDB tools: a platform for epitope prediction and analysis. Nucleic Acids Research, 52(W1), W526-W532. https://doi.org/10.1093/nar/gkae407

Young, B., Zhao, X., Cook, A. R., Parry, C. M., Wilder-Smith, A., & I-Cheng, M. C. (2017). Do antibody responses to the influenza vaccine persist year-round in the elderly? A systematic review and meta-analysis. *Vaccine*, *35*(2), 212-221.

Zhirnov, O. P., Ikizler, M. R., & Wright, P. F. (2002). Cleavage of influenza a virus hemagglutinin in human respiratory epithelium is cell associated and sensitive to exogenous antiproteases. *J Virol*, *76*(17), 8682-8689. https://doi.org/10.1128/jvi.76.17.8682-8689.2002

XII. APPENDIX

Table A1: Consumables.

Product	Catalogue Number	Company
15 ml tube	62.554.002	Sarstedt (Nümbrecht, Germany)
24 ml syringe	8300054666	Covetrus (Portland, Maine)
50 ml tube	62.547.254	Sarstedt (Nümbrecht, Germany)
70 µm strainer Falcon®	352350	Corning (Corning, New York)
96-well flat bottom ELISA plates Nun MaxiSorp	442404	Thermo Fisher Scientific (Waltham, Massachusetts)
Cover slips (Menzel)	-	Thermo Fisher Scientific (Waltham, Massachusetts)
ELISA plate lids	264122	Thermo Fisher Scientific (Waltham, Massachusetts)
Filter tip 10 µl	70.3020.255	Sarstedt (Nümbrecht, Germany)
Filter tip 100 µl	70.3030.255	Sarstedt (Nümbrecht, Germany)
Filter tip 1000 µl	70.3050.275	Sarstedt (Nümbrecht, Germany)
Filter tip 20 µl	70.760.213	Sarstedt (Nümbrecht, Germany)
Filter tip 200 µl	70.3031.255	Sarstedt (Nümbrecht, Germany)
Flow cytometry plate lids	82.1584	Sarstedt (Nümbrecht, Germany)
Flow cytometry plates	82.1582	Sarstedt (Nümbrecht, Germany)
Flow cytometry tubes	55.1579	Sarstedt (Nümbrecht, Germany)
Micro tube 1.5 ml	72.690.001	Sarstedt (Nümbrecht, Germany)
Micro tube 2 ml	72.695.500	Sarstedt (Nümbrecht, Germany)
Microscope slides	7695001	Th. Geyer (Renningen, Germany)
Multidispense Combitips®	0030089685	Eppendorf (Hamburg, Germany)
PCR-tubes 8-strip	72.991.002	Sarstedt (Nümbrecht, Germany)
Serological pipette 10 ml	86.1254.001	Sarstedt (Nümbrecht, Germany)
Serological pipette 25 ml	86.1685.001	Sarstedt (Nümbrecht, Germany)
Serological pipette 5 ml	86.1253.001	Sarstedt (Nümbrecht, Germany)
Tissue culture 24-well plate	83.3922	Sarstedt (Nümbrecht, Germany)
Tissue culture 6- well plate	83.3920	Sarstedt (Nümbrecht, Germany)
Tissue culture 96-well plate	83.3924	Sarstedt (Nümbrecht, Germany)
Tissue culture flask T175	83.3912	Sarstedt (Nümbrecht, Germany)
Tissue culture flask T25	83.3910	Sarstedt (Nümbrecht, Germany)
Tissue culture flask T75	83.911	Sarstedt (Nümbrecht, Germany)

Table A2: Laboratory equipment.

Instrument	Company
Avanti® J-26 XP Centrifuge	Beckman Coulter (Brea, California)
BDK-SK biological safety cabinet	BDK Luft- und Reinraumtechnik GmbH (Sonnenbühl, Germany)
BS48 biological safety cabinet	Tecniplast (Buguggiate, Italy)
ChemiDoc™ MP Imaging System	Bio-Rad (Hercules, California)
ELISpot plate reader Bioreader® 7000 V	BIOSYS Scientific Devices GmbH (Karben, Germany)
Fluorescence microscope BZ-X700	Keyence (Osaka, Japan)
Galaxy 170 S incubator	New Brunswick Scientific Co., Inc. (Edison, New Jersey)
HD 2200 ultrasonic homogenizator system	Bandelin Sonopuls (Berlin, Germany)
Hera Cell incubator	Heraeus (Hanau, Germany)
Liquid nitrogen tank Locator 6 Plus	Thermo Fisher Scientific (Waltham, Massachusetts)
Mastercycler nexus X2	Eppendorf (Hamburg, Germany)
Mini Trans blot System	Bio-Rad (Hercules, California)
Mini-Protean Tetra System	Bio-Rad (Hercules, California)
Mupid One electrophoresis system	Nippon Genetics Co., Ltd. (Tokyo, Japan)
NovoCyte Quanteon flow cytometer	Agilent Technologies (Santa Clara, California)
Optima™ LE-80K Ultracentrifuge	Beckman Coulter (Brea, California)
PowerPac Basic	Bio-Rad (Hercules, California)
Scanlaf Mars biological safety cabinet	LaboGene (Lynge, Denmark)
Spark® multimodal plate reader	Tecan Group Ltd. (Männedorf, Switzerland)

Table A3: Commercial kits.

Kit	Company
ELISpot Plus Mouse IFN-γ (ALP) kit	Mabtech AB (Nacka Strand, Sweden)
NucleoBond® Xtra Midi kit	Macherey-Nagel (Düren, Germany)
NucleoSpin® Blood QuickPure kit	Macherey-Nagel (Düren, Germany)
NucleoSpin® Gel and PCR-Clean-up kit	Macherey-Nagel (Düren, Germany)
NucleoSpin® Plasmid kit	Macherey-Nagel (Düren, Germany)
Pierce™ Coomassie (Bradford) Protein-Assay-Kit	Thermo Fisher Scientific (Waltham, Massachusetts)
Plasmid DNA extraction kit	Macherey-Nagel (Düren, Germany)

Table A4: Reagents used in the experiments.

Reagent	Cat. No.	Company
1 kb DNA ladder	N3232	New England Biolabs (Ipswich, Massachusetts)
3′3′,5′5′-Tetramethyl-benzidine (TMB) Liquid Substrate System	T0440	Sigma-Aldrich (St. Louis, Missouri)
4% formaldehyde	T359.1	Carl Roth (Karlsruhe, Germany)
4′,6-Diamidin-2-phenylindol (DAPI) solution	R37606	Thermo Fisher Scientific (Waltham, Massachusetts)
10-beta competent *E.coli* bacteria	-	New England Biolabs (Ipswich, Massachusetts)
Aceton	9780.1	Carl Roth (Karlsruhe, Germany)
Agarose	840004	Biozym (Oldendorf, Germany)
BamHI-HF	R3136	New England Biolabs (Ipswich, Massachusetts)
Bovine serum albumin (BSA)	3737.3	Carl Roth (Karlsruhe, Germany)
Brefeldin A Solution (1000X)	420601	Biolegend (San Diego, California)
Color Protein Standard	P7719S	New England Biolabs (Ipswich, Massachusetts)
DMSO	D8418	Sigma-Aldrich (St. Louis, Missouri)
Dulbecco's Modified Eagle's Medium (DMEM) high glucose	D5796	Sigma-Aldrich (St. Louis, Missouri)
Dulbecco's Phosphate Buffered Saline (DPBS)	14190	Thermo Fisher Scientific (Waltham, Massachusetts)
Fetal bovine serum (FBS)	10083-145 F0804	Thermo Fisher Scientific (Waltham, Massachusetts) Sigma-Aldrich (St. Louis, Missouri)
Fluorescence mounting medium	S3023	Agilent (Santa Clara, California)
Glycine	A1067	ITW Reagents Panreac (Barcelona, Spain)
HEPES solution	H0887	Sigma-Aldrich (St. Louis, Missouri)
HindIII-HF	R3104	New England Biolabs (Ipswich, Massachusetts)
Ionomycin	I9657	Sigma-Aldrich (St. Louis, Missouri)

KCl	6781.3	Carl Roth (Karlsruhe, Germany)
KH_2PO_4	3904.1	Carl Roth (Karlsruhe, Germany)
KPL TrueBlue™ Peroxidase Substrate	5510	SeraCare Life Sciences Inc. (Milford, Massachusetts)
L-Glutamine solution	G7513	Sigma-Aldrich (St. Louis, Missouri)
MEM non-essential amino acid solution	M7145	Sigma-Aldrich (St. Louis, Missouri)
Methanol	9785.1	Carl Roth (Karlsruhe, Germany)
Minimum Essential Medium Eagle	M4655	Sigma-Aldrich (St. Louis, Missouri)
NaCl	0601.1 / 3957.1	Carl-Roth GmbH (Karlsruhe, Germany)
$NaHPO_4$	X987.2	Carl Roth (Karlsruhe, Germany)
Nitrocellulose membrane	10600002	Cytiva (Marlborough, Massachusetts)
nonfat dried milk powder	A0830	ITW Reagents Panreac (Barcelona, Spain)
NotI-HF	R3189	New England Biolabs (Ipswich, Massachusetts)
Penicillin / Streptomycin	P0781	Sigma-Aldrich (St. Louis, Missouri)
PMA	P1585	Sigma-Aldrich (St. Louis, Missouri)
PNGase F	P0704	New England Biolabs (Ipswich, Massachusetts)
Protease inhibitor	A32955	Thermo Fisher Scientific (Waltham, Massachusetts)
Purple loading dye	B7024A	New England Biolabs (Ipswich, Massachusetts)
Red Blood Cell Lysis Buffer	R7757	Sigma-Aldrich (St. Louis, Missouri)
ROTI®Fair tablet	1112.2	Carl Roth (Karlsruhe, Germany)
RPMI 1640	R8758	Sigma-Aldrich (St. Louis, Missouri)
SalI-HF	R3138	New England Biolabs (Ipswich, Massachusetts)
SDS	CN30.3	Carl Roth (Karlsruhe, Germany)
Stop Reagent for TMB Substrate	S5814	Sigma-Aldrich (St. Louis, Missouri)
Sucrose	S1888	Sigma-Aldrich (St. Louis, Missouri)
SuperSignal® West Dura Extended Duration substrate	34075	Thermo Fisher Scientific (Waltham, Massachusetts)
TAE electrophoresis buffer	B49	Thermo Fisher Scientific (Waltham, Massachusetts)

Taq DNA Polymerase, recombinant	10342178	Thermo Fisher Scientific (Waltham, Massachusetts)
TRIS	A1086	ITW Reagents Panreac (Barcelona, Spain)
TRIS-buffered saline	A1086	ITW Reagents Panreac (Barcelona, Spain)
Triton X-100	93443	Sigma-Aldrich (St. Louis, Missouri)
TrypLE™ Select	12563	Thermo Fisher Scientific (Waltham, Massachusetts)
Trypsin-EDTA	252000	Thermo Fisher Scientific (Waltham, Massachusetts)
Tween-20	A4974	ITW Reagents Panreac (Barcelona, Spain)
VP-SFM medium	11681020	Thermo Fisher Scientific (Waltham, Massachusetts)
XhoI	R0146	New England Biolabs (Ipswich, Massachusetts)
X-tremeGENE HP DNA Transfection Reagent	06366244001	Roche (Basel, Switzerland)
Zombie Aqua™ Fixable Viability Kit	423101	Biolegend (San Diego, California)

Table A5: Stock solutions.

Solution	Preparation
5x Running buffer (WB)	72.5 g Glycine 15.2 g TRIS 25 ml of 20% SDS
Blocking buffer (ELISA)	1% BSA 1 M sucrose in PBS
Blocking buffer (WB)	5% nonfat dried milk powder 0.05% Tween-20 in PBS
Dilution buffer (ELISA)	1% BSA in PBS
Freezing medium	40% DMEM / VP-SFM (cell line specific) 40% heat inactivated FBS 20% DMSO
LB agar	1.5 % agar in LB medium
LB medium, pH7.5	5 g NaCl

	5g yeast extract 10 g Tryptone ad 1l demineralized H_2O
Lysis buffer (WB)	10 ml stock (1% Triton X-100, 25 mM TRIS, 1 M NaCl) 1 tablet protease inhibitor
PBS	2 g KCl 2 g KH_2PO_4 80 g NaCl 11.5 g $NaHPO_4$ ad 1 l demineralized H_2O
PBS (ELISA)	ROTI®Fair tablet in demineralized H_2O
RPMI-10	88% RPMI 1640 10% FBS 1% HEPES 1% Penicillin/-Streptomycin
Towbin buffer	24 g TRIS 114,6 g Glycine
Transfer buffer (WB)	80 ml Towbin buffer 200 ml Methanol ad 1 l demineralized H_2O

XIII. DANKSAGUNG

Zunächst möchte ich unserem ehemaligen Lehrstuhlinhaber Herrn **Prof. Dr. Dr. h.c. Gerd Sutter** danken, mir diese Arbeit auf dem hochinteressanten Gebiet der Virologie und Impfstoffen ermöglicht zu haben. Genauso möchte ich mich ausdrücklich bei Herrn **Prof. Dr. Markus Meißner** für die Abnahme der Promotionsvorprüfung und Durchsicht meiner Doktorarbeit bedanken.

Meinen Dank möchte ich **Prof. Dr. Frank Ebel** und **Prof. Dr. Monika Rinder** für das Beisitzen der Promotionsvorprüfung aussprechen.

Ein großer Dank gilt **Dr. Alina Tscherne** für die umfangreiche und aktive Betreuung während meiner Promotion. Ihre Unterstützung reichte von Laborexpertise über wissenschaftliche Fragestellungen bis hin zum Korrekturlesen meiner Doktorarbeit.

Ein besonderer Dank gilt auch **Dr. Robert Fux** und **Veronika Pilchova, PhD** für ihr fachliches Know-how und Unterstützung während dieses Projekts.

Georgia Kalodimou, PhD möchte ich für ihre Mitarbeit am Projekt, Vermittlung experimenteller Fähigkeiten und der teilweisen Durchsicht meiner Arbeit danken. Bei **Kumar Satyendra, PhD** möchte ich mich für die hilfreichen Tipps bei praktischer Arbeit und der Zusammenarbeit bei Tierversuchen bedanken.

Ein großes Dankeschön ergeht auch an **Astrid Freudenstein** und **Sylvia Jany** für die Einarbeitung und Unterstützung bei Laborarbeit.

Ebenso gilt mein Dank **Patrizia Bonert**, **Ursula Klostermeier**, **Johannes Döring** and **Axel Groß**, die uns mit ihrer Expertise in Tierversuchen unterstützten.

Ich danke allen Doktoranden, die diesen Weg mit mir geteilt haben. Ich möchte mich bei **Dr. Lisa Oberberger**, **Isabella Panhofer**, **Flora Fischer**, **Rebecca Dressler** und **Mareen Vogler** für die unterhaltsame Zeit bedanken.

Vielen Dank an **Christine Brandmüller**, **Theresa Friebis**, **Marlowe Peter**, **Dr. Nora Hesse**, **Dr. Michael Lehmann**, **Wanda Schroppa**, **Nina**

Hechtberger, **André Teichert** und **Eleni Tzikoula** für die Zusammenarbeit, sowie allen anderen Angehörigen des Instituts für die Zeit am Institut.

Von Herzen danke ich meiner Familie, die mich während der Promotion mit Freude begleitet haben. Insbesondere gilt dies meinen Eltern; ohne ihre Unterstützung wäre dieser Weg nicht möglich gewesen.